# ENGINEERING BIOMATERIAL SURFACES WITH N-CADHERIN

BY

JOHANA CAROLINA MARISOL VEGA LEONEL

DISSERTATION

Submitted in partial fulfillment of the requirements
for the degree of Doctor of Philosophy in Neuroscience
in the Graduate College of the
University of Illinois at Urbana-Champaign, 2014

Urbana, Illinois

Doctoral Committee:

Associate Professor Hyunjoon Kong, Chair
Professor Deborah E. Leckband
Professor Martha U. Gillette
Professor Charles Leroy Cox

# Abstract

N-cadherin is a key protein that is responsible for cellular adhesion to neighboring cells in mesenchymal tissues. It plays a significant role in neural development, regeneration, and pathological processes. Recently, efforts were increasingly made to better understand biological function of N-cadherin and further harness it in the assembly of biomedical devices used for sensing, diagnosis, and treatments. One of the greatest challenges in these efforts is to control the type and number of N-cadherin molecules involved in cell-cell adhesion. To address this challenge, this study utilizes recombinant N-cadherin molecules to examine biomolecular effects on cellular adhesion, angiogenic factor secretion, and neural network formation. First, cell-cell adhesion was reproduced by tethering the recombinant N-Cadherin to hydrogel surfaces (Chapter 2). Second, soluble N-Cadherin was introduced into clusters of bone marrow stromal cells (BMSCs) to examine their effects on cellular secretion of vascular endothelial growth factors and subsequent vascular network formation (Chapter 3). The soluble N-Cadherin was also used to modulate neural differentiation of BMSC clusters (Chapter 4). Finally, N-cadherin was biologically coupled to a microchanneled hydrogel to examine its effects on 3D neural differentiation of BMSCs and subsequent 3D neural network formation (Chapter 5). Overall the knowledge gained from this work may assist current efforts to better understand emergent cellular behavior and also enhance the performance of biomedical devices.

# Acknowledgements

I would like to dedicate this work to my family, who gave me the strength and support to accomplish this work. Without them this would have never been possible.

There are many people and organizations that I would like to thank for giving me the opportunity to do this work. First I would like to thank my advisers, Dr. Deborah E. Leckband and Dr. Hyunjoon Kong, for providing me with the support and guidance to complete my graduate work. I would like to thank my committee members, Dr. Martha Gillette and Dr. Charles Leroy Cox for their time, advice, corrections and efforts in supporting the completion of my thesis. Many thanks to all my lab members, their time, support and training has been of great value and indispensable in order to complete this work. I would like to thank the Neuroscience Program for their support, especially Dr. Samuel N. Beshers who was always there to provide me with support and advice.

I would like to give a big thanks to my family who has always been there from the beginning of my life, providing the means for my education and the emotional support needed in order to thrive even during hard times. I am very grateful for my wonderful family. I would like to thank my grandmother Lucila Leonel de Vega to whom I owe my strong will, discipline and diligence. Even though she is not alive to see the completion of my graduate work, her lessons were indispensable during my graduate work.

I would like finally to thank the NeuroEngineering Integrative Graduate Education and Research Traineeship (IGERT) program and the National Science Foundation Graduate Research Fellowship Program (NSF-GRFP) for providing me with the financial support during my five years of graduate work.

# Table of Contents

# Chapter 1: Introduction

## 1.1 Introduction

Multicellular organisms comprise different tissues whose shape, organization, and functions are highly regulated by cell-cell adhesion molecules [1]. Cadherins are crucial adhesive proteins at the cell-cell adhesive junctions [2] and are critical for regulating the organization, recognition, and maintenance of the structural integrity of the tissues [3,4]. During development they are involved in migration, morphogenesis, tissue patterning and the formation of the distinct tissue interfaces [4,5]. Cadherins are a large superfamily of calcium-dependent cell adhesion proteins [6]. This superfamily consists of classical cadherins, protocadherins, desmosomal cadherisn and cadherin-like proteins [3]. Classical cadherins are the most studied in this protein family, and they are named based on the tissue from which they were first isolated [3,7]. From the classical cadherins that have been identified in mammals, E- (epithelial) and N- (neural) cadherin have been the most extensively studied [8]. E- and N-Cadherin exhibit mutually exclusive expression patterns [8]. These two proteins are markers of the endothelial to mesenchymal transition, during which by E-Cadherin is down regulated and N-Cadherin is up-regulation. This process is critical for normal development [1,8].

## 1.2 N-Cadherin

N-Cadherin is a member of the classical type I cadherins, whose structures consist of an extracellular ectodomain, a single-pass transmembrane domain, and a cytoplasmic domain [3]. The extracellular ectodomain is composed by five extracellular cadherin ectodomains (EC) [1]. Their cytoplasmic domain has a juxtamembrane and C-terminal region where p120 and β-

catenins bind respectively [1]. From the five EC domains, the N-terminal EC1 domain is critical for cell adhesion and cadherin selectivity [3].The EC1 domain determines the cadherin selectivity, and the organization of cadherin adhesions also involves the EC2 and EC3 domains [3]. Strong homophilic cadherin binding occurs between EC1-EC3 regions of the ectodomains on opposing cells [3,6]. Because classical cadherins are calcium-dependent adhesion molecules, calcium is required for adhesive function [7]. Then, calcium depletion, causes the loss of cadherin function [3,7].

### 1.3 Biological role of N-Cadherin

N-Cadherin is found in different tissues including neurons, muscle, hearth and mesenchymal cells, to name few [8]. The role of N-Cadherin depends on the type of cell on which it is expressed and the environment in which the cell is found [8]. In cardiac cells it plays a critical role in maintaining the structural integrity of the heart, by maintaining strong adhesion between cardiomyocytes [8]. Cleavage of the N-Cadherin in glioblastomas is responsible for the migration of tumor cells [9]. N-Cadherin mediated adhesion is also associated with different signaling pathways that influence proliferation, differentiation and apoptosis [8]. N-Cadherin can modulate signaling processes by sequestering β-catenin at the plasma membrane, and can modulate the Wnt pathway, by regulating the cytosolic pool of β-catenin [1,8]. Deletion of the N-Cadherin gene is embryonically lethal, and causes multiple abnormalities and severe cardiovascular defects [8]. N-Cadherin also contributes to bone formation and it is critical for osteoblast interactions that regulate commitment and differentiation [10]. Disruption of N-Cadherin expression causes abnormalities in bone formation, resulting in embryonic lethality

[10]. N-Cadherin is crucial for mesenchymal condensation and chondrogenesis, and blockage or disruption of N-Cadherin expression abolishes chondrogenesis [11].

### 1.4 Biological role of N-Cadherin on cellular trophic factor secretion

It has been demonstrated that N-Cadherin it is involved in axon growth and the activation of the fibroblast growth factor receptor (FGFR) [12]. Homophilic binding of N-Cadherin blocks the FGFR function, and promotes the axonal growth [13]. Further, N-Cadherin down-regulation correlates with the decrease in vascular endothelial growth factor (VEFG) secretion, and N-Cadherin up-regulation coincides with the increase in VEGF secretion by human umbilical cord blood- mesenchymal stem cells (hUCB-BMSCs)[14].

### 1.5 Biological role of N-Cadherin on neural network formation

During the development of the nervous system, N-Cadherin is required for neurulation, reorganization of neuroectoderm, neural migration, axon guidance and fasciculation [12]. In neural network formation, N-Cadherin is required for axon extension, guidance and synapse formation [12]. As the synapses form, N-Cadherin localizes at the synaptic site, in order to induce and stabilize their interactions with their targets [12]. Therefore, N-Cadherin may act as a stop signal at the target site [12]. Suggesting that, N-Cadherin is involved in the synaptic plasticity of the neurons [13]. N-Cadherin expression is only maintained in excitatory neurons in the hippocampus [12]. All neurons express N-Cadherin initially, but not all mature neurons express N-Cadherin [12]. Therefore, N-Cadherin might be required for synapse formation, but it is not required to maintained mature synapses, there are probably other cadherins that are also involve in maintaining the synapses [12].

## 1.6 What are the challenges of studying the effects of N-Cadherin

Because N-Cadherin gene deletion is lethal, what it is known have been found through in-vitro experiments and the N-Cadherin weak allele expression in mutant animals [15]. Also, to study N-Cadherin in-vitro is challenging because it is absolutely necessary to conjugate the protein in ways that retain its biological function, in order to insure optimum cell adhesion [3]. Generally, direct conjugation of the N-Cadherin protein to the substrate can disrupt the protein structure and compromise its function. It is also difficult to control the extent and number of adhesion sites in vitro, making it difficult to decipher N-cadherin-specific effects.

## 1.7 Motivation for conjugating N-Cadherin to a substrate or using it as a soluble factor

N-Cadherin plays a critical role during development in a way that deletion of the N-Cadherin leads to abnormalities in all the systems; blood vessel formation, heart function, bone formation, neurological formation, all of this leads to failure of organ formation and function, ultimately making the embryo unviable [15,16,17]. It is known that N-Cadherin interacts with other proteins, and growth factors that regulate cellular events, however, the mechanisms are not well understood. [15]. Therefore, understanding the mechanisms by which N-Cadherin can regulate the morphology, and biological response of the cells, can be an invaluable tool to develop regeneration therapies that can aid the medical field. In order to accomplish the broad goal of studying the influence of this protein in a 3D environment and in solution, different approaches must be developed that more closely mimic how the N-Cadherin would be found in vivo.

## 1.8 Project Overview

Despite some impressive work to develop an artificial microenvironment suitable for neural cell survival, proliferation, migration and differentiation, a great challenge remains to develop techniques that would allow their complete integration with the biological systems. A challenge is to establish the role of the extracellular matrix and cell adhesion molecules such as N-Cadherin in the in vivo neural niche. This work aims to understand the role of N-Cadherin on cell adhesion, cell trophic factor secretion, and the network formation. This thesis describes the development of several techniques that enabled us to identify roles of N-Cadherin as a neurosupportive protein and as a signal transduction molecule that is critical for neural network formation. As a neurosupportive protein, it promotes cell adhesion to the extracellular matrix and synapse formation (Chapter 2). As a signal transduction protein, it is involved in trophic factor secretion and cell guidance (Chapter 3). It is also involved in regulating the ratio of BMSCs cells differentiation into gial and neuron (Chapter 3). N-cadherin ultimately supports neural network formation in three dimensional cultures and it increases network activity (Chapter 4). Overall, the knowledge gained from this thesis will be broadly useful for improving the quality of a wide array of molecular and cellular based neural network studies that can aid the neural regeneration field of study.

## 1.9 References


**1.** Adherens Junctions: From molecular mechanism to tissue development and disease. Subcellular *Biochemistry*. 2012; 60: 9- 62 and 171-249.

**2.** Leckband, D., and Sivasankar, S. Cadherin recognition and adhesion. *Curr. Opin. in Cell Biol.*2012;24:1-8.

**3.** Leckband, D., and Prakasam, A. Mechanism and dynamics of cadherin adhesion. *Annu. Rev. Biomed. Eng.* 2006; 8: 259-287.

**4.** Delva, E., and Kowalczyk, A.P. Regulation of cadherin trafficking. *NIH.* 2009; 10: 259-271.

**5.** Gomez, G.A., McLachlan, R.W., and Yap, A.S. Productive tension: force-sensing and homeostasis of cell-cell junction. *Trends in Cell Biol.* 2011; 21:499-505.

**6.** Leckband, D., and Sivasankar S. Cadherin recognition and adhesion. Current Op. in Cell Bio. 2012;24:1-8

**7.** Brasch, J., Harrison, O.J., Honing, B., and Shapiro L. Thinking outside of the cell: how cadherins drive adhesion. *Trends in Cell Biol.* 2012; 22:299-310.

**8.** Radice, G.L. N-Cadherin-Mediated adhesion and signaling from development to disease: lessons from mice. *Progress in Mol. Biol. and Trans. Sci*. 2013; 116:263-289.

**9.** Kohutek, Z.A., diPierro, Ch.G., Redpath, G.T., and Hussaini, I. M. ADAM-10-Mediated N-Cadherin cleavage is protein kinase C-α dependent and promotes glioblastoma cell migration. *The J. of Neuro.* 2009; 29:4605-4615.

**10.** Lai, Ch.F., Cheng, SL., Mbalaviele, G., Donsante, Ch., Walkins, M., Radice, G.L., and Civitelli, R. Accentuated ovariectomy-induced bone loss and altered osteogenesis in heterozygous N-Cadherin null mice. *J.of Bone and Min. Res*. 2006; 21:1897-1906.

**11.** Bian, L., Guvendiren, M., Mauck, R.L., and Burdick, J.A. Hydrogels that mimic development relevant matrix and N-cadherin interactions enhance MSC chondrogenesis.

**12.** Ranscht, B. Cadherins: molecular codes for axon guidance and synapse formation. *Int. J. Devl. Neuro.* 2000; 18: 643-651.

**13.** Skaper, S.D. Neuronal growth-promoting and inhibition cues in neuroprotection and neuroregeneration. Neurotrophic Factors: Methods and protocols. *Methods in Mol. Bio.* 2012; 846:13-22.

**14.** Lee, E. J., Choi, EK., Kang, S. K., Kim, GH., Park, J.Y., Kang, HJ., Lee, SW., Kim, KH., Kwon, J.S., Lee, K.H., Ahn, Y., Lee, HJ., Cho, HJ, Choi, S.J.,Oh, W.I., Park, YB., and Kim, HS. N-Cadherin determins individual variations in the therapeutic efficacy of human umbilical cord blood-derived mesenchymal stem cells in a rat model of myocardial infarction. *Mole. Therapy.* 2012; 20:155-167.

**15.** Susuki, S.C., and Takeichi, M. Cadherins in neuronal morphogenesis and function. *Devlop. Growth Differ.* 2008; 50:S119-S130.

**16.** Carmeliet. P., and Tessier-Lavigne, M. Common mechanisms of nerve and blood vessel wiring. *Nature.* 2005; 436**:**193-200.

**17.** Broders-Bondon, F., Paul-Gilloteaux, P., Carlier, C., Radice, G.L., and Dufor, S. N-Cadherin and β1-integrins cooperate during the development of the enteric nervous system. *Dev. Bio.* 2012; 364:178-191.

# Chapter 2: Recapitulating cell-cell adhesion using N-Cadherin biologically tethered to substrates[*].

## 2.1 Abstract

Intercellular adhesion modulated by cadherin plays an important role in diverse cellular functions including tissue morphogenesis, regeneration, and pathogenesis. However, it is a challenging task to decipher the effects of cell-cell adhesion *in vitro*, because of a difficulty in controlling the extent and numbers of cell-cell contacts. In this study, we hypothesize that tethering recombinant extracellular domains of neural cadherin with a C-terminal immunoglobulin Fc domain (N-Cad-Fc) to a substrate with an immobilized anti-Fc antibody (Fc-antibody) and a bifunctional polymer, which is reactive to both protein and substrate would allow us to recapitulate cell-cell adhesion, independent of the number of cells plated on the substrate. To examine this hypothesis, we first immobilized Fc-antibody to a polyacrylamide hydrogel and a methacrylate-substituted glass using poly(amino-2-hydroxyethyl-co-2-methacryloxyethyl aspartamide)-g-poly(ethylene glycol)-N-hydroxyl succinimide ester (PHMAA-g-PEGNHS), and then incubated the gel in medium containing defined concentrations of the recombinant N-Cad-Fc. The resulting N-Cad-conjugated substrate enabled us to modulate adhesion of bone marrow stromal cells to the gel surface by varying the surface density of N-Cad-Fc. In contrast, direct chemical conjugation of N-Cad-Fc to the gel surface did not support cell adhesion. Additionally, the glass substrate biologically tethered with N-Cad-Fc promoted neuronal adhesion significantly more than substrates coated with poly-L-lysine. We suggest that this novel biological tethering method could be broadly applicable for modifying substrates with a variety of classical cadherins to enable the systematic study of the effects of cadherin-modulated cell-cell adhesion on cellular activities.

*Portion of this chapter were previously publish: Vega L. J.C.M., Lee, M.K., Jeong, J.H., Smith,C.E., Lee, K.Y., Chung, H.J., Leckband, D.E., and Kong, H. Recapitulating cell-cell adhesion using N-cadherin biological tethered to substrates. *Biomacromolecules.* 2014; 15:2172-2179.

## 2.2 Introduction

Multi-faceted extracellular microenvironments including growth factors/cytokines and extracellular matrix (ECM), orchestrate to regulate diverse phenotypic activities of cells in a desired manner [1]. Accordingly, cells modulate complex processes of tissue development, homeostasis, regeneration and pathology [2]. In the last decades, there have been tremendous efforts to understand the role of the extracellular matrix in instructing cellular activities, using various natural or synthetic matrices with controlled properties and nano/microstructures [3,4].

Some of these studies reported that the effects of ECM properties and soluble factors were also modulated by the extent of contacts between cells [3]. This could be attributed to juxtracrine signaling; however, many results suggested that direct cellular adhesion between neighboring cells, formed by intercellular cadherin bonds, may regulate cell fate and phenotypic activities [5]. For example, contact inhibition due to the ligation of E-cadherin activates the Hippo pathway via the epithelial growth factor receptor [6]. Conversely, intercellular adhesion mediated by N-cadherin triggers myogenic differentiation via the Cdo/JNK pathway [7]. The epithelial-to-mesenchymal transition during tissue morphogenesis correlates with the down regulation of E-cadherin and the up-regulation of N-cadherin [8]. Despite these findings, few studies have systematically explored the effects of cadherin-mediated cell-cell adhesion on cell fates and phenotypic activities, because of a lack of tools to control the number of intercellular cadherin bonds. Certain efforts were made to control the effects of cadherin, by culturing different number of cells on a substrate [9,10]. This approach, however, was unable to provide a precise control on the number of cadherin interactions between the contacting cells.

Alternatively, the chemical conjugation of controlled number and type of cadherin molecules onto a substrate would allow us to recapitulate cellular adhesion to neighboring cells *in vitro*, similar to conjugation of ECM proteins binding with cellular integrins [11]. To chemically link ECM proteins to substrates, short or polymeric molecules that present chemical groups reactive to target substrates and succinimidyl groups reactive to primary amine groups of proteins are used [12]. The chemical conjugation of cadherins to substrates is challenging because chemical modifications degrade the cadherin's adhesive function. It is also difficult to ensure the accessibility of the binding site, because amine groups of N-cadherin randomly react with succinimidyl groups on substrates of interest [24].

In this study, we hypothesized that biochemical coupling of cadherin molecules engineered to present Fc-tags to substrates of interests, using an Fc-antibody, would be advantageous to promoting cell adhesion to substrates of interest (Fig.2.1), and would enable further modulation of cellular adhesion morphology and neural network formation. We examined this hypothesis by chemically coupling an Fc-antibody to a hydrogel or a glass using a polyaspartamide protein linker [12] and subsequently exposing them to a precise concentration of recombinant, Fc-tagged N-cadherin extracellular domains (N-Cad-Fc). We analyzed the benefits of biochemically immobilizing N-Cad-Fc, relative to direct chemical coupling to the substrates, in stimulating adhesion of bone marrow stromal cells and cortical neurons, two of which endogenously express N-cadherin [13]. The results suggest that this method would also be useful for conjugating other cadherins (e.g., epithelial-cadherin, vascular endothelial-cadherin, etc) or Fc-tagged adhesion proteins, in order to determine the influence of cell-cell adhesive cues on cellular activities with precise control.

## 2.3 Experimental

### *2.3.1 Materials*

#### *2.3.1.1 PHMAA synthesis*

The polysuccinimide (PSI) with the average molecular weight (Mw) of 57,000 g/mol was first synthesized by acid-catalyzed polycondensation of L-aspartic acid [14]. Designated amounts of 2-aminoethyl methacrylate, ethanolamine, and excess amounts of ethylenediamine were added sequentially to PSI dissolved in dimethylformamide, in order to prepare poly(2-amino-2-hydroxyethyl-co-2-methacryloxyethyl aspartamide) (PAHMAA) [12]. The molar ratio between 2-aminoethyl methacrylate and succinimide units of PSI was kept constant at 0.1:1. The PAHMAA was modified to present controlled number of N-hydroxyl succinimidyl (NHS) ester groups. The poly(ethylene glycol) disuccinimidyl ester (PEGDE, Mw 7,000 g/mol) was added into water dissolved with PAHMAA, and the mixture was stirred overnight to prepare PHMAA-g-PEGNHS. The resulting PHMAA-g-PEGNHS (Fig. 2.2) was extensively dialyzed against distilled water and lyophilized. The molar ratio between PEGDE to the succinimide units of PSI was varied from 0.01 to 0.1 and 0.3. The resulting degree of PEGDE substitution was quantified using the $^{1}$H nuclear magnetic resonance (NMR) spectra (Fig. 2.3).

#### *2.3.1.2 In vitro synthesis of Fc-tagged N-Cadherin (N-Cad-Fc)*

HEK293 cells previously engineered to express soluble, recombinant Fc-tagged chicken N-cad constructs (N-Cad-Fc) [15] were cultured in Dulbecco's modified Eagle Medium (DMEM, Invitrogen) supplemented with 10% fetal bovine serum (FBS, Invitrogen) and 0.4 mg/ml G418 (Sigma) as a selection marker. The N-Cad-Fc recombinant protein was collected from cell culture supernatant, filtered, and isolated using protein A affinity column (Bio-Rad)

followed by gel filtration chromatography, as described [16]. Bead aggregation measurements were performed to confirm the functional activity of the N-Cad-Fc [17].

*2.3.1.3 Fluorescent labeling of N-Cad-Fc*

N-Cad-Fc was chemically labeled with fluorescein isothiocyanate (FITC, Sigma-Aldrich). Briefly, 1 mg/mL solution of N-Cad-Fc dissolved in HEPES buffer (20mM HEPES, 50mM NaCl, 5mM $CaCl_2$) was reacted with FITC for 12 hours at 4 °C. Following the reaction, FITC-labeled N-Cad-Fc was purified by centrifugal filtration (3 kDa MWCO, Millipore), followed by dialysis in HEPES buffer at 4 °C (3.5 kDa MWCO Slide-A-Lyzer cassette, Pierce) to remove unreacted FITC.

*2.3.1.4 Biological/Chemical conjugation of N-Cad-Fc to PAAm hydrogel using Fc-antibody and PHMAA-g-PEGNHS*

Anti-Fc-antibody (Sigma) was dissolved in PBS at 250 µg/mL. PHMAA-g-PEGNHS (5 mg) was added to 0.1 mL of each Fc-antibody solution, and stirred at 4 $^{o}$C overnight. The reacted products were mixed with 100µl pre-gel solution (8 wt% acrylamide and 0.48 wt% N,N,N',N'-methylenebisacrylamide (bis-acrylamide)). Then, 10µl of 10% ammonium persulfate (APS, Aldrich) and 5µl of tetramethylethylenediamine (TEMED, Aldrich) were added to initiate the polymerization and cross-linking reactions [18]. The molar ratio of bis-acrylamide (cross-linker) and acrylamide (monomer) was kept at 0.1:1.0. The pre-gel solution was then placed on a coverslip that was pre-treated with 0.4% 3-(trimethoxysilyl propyl)methacrylate (Aldrich), and immediately covered with an untreated cover slide. After allowing the hydrogel to form for 30 min, the coverslip was gently removed from the gel. The hydrogel was washed with PBS four

times to remove unreacted Fc-antibody. Finally, the gel was incubated overnight at 4 $^{o}$C with N-Cad-Fc in HEPES buffer (20 mM HEPES, 50 mM NaCl, 5 mM CaCl) at concentrations ranging from 0 to 100 and 250 µg/ml. Then, the gel was washed three times with PBS to remove unbound N-Cad-Fc.

For the chemical conjugation of N-Cad-Fc to a hydrogel, N-Cad-Fc was dissolved in HEPES buffer at 250 µg/mL. PHMAA-g-PEGNHS (5 mg) was added to 0.1 mL of each N-Cad-Fc solution, and stirred at 4 $^{o}$C overnight. The reacted products were mixed with 100µl of pre-gel solution (8 wt% acrylamide and 0.48 wt% bis-acrylamide). Then, 10µl of 10% APS and 5 µl of TEMED were added to initiate the polymerization and cross-linking reactions. The molar ratio of bis-acrylamide to acrylamide was kept at 0.1:1.0.

The compressive elastic moduli of the hydrogels were measured with a mechanical testing system (Insight, MTS Systems). The hydrogel was compressed at a rate of 1 mm/min and the resulting stress was measured with the mechanical testing system. The elastic modulus was calculated from the slope of the measured stress versus strain curve within the first 10% of strain.

*2.3.1.5 Measurement of the surface density of N-Cad-Fc*

Hydrogels modified with FITC-labeled N-Cad-Fc were used to measure the protein density on the surface. For this analysis, the hydrogel conjugated with Fc-antibody was incubated with FITC-labeled N-Cad-Fc. The concentration of FITC-labeled N-Cad-Fc in solution was varied from 0 to 100 and 250 µg/ml. Then, the gel was washed three times with PBS to remove excess FITC-labeled N-Cad-Fc. The fluorescence from the gel surface was captured with the fluorescence stereomicroscope (Zeiss Stereolumar v12). Four images per each

condition were analyzed. In parallel, fluorescence intensities from the solution containing controlled number of FITC-labeled N-Cad-Fc were obtained to prepare a standard curve. This standard curve was used to back-calculate the density of protein on the gel surface.

*2.3.1.6 Biological/chemical conjugation of N-Cad-Fc to glass slides using PHMAA-g-PEGNHS*

A glass coverslip was first treated with 0.4% 3-(trimethoxysilyl propyl)methacrylate. The reacted products of Fc-antibody and PHMAA-g-PEGNHS were placed on top of the treated cover slide. The protein solution was incubated at 4 °C for 30 min. Then, the excess PHMAA-g-PEG- Fc-antibody was removed by washing the surface with PBS. Finally, the surface was incubated overnight with aqueous N-Cad-Fc solution a concentrations of 0, 100 and 250 µg/mL at 4 °C. Again, the surface was washed with PBS to remove excess N-Cad-Fc. Separately, for a control experiment, the N-Cad-Fc was chemically conjugated to the substrate via sequential glass surface treatment with 3-(trimethoxysilyl propyl)methacrylate and UV light-induced surface reaction of the mixture of N-Cad-Fc and PHMAA-g-PEGNHS.

*2.3.1.7 Preparation of poly-L-lysine coated glass slides*

Glass coverslips were incubated with nitric acid (70% v/v, Sigma) overnight. After washing them with double distilled water four times, the coverslips were air dried in the biosafety cabinet for ~2 hours. Coverslips were placed in an oven for two hours at 225 $^{o}$C, and then cooled at room temperature. A 0.1 mg/mL poly-L-Lysine (PLL, Sigma) solution was prepared with 0.1M Boric Acid (Sigma) solution at pH 8.5. The PLL solution was placed on the

nitric acid-treated glass coverslips and incubated overnight at 37 $^{o}$C. The coverslips were washed twice with PBS (Sigma) and allowed to air dry for 20-30 minutes under UV irradiation.

*2.3.1.8 Bone marrow stromal cell culture*

Mouse bone marrow-derived stromal cells (BBMSCs, D1 cells, ATCC) with a passage number lower than 26 were used in this study. The BBMSCs were expanded in DMEM (Invitrogen) supplemented with 10% FBS (Invitrogen) and 100 units/ml penicillin-streptomycin (PS, Invitrogen). Cells were plated on hydrogels with different surface densities of N-Cad-Fc, and further incubated in DMEM supplemented with 10 % FBS and 100 units/ml PS at 37 $^{o}$C for 12 hrs. The cell number was kept at $1.5x10^{3}$ cells/cm$^{2}$. For control experiments without calcium, which is required for cadherin activity, cells were cultured on hydrogels for 12 hrs, and the medium was replaced with calcium-free DMEM supplemented with 0.5 mM of ethylenediaminetetraacetic acid (EDTA).

*2.3.1.9 Quantification of cell surface expression levels of N-Cadherin*

A monoclonal rat antibody against the N-cadherin ectodomains, anti-N-Cad was used to label cadherin-expressing cells. BBMSCs were incubated with the anti-N-Cad for 12 hrs. Then, the cells were incubated with the secondary antibody, fluorescein-isothiocyanate (FITC)-conjugated anti-rat IgG (whole molecule, Sigma-Aldrich). The antibody labeling was conducted in phosphate buffered saline (PBS) containing 1 w/v% bovine serum albumin (BSA) at pH 7.4. The fluorescence intensities of labeled BMSCs were measured with an LSR II flow cytometer (BD Biosciences). The calibration curve for the fluorescence intensity was generated with calibrated FITC-labeled standard beads (Bangs Lab).

*2.3.1.10 Immunofluorescence imaging of BBMSCs*

After 12 hrs of culture on the hydrogels, cells were fixed with 4% (w/v) paraformaldehyde in PBS for 30 min at room temperature. Then, cells were washed twice with PBS for 5 min each time, then permeabilized with 0.5% Triton-X 100 for 10 min, and again washed twice with PBS. Permeabilized cells were blocked with 1w/v% bovine serum albumin solution (Sigma) and 0.1% sodium azide (Fisher) in PBS for 1 hr and then washed twice with PBS. Finally, cells were sequentially incubated with 50 ng/ml phalloidin-FITC solution (Invitrogen) for 1 hr at room temperature, and 100 ng/ml DAPI solution (Invitrogen) for 2 min. DIC (Differential Interference Contrast) and fluorescence images were acquired with 40x and 63x oil objectives in the laser-scanning confocal microscope (LSM700, Zeiss).

*2.3.1.11 Isolation of cortical neurons*

All procedures involving animals were reviewed and approved by the Institutional Animal Care and Use Committee at the University of Illinois Urbana-Champaign in accordance with the guidelines of the U.S. National Institutes of Health (Hee Jung Chung's Protocols 10199, 12240). Embryonic cortical neurons were obtained from dissected cortices of rat embryos at 18-19 gestation day (E18-E19) as previously described [19]. Cortices were incubated with 3 mg/ml protease 23 (Sigma) in 1X slice dissection solution (82 mM $Na_2SO_4$, 30 mM $K_2SO_4$, 10 mM HEPES, 10 mM Glucose, 5 mM $MgCl_2$ and 0.001 % Phenol Red pH 7.4) for 10 minutes at 37 $^{o}$C. The cortices were then washed with plating medium (10 % Fetal Bovine Serum (FBS), 20 % (w/v) glucose, 1% sodium pyruvate (100 mM), and 2 mM L-Glutamine in MEM mixed with Earle's BSS without L-glutamine), and dissociated in 3 mL of plating medium into single cells via repeated pipetting. The dissociated cells were plated on glass coverslips coated with poly-L-

lysine or N-Cad (N-Cad-Fc) at 6 x $10^3$ cells/$cm^2$. After 4 hrs, the medium was replaced with the maintenance medium (neural basal serum free media (invitrogen) containing B27 (invitrogen) extract, 2mM L-Glutamine and100 units/ml PS).

*2.3.1.12 Immunofluorescence imaging of neural networks*

At two weeks after plating, neurons were fixed with 4% paraformaldehyde for 30 minute, and rinsed with D-PBS three times. Following permeabilization with 0.3 % Triton-X in D-PBS for 10 min at room temperature, neurons were blocked with 5 % goat serum diluted in D-PBS overnight, and sequentially incubated with primary and secondary antibodies. The primary antibodies used were rabbit polyclonal antibodies against neuronal marker Microtubule-Associated Protein-2 (anti-MAP2, 1:1000, Sigma Aldrich) and mouse monoclonal antibodies against the glial marker Glial Fibrillary Acidic Protein (anti-GFA, 1:5000, BD Bioscience). Secondary antibodies used were Alexa Fluor 488 goat anti-mouse and Alexa Fluor 568 goat anti-rabbit antibodies [20]. Neurons were rinsed 3 times with PBS and incubated with 100 ng/ml DAPI solution for 3 minutes. The DIC and fluorescence images were acquired with laser-scanning confocal microscope (LSM700, Zeiss).

*2.3.1.13 Statistical Analysis*

All average data are presented as means ± SE. To determine significance, comparisons between groups were performed by one-way ANOVA followed by Tukey's Multiple Comparison Test ($p < 0.05$).

## 2.4 Results

### *2.4.1 Sequential, biological conjugation of N-Cad-Fc to a polyacrylamide hydrogel*

Addition of the mixture of PHMAA-g-PEGNHS with Fc-antibody into a pre-gel solution consisting of acrylamide, bis-acrylamide, initiator, and TEMED resulted in a hydrogel chemically coupled with Fc-antibody (Fig. 2.4A, 2.4B, Fig. 2.2 & 2.3). Further incubation of the hydrogel with media dissolved with N-Cad-Fc led to immobilization of N-Cad-Fc to the gel surface, as confirmed with FITC-labeled N-Cad-Fc (Fig. 2.5). The fluorescent N-Cad-Fc was localized exclusively on the gel surface. According to the previous studies, the mean pore diameter of the gel used in this study is approximately 10 nm. The hydrodynamic radius of N-Cad-Fc has not been determined, but the linear dimensions of the ectodomains with the Fc tag are ~30 nm, and the cross sectional area of each of the two ectodomains in the Fc-tagged dimers is ~5 $nm^2$. Therefore, we suggest that N-Cad-Fc minimally diffused into the gel interior [21]. The surface density of N-Cad-Fc, quantified from the measured fluorescence intensity of the gel, was proportional to the concentration of N-Cad-Fc in the medium. Given the molecular weight of N-Cadherin as 135 kDa, the actual molecular density of N-Cad-Fc was calculated. This density was 3.6 times larger at 79 $\mu g/mm^2$ (i.e., $5.8x10^{-10}$ $mol/mm^2$) compared to 22 $\mu g/mm^2$ (i.e, $1.6x10^{-10}$ $mol/mm^2$). Little N-Cad-Fc bound to the gel, when Fc-antibody was omitted. In addition, little N-Cad-Fc bound to a hydrogel prepared by mixing gel-forming polymers and Fc-antibody without PHMAA-g-PEGNHS (white bar in Fig. 2.5).

*2.4.2 BMSC adhesion modulated by biochemically coupled N-Cad-Fc on the hydrogel*

The surface density of N-Cad-Fc on the hydrogels modulated BMSC adhesion, as demonstrated by the cell spreading area, circularity, and the nuclear aspect ratio (Fig. 2.7). BBMSCs express N-Cad at a density of 5 N-Cad molecules per $\mu m^2$, as confirmed by quantitative flow cytometry. Few cells spread on the gel with an N-Cad surface density at 0 and 22 $\mu g/mm^2$ (Fig. 2.6A-I and 2.6A-II). Increasing the N-Cad-Fc density from 22 to 79 $\mu g/mm^2$ increased the cell spreading area more than three-fold (Fig. 2.6A-II, 2.6A-III, and 2.7B), and cells were more elongated, based on the measured circularity. Such decrease in circularity was more significant when N-Cad-Fc density was increased from 22 to 79 $\mu g/mm^2$ (Fig. 2.7C). Accordingly, cell nuclei became more elongated on hydrogels with higher N-Cad-Fc densities; namely, the nuclear aspect ratio increased from 1.3 to 1.6 when N-Cad increased from 22 to 79 $\mu g/ mm^2$ (Fig. 2.7D). In addition, cells adhered to gels with an N-Cad surface density of 79 $\mu g/mm^2$ exhibited more stretched intracellular actin fibers than on gels with lower N-Cad-Fc densities (Fig. 2.6A-III). In contrast, few cells adhered to hydrogels prepared without either Fc-antibody or PHMAA-g-PEGNHS (Results not shown). The cells that did settle on the gels remained mostly rounded. In addition, we tested whether CHO cells free of N-Cad on their surfaces spread on the N-Cad-Fc-conjugated glass. As expected, a minimal number of CHO cells spread on the surface, independent of the surface density of N-Cad-Fc (Fig. 2.8).

To examine whether the cell adhesion to the hydrogel was cadherin-specific, several control experiments were performed. Competition with soluble N-Cad-Fc at 100 µg/ml reduced cell adhesion on the gel (Fig. 2.9). Alternatively, we removed calcium, which is required for cadherin activity (Fig. 2.10A). Initially, cells were fully extended on the gel when incubated in

calcium-supplemented medium. However, replacing the medium with the calcium-depleted DMEM containing EDTA caused a decrease in the cell spreading area with increasing incubation time in the calcium-depleted media. Within three hours, more than half of cells were detached from the gel (Fig. 2.11).

### *2.4.3 Directly coupled N-Cad minimally stimulates cell adhesion to hydrogels*

The importance of the linking method on N-Cad-Fc activity was demonstrated with gels in which N-Cad-Fc was directly coupled to PHMAA-g-PEGNHS (Fig. 2.12). The chemical conjugation also allowed immobilization of N-Cad-Fc to the gels, as confirmed with FITC-labeled N-Cad-Fc (Table 2.1). However, few cells adhered to the hydrogel, compared to gels with biologically conjugated N-Cad-Fc. In addition, cells minimally spread on the gel, which was similar to cells adhered to the gel free of N-Cad-Fc (Fig. 2.13 and 2.14).

### *2.4.4 N-Cad-Fc tailors the neural network phenotype in vitro*

Subsequent studies demonstrated that N-Cad-Fc biologically coupled to glass substrates can modulate cortical neuron and glial cell adhesion to the substrate and further neurite outgrowth. It is well known that both neurons and glia express endogenous N-Cad [22,23]. The sequential treatment of the glass with 3-(trimethoxysilyl propyl)methacrylate and ultraviolet (UV) light-induced surface reaction of the mixture of Fc-antibody and PHMAA-g-PEGNHS resulted in a glass substrate with immobilized Fc-antibody. The subsequent exposure of modified glass substrate with N-Cad-Fc led to the N-Cad-Fc conjugated glass substrate, as confirmed by fluorescence (results not shown). Separately, chemical reaction between N-Cad-Fc and PHMAA-g-PEGNHS on the silane-treated glass also resulted in immobilization of N-Cad-Fc to the glass.

Interestingly, in confocal images, neurons identified with microtubule-associated protein (MAP2) adhered to the N-Cad-Fc conjugated substrate more extensively than glial cells, which were identified with glial fibrillary acidic protein (GFAP) (Fig. 2.15). In contrast, more glial cells were adhered to the poly-L-lysine (PLL)-coated glass substrate (Fig. 2.15). Additionally, the glial cells spread more extensively on the PLL-coated glass substrate, while the neuron cells were extended more on the N-Cad-Fc conjugated substrate (Fig. 2.16A). The ratio of glia to neurons on PLL-coated glass was approximately 3:1, while that on the glass biologically conjugated with N-Cad-Fc using Fc-antibody was 1:1 (Fig. 2.16B). In addition, the substrate biochemically conjugated with N-Cad-Fc stimulated neurite outgrowth more significantly than the substrate chemically conjugated with N-Cad-Fc (Fig.2.17).

## 2.5 Discussion

This study demonstrates a new method to tether recombinant N-Cad-Fc to hydrogels, and the capacity of the thus modified hydrogels to regulate cell adhesion and neural network formation, by tuning the surface density of N-Cad-Fc. Moreover, biochemical coupling resulted in more potent N-Cad-Fc activity than direct chemical attachment to the surface. The N-Cad-Fc was coupled to a polyacrylamide hydrogel surface by first chemically conjugating Fc-antibody to the gel using PHMAA-g-PEGNHS and secondly incubating the gel surface with N-Cad-Fc. The resulting hydrogel enabled us to modulate BMSC adhesion to the gel surface by varying the N-Cad-Fc surface density. Several control experiments confirmed that cell adhesion to N-Cad-Fc modified substrates was cadherin specific. Finally, the results demonstrate that biochemically bound N-Cad-Fc on glass promoted greater attachment of neurons than glia, when dissociated cortical neurons were plated.

Two likely explanations for the increased biological activity of antibody-immobilized N-cad-Fc is the avoidance of chemically modifying functionally sensitive sites on the proteins and the proper orientation of the ectodomain critical for binding to cell surface cadherin [24]. Cadherins consist of an extracellular domain, a transmembrane domain and a cytoplasmic domain [24]. The recombinant N-Cad used in this study has a Fc-tag at the C terminal of the five extracellular domains (EC5), thus leaving the EC1 domain [25] to be available for association with cellular N-Cad on the gel surface. The extent of cell spreading on surface density of N-Cad-Fc on the gel is therefore attributed to the change in the number of cadherin bonds formed between recombinant N-Cad-Fc and cell surface N-Cad [8,26]. By contrast, we suggest that chemical conjugation of the N-Cad-Fc directly to the gel fails to expose the extracellular domain of N-Cad-Fc to cellular N-Cad, thus resulting in poor cell adhesion and limited cell spreading to the gel.

Two controls confirmed the N-Cad specificity of cell adhesion on the modified hydrogels. Control, competitive binding experiments with excess, free recombinant N-Cad-Fc confirmed that the cell adhesion and spreading modulated by surface density of N-Cad-Fc was due to specific binding between immobilized, recombinant N-Cad-Fc and cellular N-Cad. Additionally, the disruption of cell adhesion by calcium depletion, which inactivates cadherins, further verifies that the cell adhesion is N-Cad-specific.

In addition, biochemically tethering N-Cad-Fc to a glass substrate preferentially promoted neural cell adhesion relative to glia [24], N-Cadherin is essential for shaping brain structure and for assembling functional neural circuits [27]. N-Cad is also important in neural network formation and axon guidance, because the intercellular cadherin association activates

the growth cone motility and neurite outgrowth [25,28]. It is known that neuron cells abundantly express N-Cad, while glial cells express limited number of N-Cad [27]. We suggest that biochemically coupling N-Cad-Fc to the glass surface results in less cadherin inactivation and a more advantageous presentation of the binding domain to N-Cadherin on neuronal cell surfaces and subsequent cell adhesion. It is well known that intercellular N-Cad association is essential for synaptic formation [28]. These data suggest that N-cadherin adhesion may also promote neural adhesion and growth.

## 2.6 Conclusion

Overall, this study presents a novel cell culture platform capable of recapitulating intercellular adhesion signals without the need to control the degree of cell-cell contacts. The platform was prepared by tethering the recombinant extracellular domains of N-Cad-Fc to a hydrogel using a PHMAA protein linker reacted with Fc-antibody. We suggest that such biochemical tethering preserves protein function, exposes ectodomains to cellular N-Cad, and thus enables the control of the cell adhesion by varying the surface density of N-Cad-Fc. This results in better outcomes than direct chemical conjugation of N-Cad-Fc to the gel surface. Additionally, biochemcially tethering N-Cad-Fc to glass surfaces resulted in preferential neuron adhesion and subsequent neural network formation on the substrate. This N-Cad-Fc tethering could thus be readily extended to modify a variety of hydrogel, glass, and plastic substrates with various cadherin family members, in order to systematically study diverse cellular activities modulated by cell-cell adhesion. In addition, the biological tethering of N-Cad would be useful to modifying various biomaterial systems used for cell therapies and tissue regeneration therapies.

*Acknowledgments*

This work was supported by National Science Foundation (CAREER: DMR-0847253 to H.K., STC-EBICS Grant CBET-0939511 to H.K, NSF CMMI 10-29871 to L.D, NSF Graduate Fellowship to J.V.), and The University of Illinois' Research Board. (Supporting Information is available online from Wiley InterScience or from the author).

## 2.7 Figures and tables

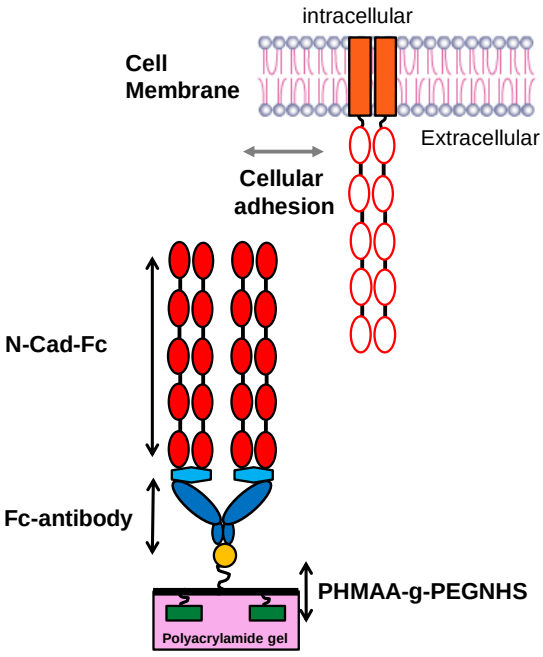


**Figure 2.1.** Schematic describing a strategy to conjugate N-Cad-Fc to a polyacrylamide hydrogel using PHEA-g-PEGNHS reacted with Fc-antibody. The PHEA-g-PEGNHS linked with Fc-antibody was first immobilized on the polyacrylamide gel, followed by incubation with N-Cad-Fc.

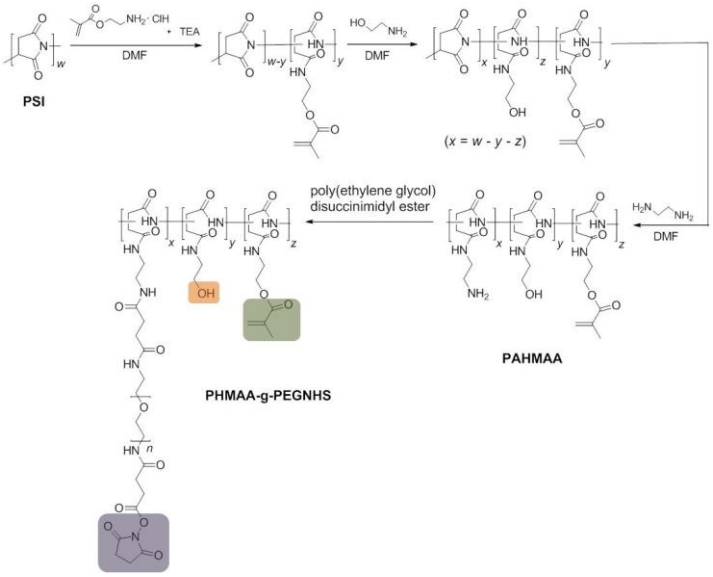


**Figure 2.2.** Chemical synthesis of PHMAA-g-PEGNHS

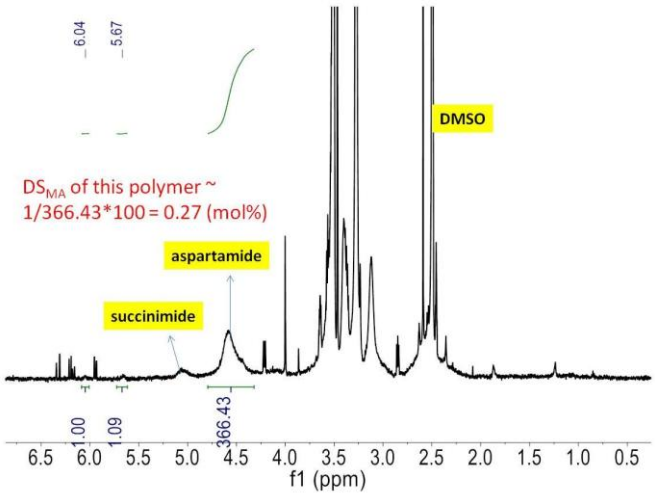


**Figure 2.3** $^{1}$H NMR of PHMAA-g- PEGNHS

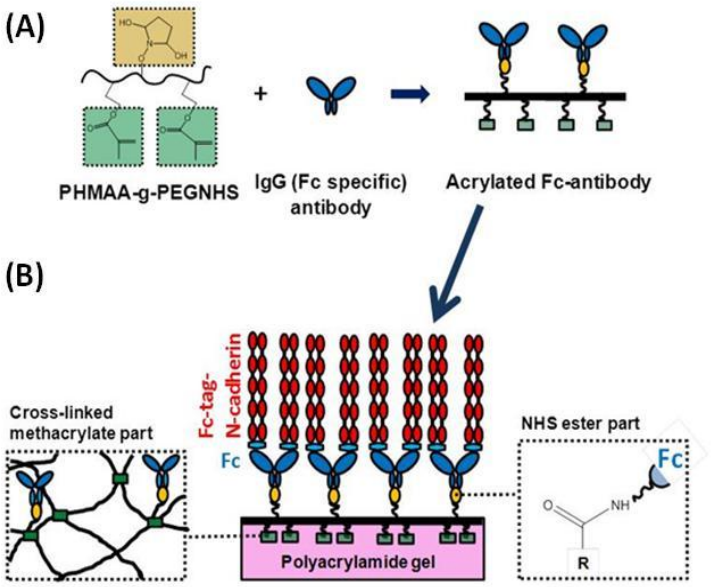


**Figure 2.4.** Biological conjugation of N-Cad-Fc to a hydrogel using PHMAA-g-PEGNHS and Fc-antibody. (A) A scheme for reaction between PHMAA-g-PEGNHS and Fc-antibody. (B) Schematic describing a sequential immobilization of N-Cad-Fc to a polyacrylamide hydrogel using a reacted product of PHMAA-g-PEGNHS and Fc-antibody.

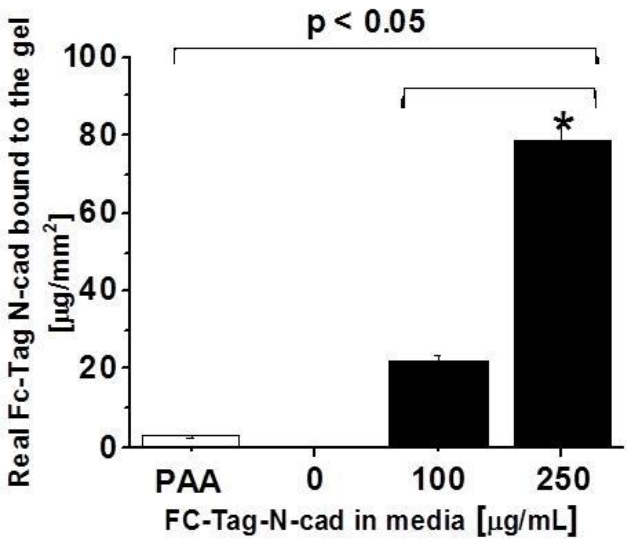


**Figure 2.5** Effects of the concentration of N-Cad-Fc in the incubation media on surface density of N-Cad-Fc linked to the gel surface. The last three bars represent conditions to link N-Cad-Fc using PHMAA-g-PEGNHS and Fc-antibody. The first, white bar (PAA) represents a condition to incubate a hydrogel prepared without PHMAA-g-PEGNHS in medium containing 100 μg/ml N-Cad-Fc. Four images per each sample were analyzed. The difference in values between conditions is statistically significant (*$p < 0.05$).

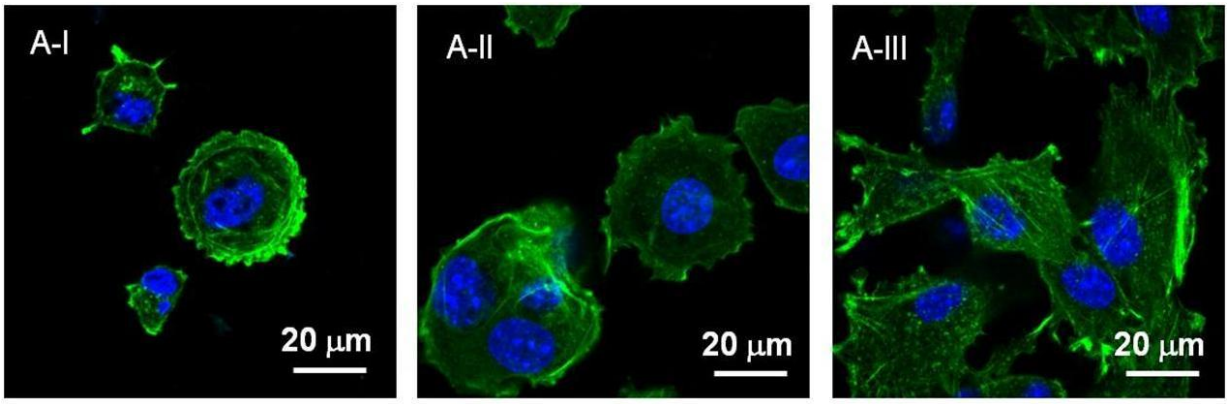


**Figure 2.6** Fluorescent images of BBMSCs plated on gels with varied N-Cad-Fc densities of 0 (A-I), 22 μg/mm$^2$ (A-II), and 79 mm$^2$ (A-III). Green and blue colors in these images represent cellular actin fibers and nucleus, respectively.

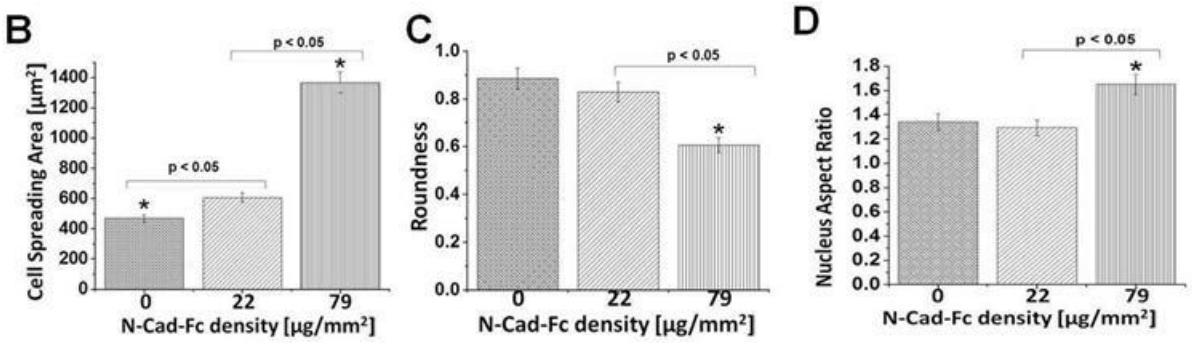


**Figure 2.7** Statistical analysis of cells in figure 2.6. (B) Effects of N-Cad-Fc density on spreading area of cells. (C) Effects of N-Cad-Fc density on roundness of cells. (D) Effects of N-Cad density on aspect ratio of the cells. The values and error bars in plots (B)-(D) represent average values and standard deviation of the four images (1 mm x 1 mm). At least 120 cells were analyzed per image. * represents statistical significance between conditions.

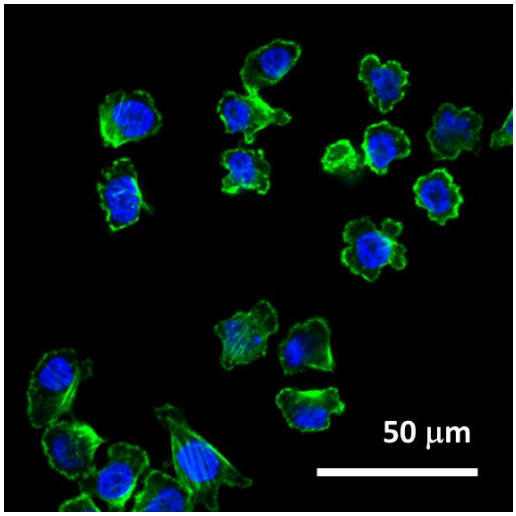


**Figure 2.8.** Fluorescent image of CHO cells grown on the N-Cad-Fc-conjugated glass.

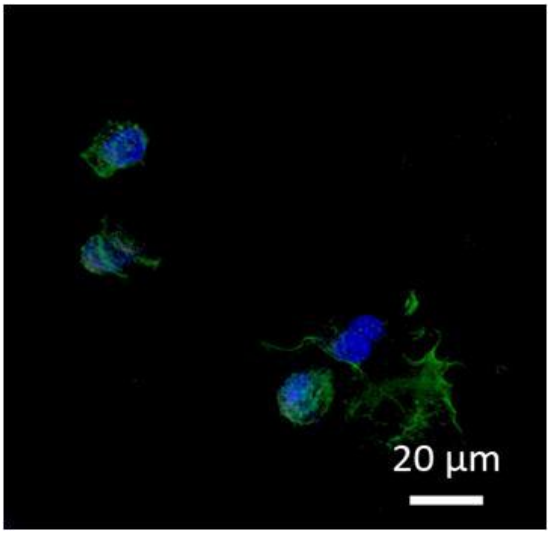


**Figure 2.9.** Fluorescent image of BBMSCs cells cultured in the media supplemented with free 100 µg/ml of N-Cad-Fc. The gel was modified to present N-Cad at surface density of 22 µg/mm$^2$ using PHMAA-g-PEGNHS and Fc-antibody. In the image, green and blue colors represent cellular actin fibers and nucleus, respectively.

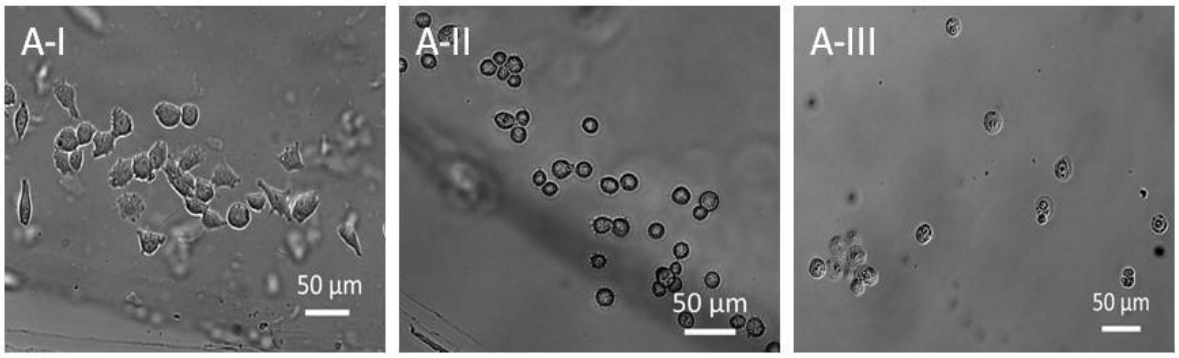


**Figure 2.10** Effects of calcium depletion in cell culture media on cellular adhesion to the hydrogel coupled with N-Cad-Fc. (A-I) BBMSCs cultured in the calcium supplemented normal media. (A-II) BBMSCs incubated in calcium-depleted media for one hour. (A-III) BBMSCs incubated in calcium-depleted media for three hours.

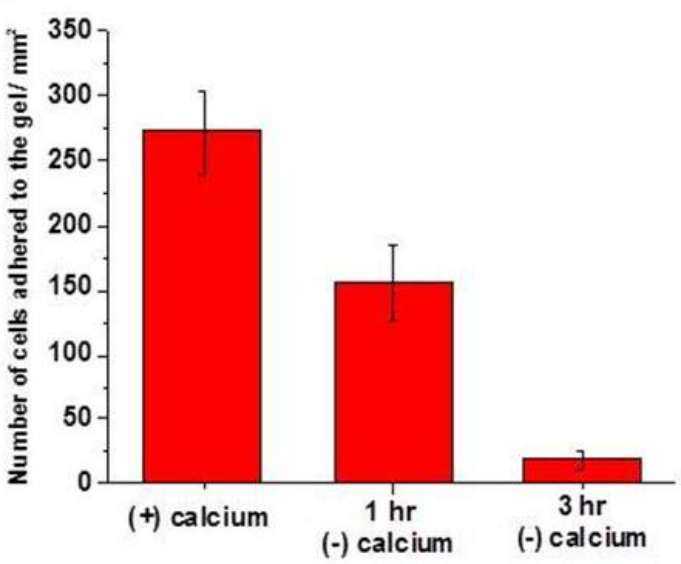


**Figure 2.11.** Quantitative analysis of the number of BBMSCs adhered to the gel during incubation in the calcium-depleted media in figure 2.8. Four images (300 µm x 200 µm) per condition were analyzed.

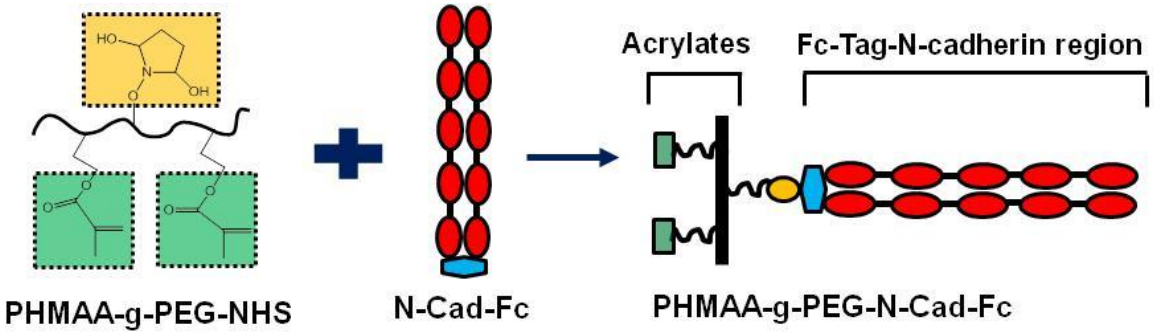


**Figure 2.12.** Schematic describing the chemical conjugation of N-Cad-Fc to a hydrogel via PHMAA-g-PEGNHS.

| N-Cad-Fc Conjugation method | Mass density of N-Cad-Fc ($\mu g/mm^2$) | Molecular density of N-Cad-Fc ($x10^{-10}/mm^2$) |
|---|---|---|
| **Chemical conjugation** | 92 | 6.8 |
| **Biological conjugation** | 0 | 0 |
| | 22 | 1.6 |
| | 79 | 5.8 |

**Table 2.1.** Mass and molecular density of N-Cad-Fc conjugated to a hydrogel.

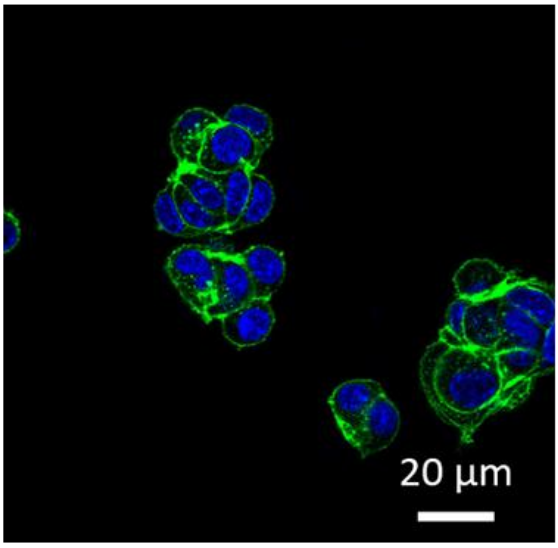


**Figure 2.13** Fluorescent images of BBMSCs cultured on gels with chemically coupled N-Cad-Fc at a surface density of 92 $\mu g/mm^2$. In the image, the green and blue coloration represents actin fibers and nucleus, respectively.

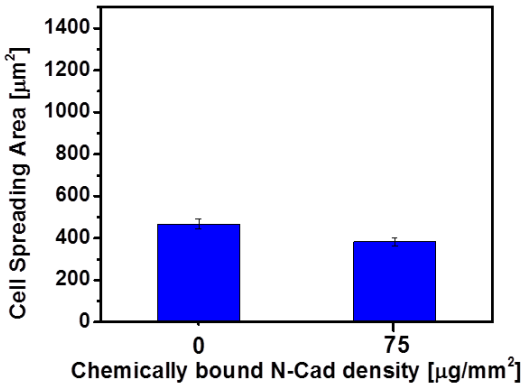


**Figure 2.14** Effects of direct, chemical conjugation of N-Cad-Fc to PHMAA-g-PEGNHS on BBMSCs' adhesion to a hydrogel. Effects of N-Cad-Fc chemically bound to the gel on cellular spreading area. Four images (1 mm x 1 mm) per condition were analyzed. At least 120 cells were analyzed per image.

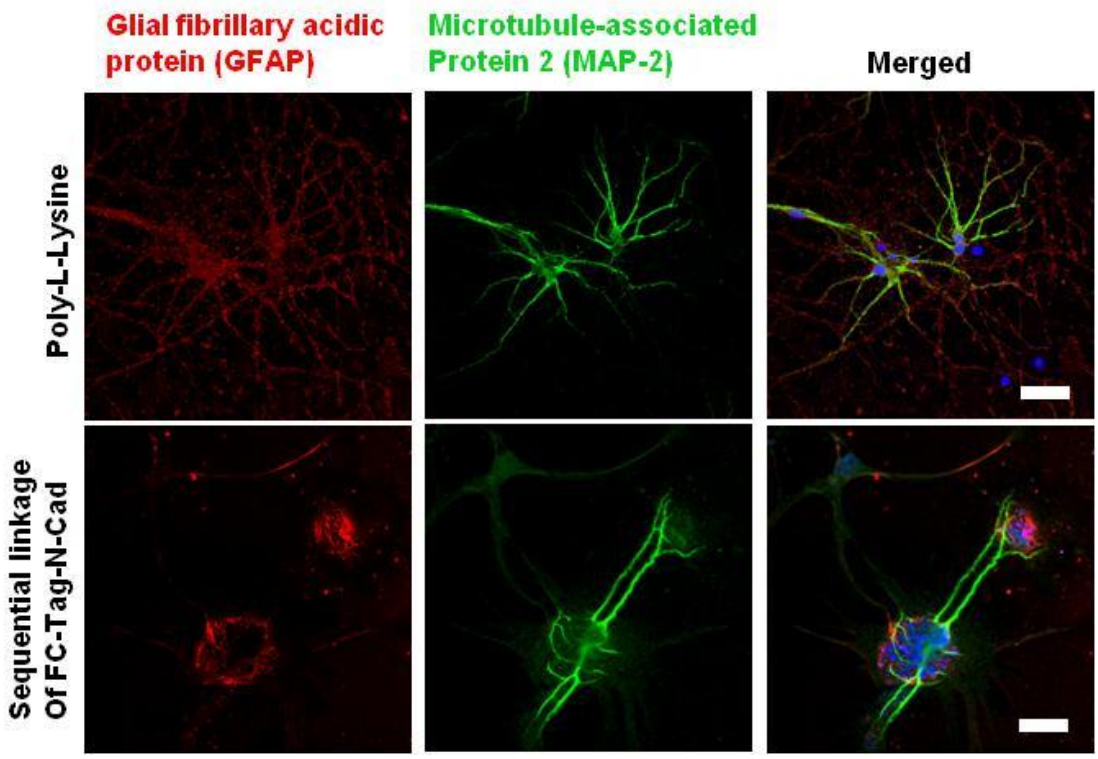


**Figure 2.15.** Fluorescent images of E19 cortical neurons cultured on the glass surface modified with poly-L-Lysine and N-Cad-Fc. Glial cells were identified with GFAP (shown in red), cortical neurons were identified with MAP-2 (green), and cellular nuclei were stained with DAPI (blue). (B) Analysis of the spreading area of glia and neurons.

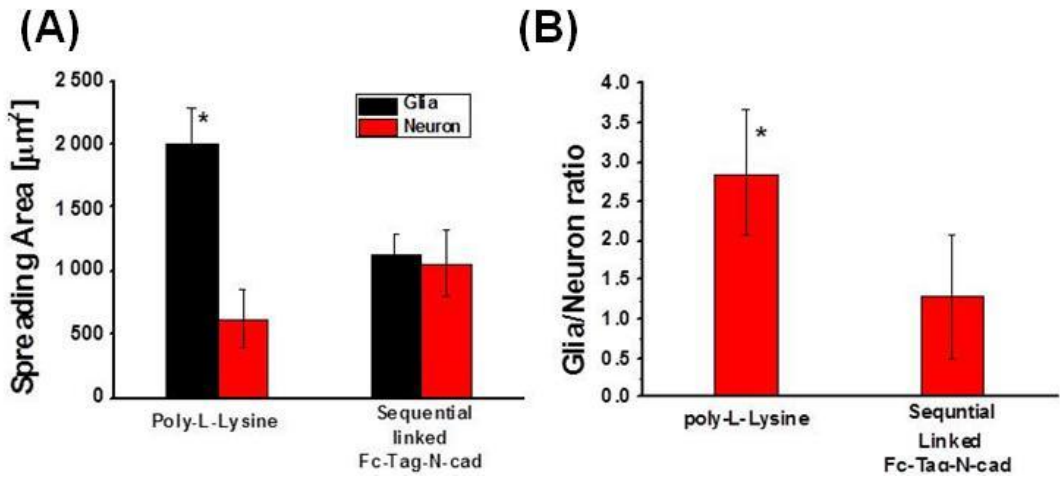


**Figure 2.16** Analysis of the ratio between glia and neuron. The values and error bars in plots (A) and (B) represent average values and standard deviation of the four images (500 µm x 500 µm). At least 120 cells were analyzed per image. N-Cad-Fc was conjugated to the glass using Fc-antibody.

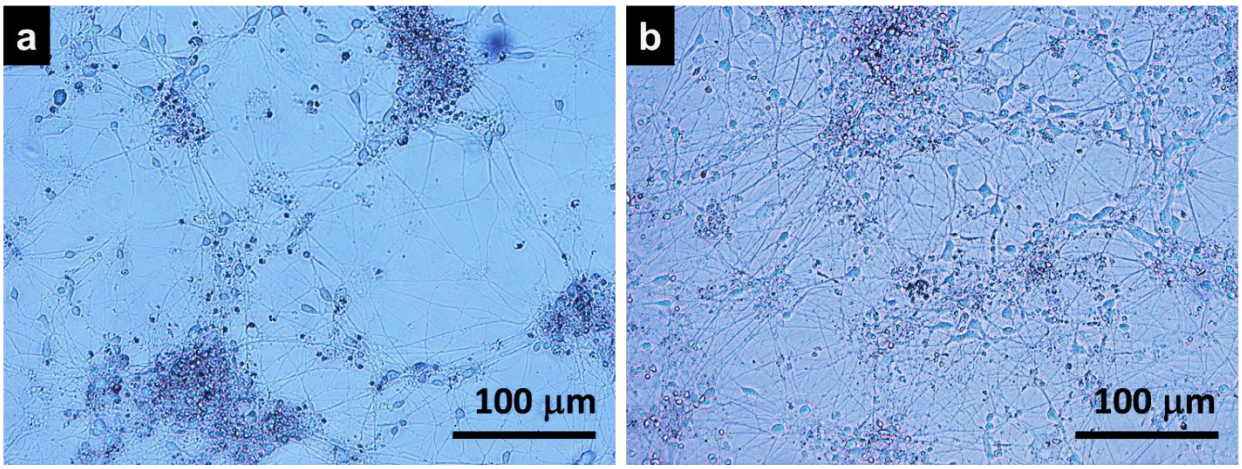


**Figure 2.17.** Optical images of neural network formed on the glass surface bound with N-Cad-Fc either by (a) chemical conjugation or (b) biological conjugation using Fc-antibody. Images were captured 6 days after seeding cells on the glass substrate.

## 2.8 References


**1.** Adamas, J. C. and Watt, F. M. Regulation of development and differentiation by extracellular matrix. *Development.* 1993; 117**:**1183-1198.

**2.** Trappmann, B., Gautrot, J.E., Connelly, J.T., Strange, D.G.T., Li, Y., Oyen, M.L., Cohen, S.. Boehm, H., Li, B., Vogel, V., Spatz, J.P., Watt, F. M., and Huck, W.T.S. Extracellular-matrix tethering regulates stem-cell fate. *Nat. Mater.* 2012**;** 11: 642-649.

**3.** Kohara, H. and Tabata, Y. Review: Tissue engineering technology to enhance cell recruitment for regeneration therapy. *J. Med. Bio. Eng.* 2010**;** 30: 267-276.

**4.** Zhang, R. and Ma, P. X. Synthetic nano-fibrillar extracellular matrices with predesigned macroporous architectures. *J. Biomedical Materials Research.* 2000; 52**:**430-438.

**5.** Halbleib, J. M. and Nelson, W.J. Cadherin in development: cell adhesion, sorting, and tissue morphogenesis. *Genes and development.* 2006; 20**:** 3199-3214.

**6.** Kim, N, Koh, E., Chen, X., and Gumbiner, B.M.E-cadherin mediates contact inhibition of proliferation through Hippo signaling-pathway components. *Pro. Natl. Acad. Sci*. 2011; 108**:** 11930-11935.

**7.** Charrasse, S., Meriane, M., Comunale, F., Blangy, A., and Gauthier-Rouvière, C. J. N-cadherin-dependent cell-cell contact regulates Rho GTPases and β-catenin localization in mouse C2C12 myoblasts. *J. Cell Biol*. 2002; 158**:** 953-965.

**8.** Derycke, L. D. M. and Bracke, M.E. N-cadherin in the spotlight of cell-cell adhesion, differentiation, embryogenesis, invasion and signaling. *Int. J. Dev. Biol*. 2004; 48**:** 463-476.

**9.** Collazos-Castro, J.E.; Hernández-Labrado, G.R.; Polo, J.L.; Garía-Rama, C. N-cadherin- and L1-functionalised conducting polymers for synthetic stimulation and guidance of neural cell growth. *Biomaterials.* 2013; 34: 3603-3617.

**10.** Yue, X.S. Murakami, Y., Tamai, T., Nagaoka, M., Cho, C.S., Ito, Y., and Akaike, T. A fusion protein N-cadherin-Fc as an artificial extracellular matrix surface for maintenance of stem cell features. *Biomaterials.* 2010; 31: 5287-5296.

**11.** Underhill, G.H., Galie, P., Chen, C.S., and Bhatia, S.N. Bioengineering methods for analysis of cells in vitro.*Annu. Rev. Cell Dev. Biol.* 2012; 28: 385-410.

**12.** Cha, C., Jeong, J.H., Tang, X., Zill, A.T., Prakash, Y.S., Zimmerman, S.C., Saif, T.A., and Kong, H. Top-down synthesis of versatile polyaspartamide linkers for single-step protein conjugation to materials *Bioconjugate Chem.* 2011; 22: 2377-2382.

**13.** Ouyang, M., Lu, S., Kim, T., Chen, C.E., Seong, J., Leckband, D.E., Wang, F., Reynolds, A.B., Schwartz M.A., and Wang, Y. N-cadherin regulates spatially polarized signals through distinct p120ctn and β-catenin-dependent signaling pathways *Nat. Commun.* 2013**;** 4: 1-12.

**14.** Kang, H.S., Yang, S.R., Kim, J.D., Han, S.H., and Chang, I.-S. Effects of grafted alkyl groups on aggregation behavior of amphiphilic poly(aspartic acid). *Langmuir.* 2001**;** 17: 7501-7506.

**15.** Lambert, M., Padilla, F.,and Mege, R-M. Immobilized dimmers of N-cadherin-Fc chimera mimic cadherin-mediated cell contact formation: contribution of both outside-in and inside-out signals. *J. Cell Sci.* 2000**;** 113: 2207-2219.

**16.** Chappuis-Flament, S., Wong, E., Hicks, L.D., Kay, C.M., and Gumbiner, B.M. Multiple cadherin extracellular repeats mediate homophilic binding and adhesion. *J. Cell Biol.* 2001; 154: 231-243.

**17.** Sivasankar, S., Brieher, W., Lavrik, N., Gumbiner, B., and Leckband, D. Direct molecular force measurements of multiple adhesive interactions between cadherin ectodomains. *Proc. Natl. Acad. Sci.* 1999; 96: 11820-11824.

**18.** Tse, J.R., and Engler, A.J. Preparation of hydrogel substrates with tunable mechanical properties *Curr. Protoc. Cell Biol.* 2010; Chapter 10, Unit 10 16, doi:10.1002/0471143030.cb1016s47.

**19.** Lee, H.K., Kameyama, K., Huganir, R.L., and Bear, M.F. NMDA induces long-term synaptic depression and dephosphorylation of GluR1 subunit of AMPA receptors in hippocampus *Neuron* 1998; 21, 1151-1162.

**20.** Intracellular calcium assays in dissociated primary cortical neurons: Doering, L. C., Editor. Springer protocols handbooks. 4th ed. McMaster University, Hamilton, ON, Canada. *Humana Press*; 2010: 125-136.

**21.** Holmes, D.L., and Stellwagen, N.C. Estimation of polyacrylamide gel pore size from fergwson plots of linear DNA fragments11. Comparison of gels with different crosslinker concentration, added agarose and added linear polyacrylamide. *Electrophoresis* 1991**;** 12: 612-619.

**22.** Wanner, I.B., Guerra, N.K., Mahoney, J., Kumar, A., and Wood, P.M. Role of N-cadherin in Schwann cell precursors of growing nerves. *Glia.* 2006; 54: 439.

**23.** Jossin, Y.; Cooper, J.A. Reelin, Rap1 and N-cadherin orient the migration of multipolar neurons in the developing neocortex.*Nat. Neurosci.* 2011; 14: 697-703.

**24.** Leckband, D. and Prakasam, A. Mechanism and dynamics of cadherin adhesion. *Annu. Rev. Biomed. Eng*. 2006;8: 259-287.

**25.** Chappuis-Flament, S., Wong, E., Hicks, L.D., Kay, C.M., and Gumbiner, B.M. Multiple cadherin extracellular repeats mediate homophilic binding and adhesion.*J. Cell Biol.* 2001**;** 154: 231-243.

**26.** Hansen, S.M., and Berezin, V. Signaling mechanisms of neurite outgrowth induced by cell adhesion molecules NCAM and N-Cadherin Bock, E. *Cell Mol. Life Sci.* 2008; 65: 3809-3821.

**27.** Suzuki, S.C., and Takeichi, M. Cadherins in neuronal morphogenesis and function. *Dev. growth Differ.* 2008; 50: S119-S130.

**28.** Ranscht, B. Cadherins: molecular codes for axons guidance and synapse formation. *Int. J. Dev. Neurosci.* 2000; 18: 643-651.

# Chapter 3: Soluble N-Cadherin induced BMSCs spheroids secretion of VEGF and blood vessel formation in chicken embryos

## 3.1 Abstract

Bone marrow-derived mesechymal stem cells (BMSCs) are a potentially invaluable tool for treating vascular diseases, because they are able to secrete different factors that decrease the inflammatory response as well as able to secrete angiongenic factors such as VEGF which induces angiogenesis. N-Cadherin (N-Cad) is a key player in the signal transduction for endothelia-mesenchymal transition (EMT) and it is present in BMSCs as well as in endothelial cells (ECs). In BMSCs it is mostly found in adhesion junctions (AJ) while in ECs plays the role of signal transduction and vascular endothelia cadherin (VE-Cad) is found in AJ of ECs. Here, we were able to induce BMSC spheroid formation with N-Cad-Fc and to further induce secretion of VEGF by the spheroids. When these spheroids were implanted in the chicken choroiallantonic membrane (CAM), they were able to induce new blood vessel formation in chicken embryos. Also, the permeability of inflamed ECs was decreased when co-cultured with BMSC induce N-Cad-Fc We also found a correlation with decreased N-Cad mRNA expression with secretion of VEGF by BMSCs.

## 3.2 Introduction

Stem cell differentiation and cell function are highly regulated by the intrinsic and extrinsic signals produced in their niche [1]. Cadherins are important cell adhesion molecules that are involved in organized cell division, cell arrangement during development, regulating apoptosis, maintaining tissue morphology, cell differentiation and establishing tissue polarity [2]. Cadherins are a large superfamily of calcium dependent cell adhesion proteins [2]. From the classical cadherins N-cadherin (N-Cad) and E-cadherin (E-Cad) are involved in epithelial - mesenchymal transition (EMT) [3]. The EMT is vital for development and involves the down regulation of E-cadherin and up-regulation of N-cadherin [3].

Classical cadherins form membrane-spanning complexes that mediate intercellular binding via their extracellular domains and associate with actin cytoskeleton via the intracellular region [4]. Classical cadherins are a transmembrane protein with an extracellular region which provides the adhesive function [5] and a cytoplasmic segment which can be divided into two major domains: the juxtramembrane domain (JMD) that provides a specific binding site for p120 catenin and p120 related proteins, and the catenin-binding domain (CBD) which specifically binds β-catenin and plakoglobin [4]. This interaction is critical for regulating the stability of cadherin-catenin cell-cell adhesion complexes at the cell surface, as down regulation of p120 results in internalization of cadherins [4]. Changes in the rate of cadherin synthesis or adhesion could impact the expression of genes co-regulated by β-catenin and p120catenin [4]. Therefore, endocytosis, degradation, and recycling of cadherins are crucial for dynamic regulation of adherens junctions and control of intracellular machinery [4].

Mesenchymal stem cells (MCS) are capable of self-renewal and multi-lineage differentiation, and they can be isolated from different tissues such as bone marrow [1]. Therefore, they are considered as a potential source for regenerative medicine [1]. The ability of bone marrow-derived MSCs (BMSCs) to migrate to the area of injury has encouraged investigation of BMSCs as therapeutic tools [6]. For example, systemically administered BMSCs have been shown to improve recovery in animal models of stroke and myocardial infarction [6]. The role of BMSC has stimulated revascularization of ischemic tissues [7]. In all cases, BMSC either differentiates into the type of cells at the site of injury or induces vascularisation and cell differentiation due to their secreted factors [8,11].

Three-dimensional (3-D) cultured methods have shown to provide a cellular environment more consistent with the in vivo niche, thereby allowing the cells to assume their native morphology and biological function [9]. Therefore, we hypothesized that by using the hanging drop method (Fig. 3.1) to culture BMSCs we would be able to induce BMSCs to form spheroids without an exogenous biomaterials which allows the study of their intrinsic and extrinsic signals. Furthermore, adding free recombinant extracellular domains of neural cadherin with a C-terminal immunoglobulin Fc domain (N-Cad-Fc) to the BMSC spheroid culture medium could alter the lifetime of cell surface cadherin receptors, thereby causing the cells to activate the gene expression and secretion of VEGF. Secretion of VEGF by BMSC under basal conditions and the enhancement of VEGF secretion into the supernatant by hypoxia had previously been reported [10]. Therefore, VEGF production by BMSC may be a crucial factor responsible for an angiogenic potential of BMSC [11]. Implantation of spheroids cultured with N-Cad-Fc can induce new blood vessel formation in chicken embryos.

## 3.3 Experimental

### *3.3.1 Materials*

#### *3.3.1.1 Bone marrow stromal cell (BMSC) culture*

Mouse bone marrow-derived stromal cells (BMSCs, D1 cells, ATCC) with a passage number lower than 26 were used in this study. The BMSCs were cultured in Dulbecco's modified Eagle' Medium (DMEM; Invitrogen) supplemented with 10% fetal bovine serum (FBS; Invitrogen) and 100 units/ml penicillin-streptomycin (PS; Invitrogen). Cells were cultured in a tissue culture flask up to 70% confluence.

#### *3.3.1.2 Quantification of cellular cadherin expression levels*

A monoclonal rat antibody against the N-cadherin ectodomains, anti-N-Cad was used to label cadherin-expressing cells. BMSCs were incubated with the anti-N-Cad for 12 hrs. Then the cells were incubated with the secondary antibody, fluorescein-isothiocyanate (FITC)-conjugated anti-rat IgG (whole molecule, Sigma-Aldrich). The antibody labeling was conducted in phosphate buffered saline (PBS) containing 1 w/v% bovine serum albumin (BSA) at pH 7.4. The fluorescence intensities of labeled BMSCs were measured with an LSR II flow cytometer (BD Biosciences). The calibration curve for the fluorescence intensity was generated with calibrated FITC-labeled standard beads (Bangs Lab).

#### *3.3.1.3 Spheroid Formation*

Spheroids were generated by using the hanging drop method (Fig. 3.1) [12]. Thirty spheroids were used per condition and each spheroid was made by the aggregation of 30,000 BMSCs in 30µl of medium, spheroids were cultured for three days before harvesting them. Four

conditions were initially tested in which the medium would contain 10% of FBS or 1% for FBS and with and without 100µg/ml of Fc-Tag-N-Cadherin (N-Cad-Fc)(Fig 3.2).

*3.3.1.4 N_Cadherin Protein*

HEK293 cells previously engineered to express soluble recombinant canine chicken N-cadherin-Fc constructs (N-cad-Fc)[13] were cultured in Dulbecco's modified Eagle' Medium (DMEM; Invitrogen) supplemented with 10% fetal bovine serum (FBS; Invitrogen) and 0.4mg/ml G418 (Sigma, St Louis, MO) as a selection marker. The ckN-cad-FC construct was purified from the conditioned medium using Protein A affinity column (Bio-Rad) followed by gel filtration chromatography, as described [14]. Bead aggregation measurements confirmed the functionality of the N-cadherin [15].

*3.3.1.5 Collagen Gels*

Pure collagen gels were prepared by mixing pre-chilled bovine collagen type I solution (3.0 mg/mL, Advanced BioMatrix), DMEM medium with 10%FBS and either the BMSCs spheroids form in the presence or absence of Fc-Tag-N-Cadherin or single BMSCs cells with/out Fc-Tag-N-Cadherin, and reconstituting solution in a ratio of 8:4:1. The reconstituting solution was a mixture of 0.26 M of sodium bicarbonate (NaHCO3), 0.2 M 4-(2-hydroxyethyl)-1-piperazineethanesulfonic acid (HEPES), and 0.04 M of sodium hydroxide (NaOH). The mixture was subsequently incubated in 13mm mateck dish at 37$^{o}$C for 4h to form 3D collagen hydrogels with 13 mm diameter and approximately 1 mm thickness.

*3.3.1.6 VEGF Secretion Analysis*

The capture antibody was suitably diluted in PBS and then used to coat 96-well microplates at 50µl per well. The plates were incubated overnight at $4^{o}$ C. Free binding spaces were blocked with the appropriate reagent diluent and test samples and standards were applied at suitable concentrations. Then 100µl per well of samples or standards were added. After a 2 hr incubation, biotinylated detection antibody was added, followed by Streptavidin-HRP. The plate was washed before each successive step with 0.05% Tween 20 in PBS. Substrate solution (H2O2 and tetramethylbenzidine, DY994; R&D Systems, Inc.) was added and developed for 20 min at room temperature. The color development was terminated by the addition of 25µl of stop solution (2N H2SO4). The observance intensity was determined immediately using a microplate reader (Synergy HT, Bioteck) set at dual wavelengths of 450nm and 540nm. The 540nm reading was subtracted from the 450nm reading.

*3.3.1.7 In Vivo Implantation of spheroids/single cell-hydrogel constructs and analysis of images explants.*

The effects of the spheroids/single cell hydrogel constructs on angiogenesis were examined by implanting them onto chicken choroiallantonic membrane (CAM) according to a previously developed method [16]. Partially, fertilized chicken eggs (Hy-Line W-36) were obtained from the University of Illinois Poultry Farm. Following the initial incubation, a small window (1.0·1.0 cm) was created by removing a portion of the shell on top of each egg. After formation of BMSC spheroids (3 days), the spheroid/single cell–hydrogel constructs were implanted into the CAM of individual embryos. The diameter and thickness of the hydrogel were kept constant at 13 and 1 mm, respectively. After incubation for 7 days, the membrane was fixed

with 4w/v% paraformaldehyde in PBS overnight to image the vascular structure. The fixed membrane was also embedded in Parafilm, and tissue sections were stained with hematoxylin and eosin (H&E) and Anti-alpha smooth muscle actin staining (α-SMA) antibody. The inflammatory response was also assessed by quantifying the area occupied by immune cells and fibrotic tissue.

*3.3.1.8 Immunofluorescence imaging of BMSCs*

Spheroids were fixed with 4% (w/v) paraformaldehyde in PBS overnight at room temperature. Then, cells were washed twice with PBS for 5 min each time, permeabilized with 0.5% Triton-X 100 for 30 min, and again washed twice with PBS. Permeabilized cells were blocked with 1w/v% bovine serum albumin solution (Sigma) and 0.1% sodium azide (Fisher) in PBS for overnight and then washed twice with PBS. Finally, cells were sequentially incubated with 50 ng/ml phalloidin-FITC solution (Invitrogen) for overnight at room temperature, and 100 ng/ml DAPI solution (Invitrogen) for 10 min. DIC (Differential Interference Contrast) and fluorescence images were acquired with 40x and 63x oil objectives in the laser-scanning confocal microscope (LSM700, Zeiss).

*3.3.1.9 Immunofluorescence quantification of Fc-Tag-N-Cadherin present on BMSCs*

Spheroids were fixed with 4% (w/v) paraformaldehyde in PBS overnight at room temperature. Then cells were washed twice with PBS for 5 min each time, then permeabilized with 0.5% Triton-X 100 for 30 min, and again washed twice with PBS. Permeabilized cells were blocked with 1w/v% bovine serum albumin solution (Sigma) and 0.1% sodium azide (Fisher) in PBS for overnight and then washed twice with PBS. Spheroids then were left overnight with Cy

3-conjugated AffiniPure Goat Anti-Human IgG Fc Fragment Specific (Jackson ImmunoResearch). Spheroids then were washed three times with PBS, followed by incubation with DAPI (Invigrogen) for 10 min, and finally washed three times with PBS. DIC (Differential Interference Contrast) and fluorescence images were acquired with a laser-scanning confocal microscope (LSM700, Zeiss), using 40x and 63x oil immersion objectives.

*3.3.1.10. Cadherin gene expression*

BMSC spheroids were prepared as described previously (3.3.1.3). Fifteen spheroids per condition were use to analyze mRNA expression in cells cultured under the three conditions (control or treatment with either N-Cad-Fc or with E-Cad-Fc). Each condition was tested in replicates of three, for a total of seventy five spheroids per condition. RelicaPrep RNA cell Miniprep System from Promega was used to isolate the mRNA from cells in each condition (the protocol was followed according to the manufacturing instructions). Then cDNA was amplified from each sample with 60ng of RNA and superscript III from Invitrogen. To analyze the expression of N-Cadherin (CDH2) or E-Cadherin (CDH1), we used TagMan Gene Expression Assays, which were run on the Biosystems 7900HT Fast Real-Time PCR System.

*3.3.1.11 Transwell assay for spheroids*

The effect of spheroids on the permeability of mouse endothelial cells was examined with a co-culture assay in Transwell (Sup.Fi.6). Mouse endothelial cells were seeded at a density of $5\times10^4$ per insert of the 24-well Transwell (0.4 μm pore polyester membrane insert, Corning, USA) and incubated for two days at 37° C. Then the medium was changed with 10 ng/ml TNF-α (GenScript, USA) in basal DMEM (Gibco, USA) and incubated for one day at 37° C to inflame

the endothelial cells. The spheroids, cultured for three days in the presence of N-Cad-Fc, E-cad-Fc or without any additive, were collected and added to the bottom well of a Transwell chamber at 37°C, and cultured for one more day.

The permeability of mouse endothelial cells, after co-culturing with spheroids was tested with Dextran- Alexa 488 (Mw 3000, Thermo Fisher Scientific, USA) added to the insert at a final concentration of 0.05 mg/ml. The Transwell plate with the endothelial monolayers was incubated for one hour at 37° C, and then 90 µL from each well was collected from the upper chamber and measured the emission intensity at 535 (± 20) nm at the excitation of 485 (± 20) nm using a microplate reader (Infinite 200Pro, Tecan Group Ltd.).

## 3.4 Results

### *3.4.1 Synergistic effects of FBS and N-Cadherin*

No cell aggregation was observed by BMSCs culture by the hanging drop method (Figure 3.1) with 1% of FBS in DMEM in the presence or absence of N-Cadherin protein consequently no spheroids were formed (not shown). On the contrary, in the presence of 10% FBS in DMEM BMSCs spheroids formed with and without either N-Cad-Fc or E-Cad-Fc (Fig. 2A-C). Comparison of the spheroids area previously treated with E-Cad-Fc and N-Cad-Fc showed no statistical significance difference (Fig. 2D) on either day 1 (328 µm ± 52, 326 µm ± 35, and 345 µm ± 34 diameter respectively) or day 3 ( 443 µm ± 50, 448 µm ± 79 and 448 µm ± 62 diameter respectively).

### *3.4.2 Analysis of E-Cadherin and N-Cadherin expression by spheroids*

Immunofluorescence imaging (Fig.3.4) revealed that there was not a statistically (Fig. 3.5D) significant difference in the ratio of N-Cad present on the spheroids cultured without added protein (Fig. 3.4AI &3.4AII), N-Cad-Fc (Fig. 3.4B-I & 3.4B-II) or E-Cad-Fc (Fig. 3.4 C-I & 3.4C-II). On the contrary, there was a statistically significant increase in the ratio of E-Cad present on the spheroids cultured with E-Cad-Fc (0.6±0.03, Fig. 3.4B-I, 3.4B-III & 3.5E) when compared to the spheroids cultured without protein (0.2±0.01, Fig.3.4A-I, 3.4A-III & 3.5E) or N-Cad-Fc (0.1±0.005, Fig. 3.4C-I, 3.4CII & 3.5E). To confirm that the detected cadherins was only due to cellular cadherin and not the cadherin added to the media, we stained spheroids with anti-Fc antibody. There was no Fc-tagged cadherin on the spheroids, indicating that all of the protein stained was the cellular cadherins. (Fig. 3.6)

Spheroids were cultured with added anti-N-Cad antibodies, anti-E-Cad antibodies or both antibodies. On day one, no spheroid form on Anti-E-Cad or Anti-N-E-Cad, however BMSCs cultured on anti-N-Cad did partially aggregate and formed a spheroid like structure (Fig.3.7). On day 3 all three conditions were found to form a spheroid like structure (Fig. 3.8). The size of this structure was significantly larger than spheroids cultured with cadherin extracellular domains (anti-N-Cad: 485μm ± 51, anti-E-Cad: 710 μm ± 160, or both anti-E and anti-N-Cad antibodies: 760 μm ± 170 in diameters). Spheroids cultured with Anti-N-Cad (0.37±0.019) show a statistically significant decrease of N-Cad ratio when compared to the ratio of N-Cad in spheroids cultured with Anti-E-Cad (0.51±0.025)(Fig. 3.9I) and to the ratio of N-Cad in spheroids cultured with N-Cad-Fc (0.43±0.02) (Fig. 3.10A). However, when stained for E-Cad on spheroids cultured with Anti-N-cad the ratio of E-Cad (0.19±0.096, Fig 3.9J) significantly

decrease when compared to the ratio of E-Cad in spheroids cultured with Anti-E-Cad (0.46±0.02,Fig. 3.9J). Comparison of the ratio of E-Cad in spheroids cultured with E-Cad-Fc (0.6±0.03, Fig. 3.5E) to any other condition shows a statistically significant increase of E-Cad (Fig. 3.10B). In the case of spheroids cultured with Anti-E-Cad they show a statistically significant increase of E-Cad and N-Cad when compared to spheroids cultured with Anti-N-Cad and Anti-E-N-Cad (Figs. 3.9I and 3.9J). Further, the ratio of N-Cad from spheroids cultured with Anti-E-Cad (0.5±0.025 ) compared to the ratio of N-Cad of spheroids cultured with E-Cad-Fc (0.4±0.02) shows a statistically significant increase of N-Cad ratio (Fig. 3.10A) and a significant decrease of E-Cad ratio (0.46±0.02 Anti-E-Cad) (Fig. 3.10B). When results obtained under all conditions were compared, we found that spheroids cultured with Anti-E-N-Cad show a significant decrease of E-Cad ratio (0.1±0.005) and N-Cad ratio (0.17±0.009) (Fig.3.9I-3.9J 3.10A-3.10B).

### *3.4.3 Cadherin gene expression*

Spheroids cultured with complete media, containing N-Cad-Fc or E-Cad-Fc were analyzed for their N-Cad and E-Cad mRNA expression (Fig. 3.11). Real time PCR show a significant statistical decrease on mRNA expression of N-Cad and E-Cad when spheroids were cultured with N-Cad-Fc or E-Cad-Fc in comparison with spheroids cultured without protein. Significant decrease of the expression of E-Cad was found with spheroids cultured with N-Cad-Fc compared to spheroids cultured with E-Cad-Fc. There was no difference in the amount of the N-Cad gene expression between spheroids cultured with either soluble E-Cad-Fc or N-Cad-Fc.

### *3.4.4 Detection of VEGF in supernatant of spheroid/single cell BMSC*

Supernatant collected from BMSCs cultured in alginate gels without N-Cad-Fc; BMSCs cultured in 3-D collagen gels with N-Cad-Fc; and spheroids formed in the presence and absence of E-Cad-Fc and N-Cad-Fc (but not in alginate gels) were analyzed for the expression of VEGF in picograms (pg). A significant increase in concentration of VEGF was found on spheroids cultured in the presence of N-Cad-Fc (254.4±3.6pg) when compared to any of the other conditions (Fig. 3.12). Spheroids cultured with E-Cad-Fc (201±16 pg) showed an increase of VEGF when compared to any of the BMSCs cultured on glass or collagen gel with soluble N-Cad-Fc or compared to spheroids cultured with no added protein. N-Cad-Fc was found to induce the secretion of VEGF in single cells that were cultured in 3-D collagen gels (157.6 ±15.6 pg), when compared to single cells cultured on glass, in the absence of N-Cad-Fc (128 ± 11 pg) (Fig. 3.12). VEGF secretion by spheroids in the absence of N-Cad-Fc (121.4±9.8 pg) was found to secrete lower amount of VEGF secreted by single BMSC cells cultured on glass (127.6±11pg) (Fig. 3.12).

VEGF secretion was also analyzed with spheroids cultured in the presence of Anti-N-Cad, or in the presence of both Anti-E-Cad and Anti-E-N-Cad antibodies (Fig. 3.13). Statistical analysis showed a significant increase in VEGF secretion by spheroids cultured with Anti-N-cad (210±8.5 pg) when compared to the spheroids cultured in the absence of protein or in the presence of Anti-E-Cad and Anti-E-N-Cad. However, when compared to the amount of VEGF secreted by spheroids cultured with N-Cad (254.4±3.6pg), there was no significant increase

(Fig.3.14). Spheroids cultured in the presence of N-Cad exhibited the highest level of VEGF secretion by the BMSCs.

### *3.4.5 In-Vivo angiogenesis induction*

Spheroids previously treated with or without N-Cad-Fc where embedded in collagen gels, per comparison free BMSCs cells with and without N-Cad-Fc were also encapsulated in collagen gels and all these four conditions were implanted in chicken embryos (Fig. 3.15). After 7 days of implantation, the blood vessels were analyzed in each condition by measuring the area of the blood vessel by the cross sectional area of the sample ($mm^2/mm^2$). The spheroids that were pre-treated with N-Cad-Fc induced significantly higher levels of blood vessel formation (0.26±0.05 $mm^2/mm^2$ blood vessel density) than the spheroids formed in the absence of N-Cad-Fc (0.107±0.012 $mm^2/mm^2$ blood vessel density) (Fig. 3.16). There was no significant difference found between the blood vessels formed when we used free BMSCs encapsulated in collagen gels with (0.6±0.026 $mm^2/mm^2$ blood vessel density) or without (0.153±0.03 $mm^2/mm^2$ blood vessel density) N-Cad-Fc (Fig. 3.16). Significantly fewer blood vessels developed in the presence of spheroids cultured in collagen gels without N-Cad-Fc (Fig. 3.16).

### *3.4.6 In-Vitro permeability studies*

Endothelial cells (C166) co-cultured with spheroids with and without N-Cad-Fc and E-Cad-Fc, as well as controls without spheroids, were used for endothelial permeability studies. The statistical analysis of this data (Fig. 3.17) show a significant decreased in permeability of the endothelial cells due to the presence of spheroids cultured with/out N-Cad. However, the permeability of endothelial cells decreased to a lesser extent when compared to the results

obtained when endothelial cells were co-cultured with spheroids that were treated with/without N-Cad-Fc.

## 3.5 Discussion

In our study we were able to cultured bone marrow-derived MSC (BMSCs) in free scaffold 3-D spheroids in the presence of N-Cad-Fc and E-Cad-Fc. Synergistic effects by the cadherins with the serum in the media were found to be essential by the BMSCs in order to form the spheroids. Also, the presence of soluble cadherins in the media resulted in an increase in cell proliferation, which was confirmed by the increase in the size of the spheroids (Fig. 3.3). No significant difference was found in relation with the spheroids cultured without any protein. However, it confirmed the cell proliferation and viability of the cultures during the 3 days without exogenous matrix. Cadherins are known to interact with the Wnt canonical pathway [17]. There studies that suggest that there is a downstream involvement of β-catenin in Wnt regulation of MSC self-renewal [17].

Cadherins are known for being non static structures (which is a key mechanism for modulating adhesion strength) and their ability to adjust the amount of cadherins present on the plasma membrane, which is determined by the endocytosis and synthesis of cadherins [4]. The presence of cadherins in the media was able to modulate the amount of cadherins express in the plasma membrane as could be seen in the subtle increase of N-Cad in spheroids cultured with N-Cad-Fc (Fig. 3.5D) and the significant decrease of E-cad of spheroids cultured with E-Cad-Fc (Fig. 3.5E). We can hypothesized that the presence of cadherins in the media might form trans interactions with the plasma membrane cadherins present in the cells preventing the endocytosis

of either N-Cad or E-Cad respectively to the treatment. Previous studies have shown that adding antibodies against the extracellular domain of cadherins can block the trans interactions which increase the endocytosis of the cadherins [4]. Which, we confirmed by culturing the BMSCs with anti-N-Cad, anti-E-Cad and anti-N-E-Cad in which no spheroid formation was seen on day 1 of the treatment (Fig. 3.7). Longer periods cultured of the BMSCs with the antibodies after 3 days of cultured show a spheroid formation for all conditions (Fig. 3.8). This can be explained by the internalization of the antibody due to the endocytosis. Once an antibody binds to the cadherin it prevents the trans interactions and triggers the endocytosis. The antibody is assumed to remain bound to the cadherin through the endosomal pathway until the acidic pH of the lysosome dissociates the antibody/cadherin complex and degrades both [18]. Which can explain the spheroid formation after 3 days in culture with the antibodies, one can assume that new cadherins were synthesized on the plasma membrane. Blocking of E-cad causes the increase of N-Cad and decrease of E-Cad when this was compared to spheroid cultured with E-Cad (Fig. 3.10). The same scenario is seen when spheroids were cultured with anti-N-Cad where there was a decrease on N-Cad and an increase on E-cad compared to spheroids cultured with E-Cad (Fig. 3.10). This is due to the down-regulation of E-Cad which is associated to the up-regulation of N-Cad and vice versa [4]. Blocking both cadherins proved the down-regulation and up-regulation of E-Cad and N-Cad. This was the only condition that causes a decrease on the expression of both cadherins even after three days in culture, possibly because the cells now has to synthesized both cadherins.

N-cad besides influencing the cell-cell interactions it is also involve in a series of signal pathways that can turn on the expression of different genes. This is due to the binding of β-catenin, plakoglobin and p120-catening to the cytoplasmic region of N-Cad [19]. By

sequestering β-catenin at the plasma membrane, N-cad can regulate the cytosolic amount of β-catenin and thereby regulate the Wnt or Wnt/β-catenin [19,20]. β-catenin drives von Hippel Lindau (VHL) expression which directly interacts with HIF-2α (hypoxia-induce expression-2α) decreasing β-catenin/TCF4 signaling resulting in a pro-angiogenic response [20]. So, down-regulation of N-Cad leaves more β-catenin in the cytoplama available to interact with Wnt, causing the activation of HIF-2α, which correlates with the decrease in mRNA expression of N-Cad that is observed on spheroids that were cultured with N-cad-Fc compared to the controls and the spheroids cultured with E-Cad-Fc (Fig. 3.11). Explaining how the presence of N-Cad can modulate the secretion of VEGF by spheroids cultured with N-Cad-Fc (Fig.3.12).

Increase vascularization due to the BMSCs spheroids with N-Cad-Fc imbedded in 3-D collagen gels in the chicken embryos (Fig. 3.16) can be explained by the secreted VEGF. Angiogenesis is the formation of vessels from preexisting vasculature and VEGF it is known for directing and rerouting endothelial cells into new vascular structures [21,22]. Although, some research have shown that implanted MSC favor the angiogenesis blood-derived MSC [23], we showed that this capability of the BMSCs it is increase in the presence of N-Cad-Fc (Fig. 3.16).

The cell permeability studies (Fig. 3.17) were performed by inducing inflammation of endothelial cells (ECs). The ECs form barriers that are in control of the vascular permeability for solutes and blood proteins [24]. An increase on permeability can be induced by modulating the AJ which cadherins play a vital role. The ECs are known to express N-cad, which can regulate vascular endothelial-cadherin (VE-Cad) in the AJ of the endothelial cells [24]. BMSCs are known from secreting different factors and one of them is angiopoiten (Ang-1), which decreases vascular permeability by increasing the AJ between ECs [25]. It is possible that the inflammation

of the ECs is triggering the protective effects in BMSCs and they secrete Ang-1 which would reduce the permeability of ECs by preventing the endocytosis of VE-Cad. It seems that culturing the BMSCs spheroids with N-Cad-Fc can make them more susceptible to the environment (Fig. 3.17).

It is unclear the synergistic effect that N-Cad and VEGF play on directing the migration and cell differentiation of BMSC cells. We have shown that it is possible to replicate the angionenic effects in vivo by N-Cad-Fc induced BMSC spheroids as well as their protective effects during disease of ECs by reducing their permeability due to the inflammation. Further studies need to be completed in order to understand the mechanisms by which N-Cad interacts with VEGF to induce the angiogenesis in normal tissue, and in a disease tissue they turn on the protective signals. This could be critical knowledge in order to aid vascular diseases.

## 3.6 Conclusion

We have demonstrated that it is possible to modulate the secretion of trophic factors such as VEGF by BMSC with soluble N-Cad-Fc. Also, cells did aggregate in the presence of N-Cad-Fc and E-Cad-Fc, proving that they did not stop cell-cell adhesion. Spheroids cultured with N-Cad-Fc where able to increase the blood vessel formation in chicken implants. Also, the presence of the N-Cad-Fc in the spheroids decreased permeability in endothelial cells cultured in vitro. Further studies could be performed to investigate if BMSC cultured with E-Cad-Fc and implanted in chicken embryos would also have and angiogenic effect and if this would be lower than the one obtained with spheroids cultured with N-Cad-Fc. Overall, this could be an

invaluable technique to study how cadherins modulate other proteins and interact with cells in vivo.

*Acknowledgement*

This work was supported by National Science Foundation (CAREER: DMR-0847253 to H.K., STC-EBICS Grant CBET-0939511 to H.K., NSF CMMI 10-29871 to L.D., NSF Graduate Fellowship to J.V.), and The University of Illinois' Research Board.

## 3.7 Figures and Tables

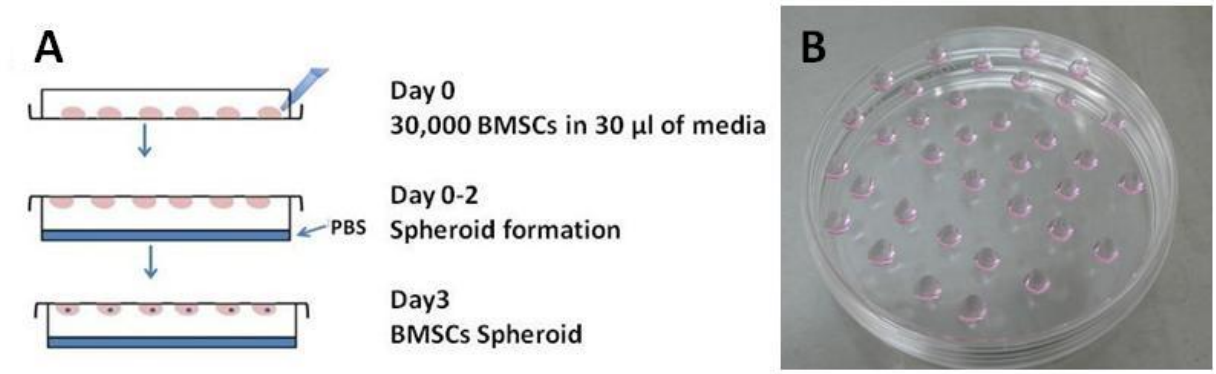


**Figure 3.1**. **A**. Schematics of how BMSC spheroids are culture. **B.** Picture of how the drops look from a top view of the tissue culture dish.

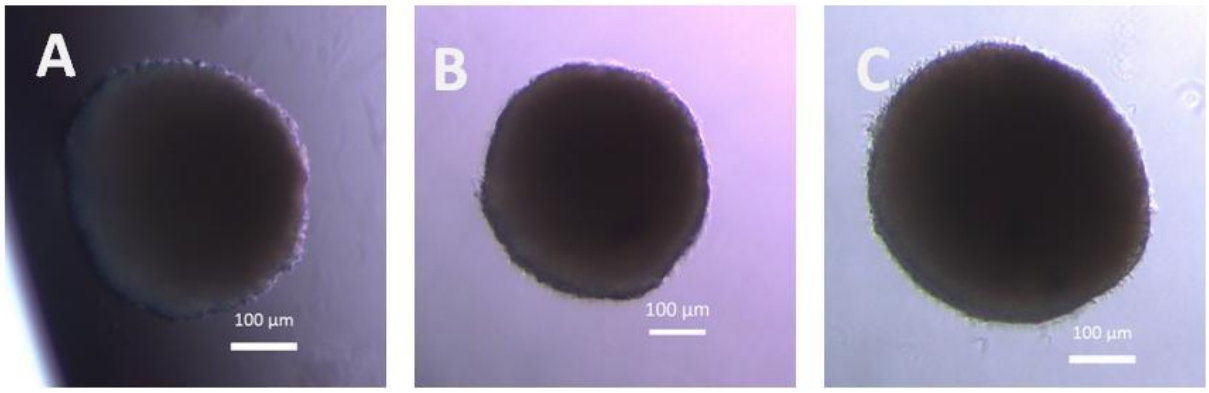


**Figure 3. 2 . B**MSC form spheroids cultured by hanging drop method in the presence of 10% FBS on day 3. **A.** Spheroids cultured in DMEM with 10% FBS, with a diameter of 443µm ± 50. **B.** Spheroids cultured on DMEM with 10% FBS and 100µg/ml of Fc-Tag-E-Cadherine, with a diameter of 448µm ± 79. **C.** Spheroids cultured on DMEM with 10% FBS and 100µg/ml of Fc-Tag-N-Cadherine, with a diameter of 475µm ± 62.

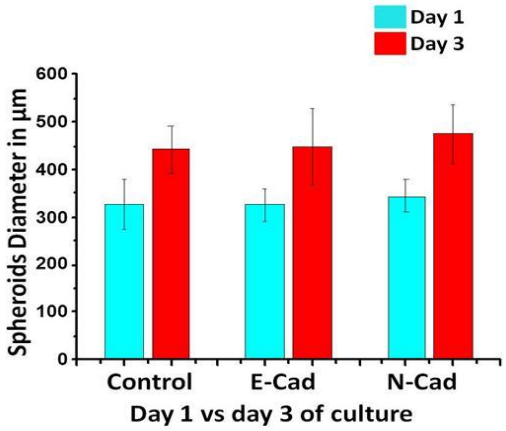


**Figure 3.3** Statistical analysis of the spheroids area presented in terms of the diameter obtained on day 1 and day. There was a statistical significant difference on size on day 3 of cultured. Spheroids cultured with N-Cad presented a larger area when compared to any of the other conditions. The Thirty spheroids were cultured per condition and analyzed. p value < 0.05.

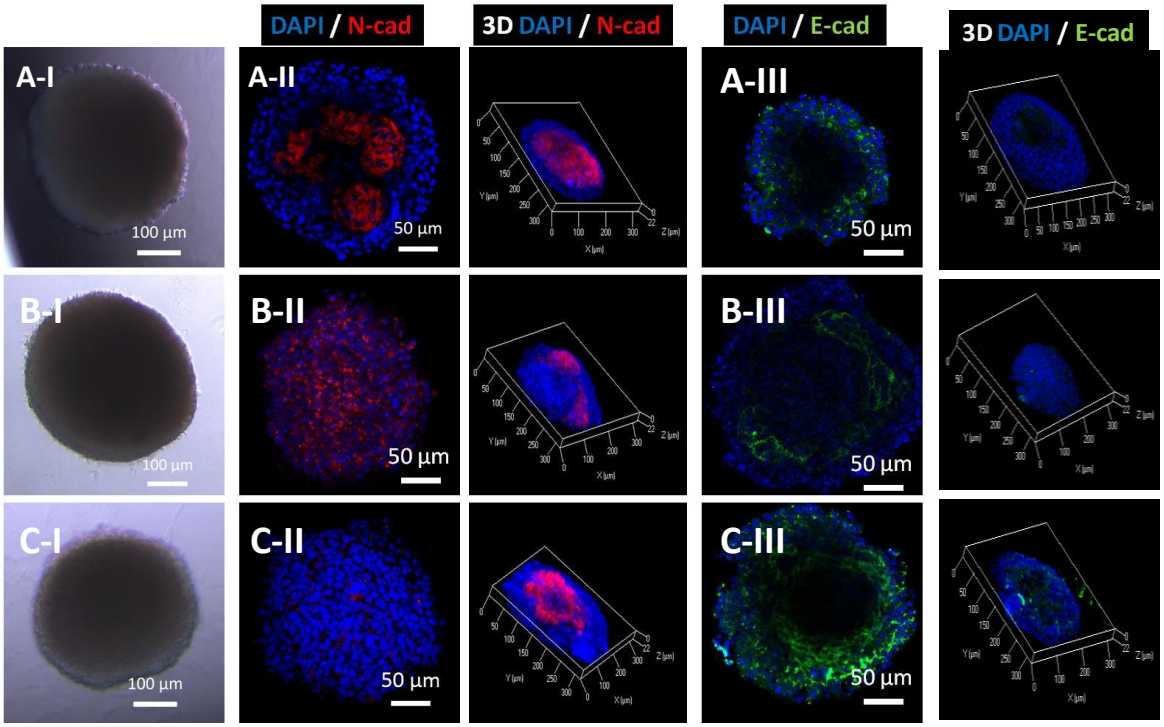


**Figure 3.4** Phase contrast and fluorescent images of spheroids cultures on day 3 and statistical analysis of the cadherins on the spheroids. The controls (AI) were stained for N-cad (A-II ) and E-Cad (A-III) **.** Spheroids cultured with E-Cad-Fc (B-I) were stained for N-Cad (B-II) and E-Cad (B-III). Shperoids cultured with N-cad-Fc (C-I) were stained for N-Cad (C-II) and E-Cad(C-III).

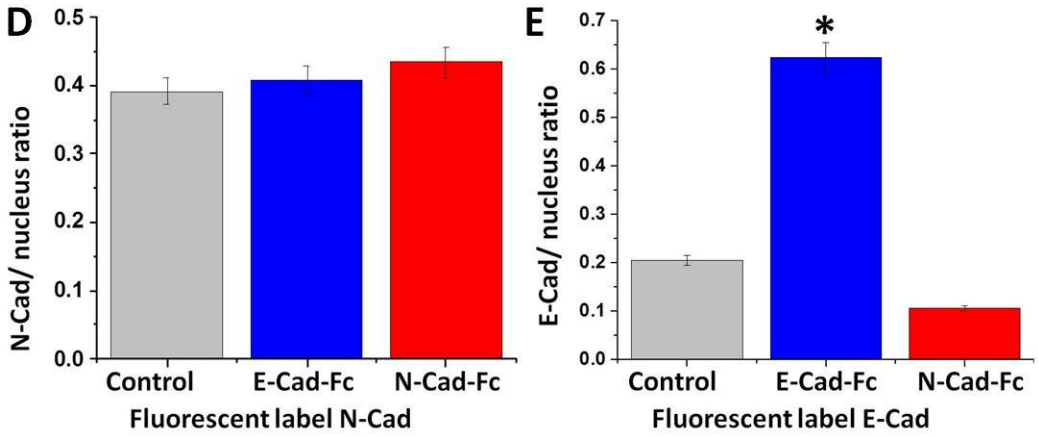


**Figure 3.5** Statistical analysis of the immunofluorescent studies of the spheroids. **D.** Statistical analysis of N-Cad on the three conditions. No statistical significant difference was found among conditions despite the small increase of N-Cad on shperoids cultured on N-Cad-Fc, that can be observe chart. **E.** Statistical analysis of E-Cad for all conditions. Significant statistical increase of E-Cad on spheroids cultured with E-Cad-Fc, p value <0.05.

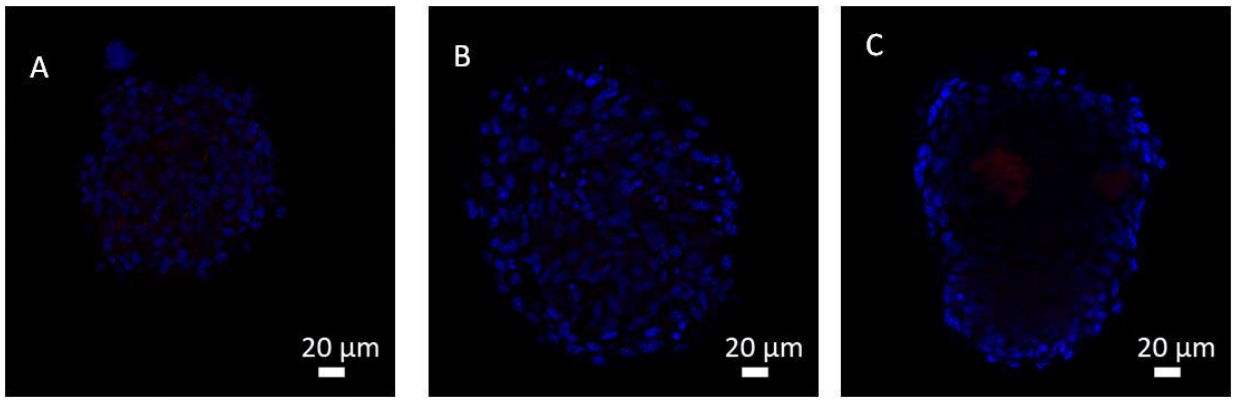


**Figure 3.6.** Spheroids fluorescently label with anti-Fc. No Fc-Tag-N-Cad or Fc-Tag-E-Cad was detected on control **(C),** E-Cad **(B)** and N-Cad **(C)** . The statistical analysis confirm the absence of the Fc-Tag-Cadherins, the values were cero.

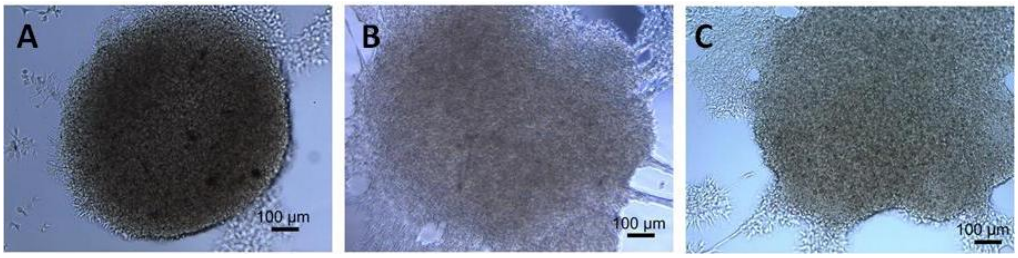


**Figure 3.7** Day 1 of spheroids cultured on the presence of Anti-N-Cad **(A),** Anti-E-Cad **(B)** and Anti-N-E-Cad **(C).**

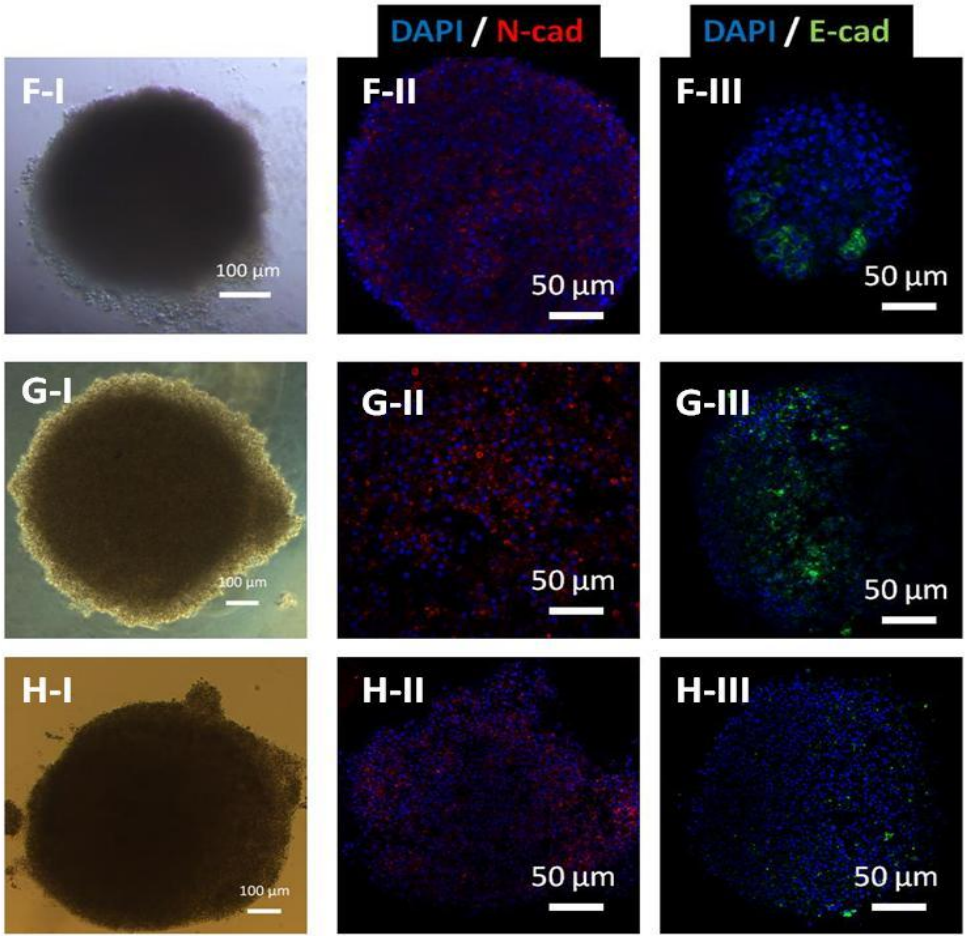


**Figure 3.8. Day 3** Phase contrast and immunofluorescent images of BMSCs spheroids cultured in the presence of Anti-N-Cad (FI-III) , Anti-E-Cad (GI-III) and Anti-E-N-Cad (HI-III).

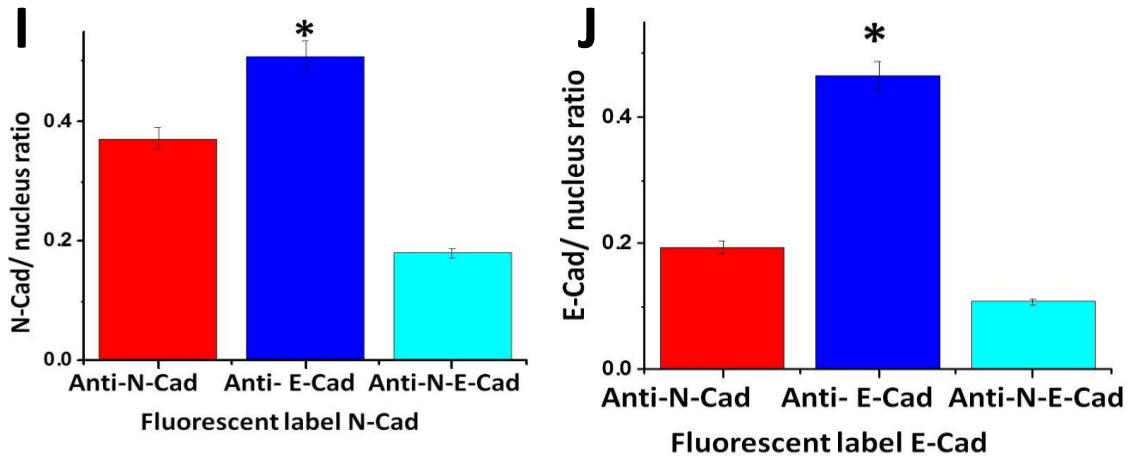


**Figure 3.9** Statistical analysis of the N-Cad present on the spheroids show a significant increase of N-Cad( I) and E-Cad (J)on spheroids cultured with Anti-E-Cad, p-value<0.05. Significant decreased was found of N-Cad and E-Cad on spheroids cultured with Anti-N-E-Cad, p-value <0.05.

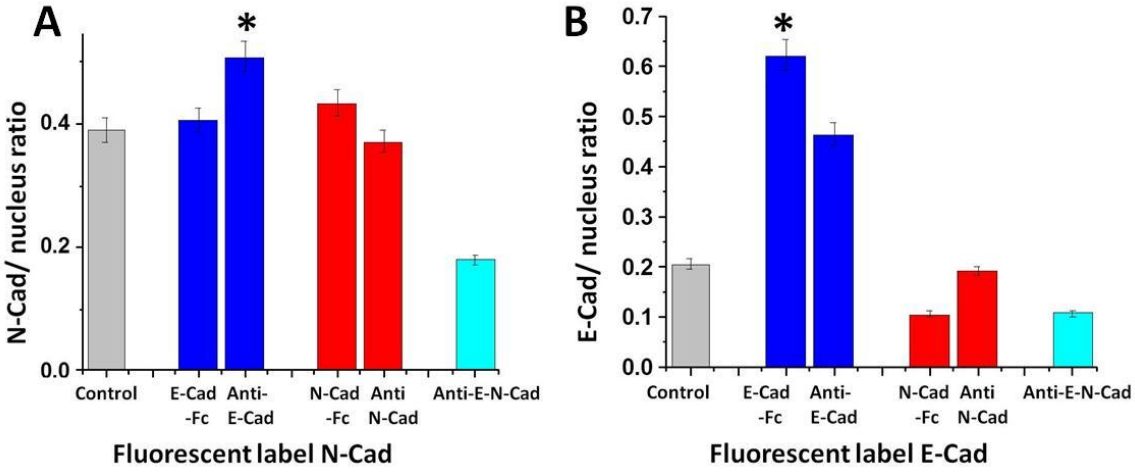


**Figure 3.10.** Statistical comparison of N-Cad (A) and E-Cad (B) on all the conditions. N-Cad was found to be significantly increased on spheroids treated with Anti-E-Cad when compared to any other conditions (A). On the contrary E-Cad was significantly increased on the spheroids cultured with E-cad-Fc (B). A statistically significant decrease of E-Cad was found on spheroids cultured with N-Cad-Fc (B). Blocking N-Cad and E-Cad cause a significant decrease of both proteins in comparison with the controls. p-value<0.05.

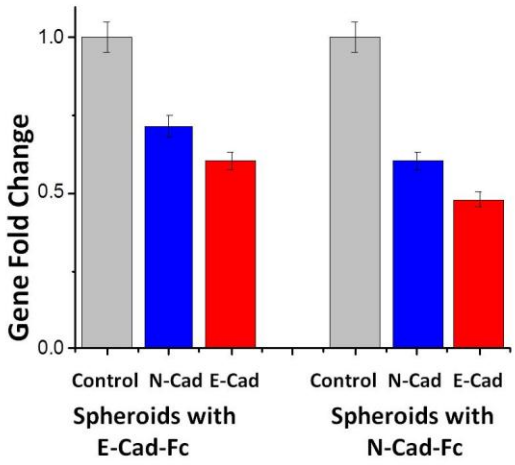


**Figure 3.11.** MRNA expression of the N-Cad and E-Cad genes in the spheroids cultured in the presence of E-Cad-Fc and N-Cad-Fc in the media respectively. No statistical significant change was found in the gene expression, possible due to the presence of the Cadherin in the media preventing endocytosis of the cadherin into the cells

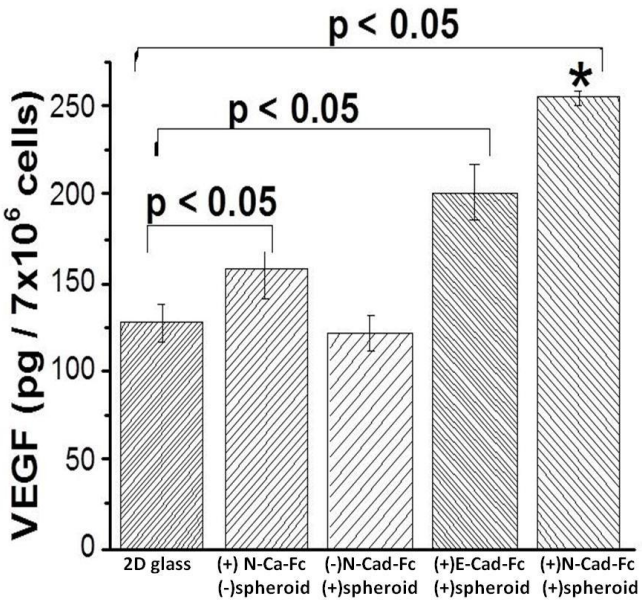


**Figure 3.12**. Spheroids form in the presence N-cad (100ug/ml) was found to induce significantly higher secretion of VEGF than any other conditions, this was confirmed by t-test of N-cad against all the other conditions ($p<0.05$). N-cad introduce to the monolayer cultures of MSC (100ug/ml) was found to induce higher secretion of VEGF this was confirmed by t-test between MSC cultured in the absence of N-cad on monolayers ($p<0.05$). There was not a significant difference between the VEGF secreted by spheroids or monolayers in the absence of N-cad. Also there was not a statistical difference between the VEGF secreted by the spheroids compared to the VEGF secrete by monolayers in the presence of N-cad.

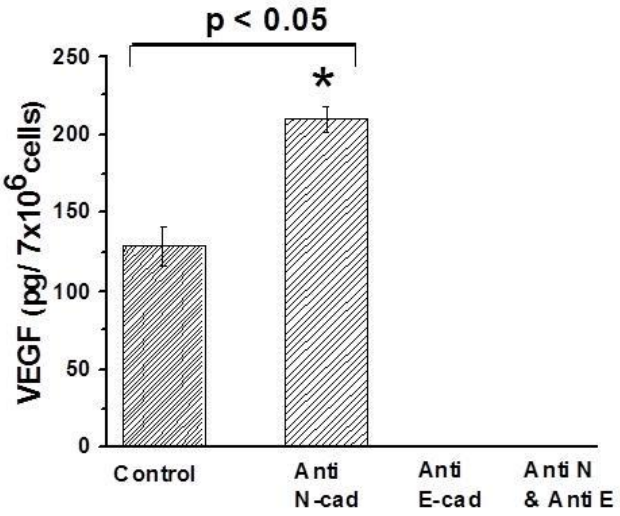


**Figure 3.13**. Analysis of the VEGF expression of spheroids cultured with Anti- N-cad, Anti-E-Cad and Anti-N and E Cad. N-cad was found to induce significantly higher secretion of VEGF than any other conditions, this was confirmed by t-test of N-cad against all the other conditions ($p<0.05$). The T-test did not find any significant difference between E-cad and Anti-N-cad induced VEGF secretion. The presence of E-cad or Anti-N-cad do induce higher secretion of VEGF when these are compared to the control (no protein).

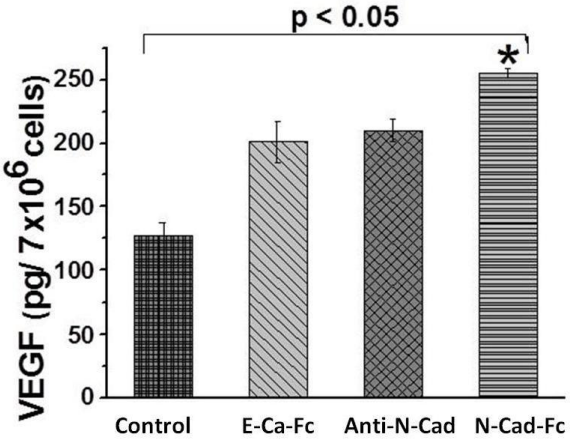


**Figure 3.14.** N-cad was found to induce significantly higher secretion of VEGF than any other conditions, this was confirmed by t-test of N-cad-Fc against all the other conditions ($p<0.05$). T-test did not found any significant difference between E-cad-Fc and Anti-N-cad induced VEGF secretion. The presence of E-cad-Fc or Anti-N-cad do induce higher secretion of VEGF when this are compared to control (no protein ).

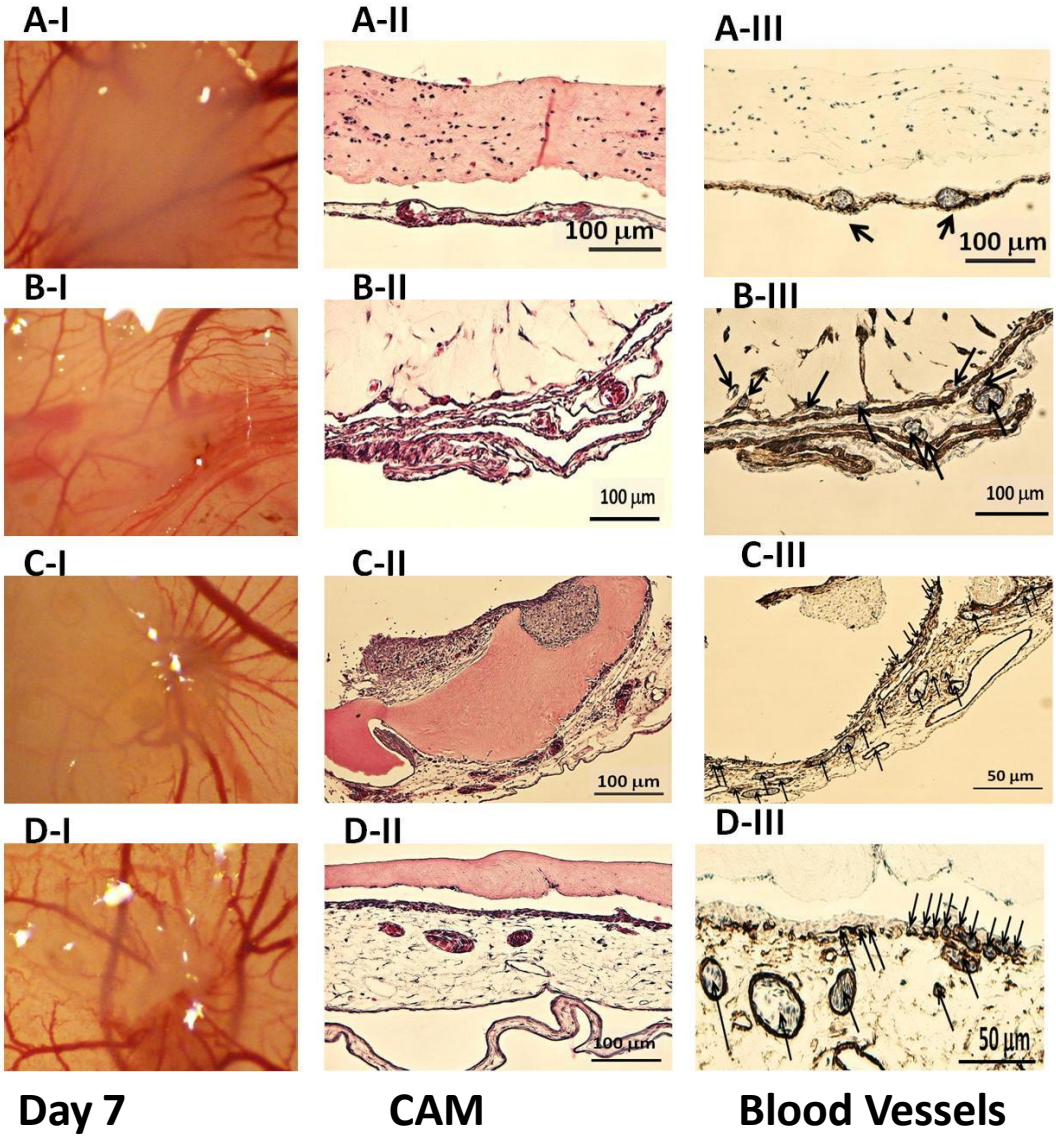


**Figure 3.15.** CAM in vivo studies of N-cad-Fc induce MSC spheroids and free BMSCs encapsulated in collagen gels. Free BMSCs were encapsulated in collagen gels **(A-I)** and were stained for H&E **(A-II)** and α-SMA (**A-III).** Collagen gels with free BMSCs with N-Cad-Fc **(B-I)**, H&E **(B-II)** and α-SMA (**B-III).** Spheroids culture with N-Cad-Fc and encapsulated in collagen gels **(C-I)**, H&E **(C-II)**, and α-SMA (**C-III).** Spheroids without N-Cad-Fc in collagen gels **(D-I)**, H&E **(D-II)**, and α-SMA (**D-III).**

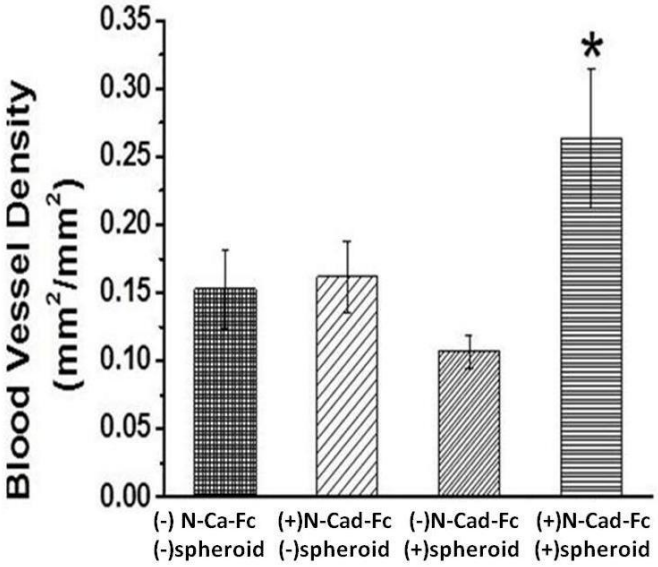


**Figure 3.16.** Statistical analysis of the blood vessels formed due to implanted collagen gels. Higher significant blood vessel formed due to the implanted spheroids cultured with N-Cad. Significant fewer blood vessels were formed in the presence of spheroids cultured in the absence of N-Cad. p-value 0.05.

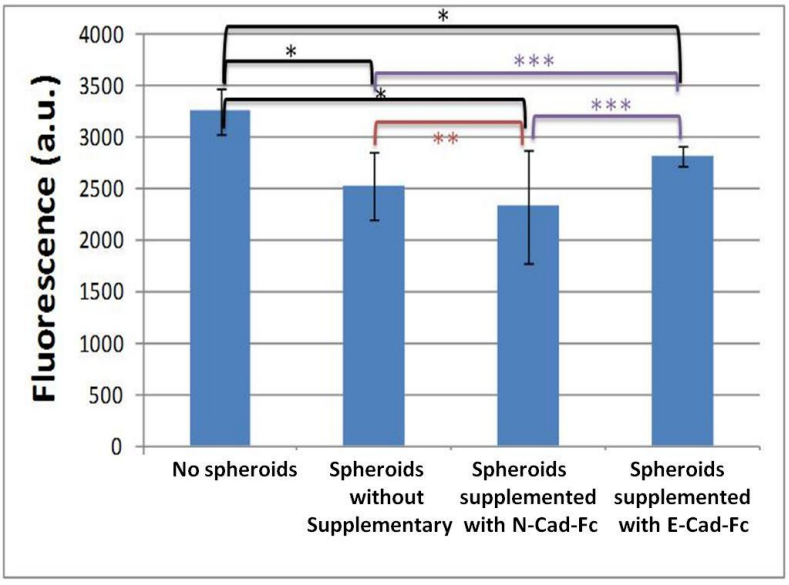


**Figure 3.17.** Statistical analysis of permeability studies. p* < 0.05: All the conditions with spheroids have been shown to **decrease the permeability** of the inflamed endothelial cells (C166) p** > 0.05: Spheroids, **either supplemented with N-Cad or not**, can decrease the permeability of the inflamed C166 **to a similar extent p***** < 0.05: Spheroids supplemented with E-Cad decreased the permeability of the inflamed C166 **to a smaller extent compared to the 3rd and 4th conditions.**

## 3.8 References


**1.** Yeh, HY., Liu BH., and Hsu, SH. The calcium-dependent regulation of spheroid formation and cardiomyogenic differentiation of MSC on chitosan membranes. *Biomaterials.* 2012; 33: 8943-8954.

**2.** Leckband, D., and Prkasam, A. Mechanism and Dynamics of Cadherin Adhesion. Annu. *Rev. Biomed. Eng.* 2006; 8: 259- 287.

**3.** Halbleib, J, M., and Nelson, W J. Cadherins in development: cell adhesion, sorting and tissue morphogenesis. 2006; 20: 3199-3214.

**4.** Adherens Junctions: From molecular mechanism to tissue development and disease. *Subcellular Biochemistry.* 2012; 60: 9- 62 and 171-249.

**5.** Brash, J., Harrison, O J., Honing, B., and Shapiro, L. Thinking outside the cell: how cadherins drive adhesion. *Trends in Cell Bio.* 2012; 22: 299-310.

**6.** Mahmood, A., Lu, D., Lu, M., and Chopp, M. Treatment of traumatic brain injury in adult rats with intravenous administration of human bone marrow stromal cells. *Neurosurgery.* 2003; 53: 697-703.

**7.** Chen, J., Li, Y., Katakowski, M., Chen, Xiaoguang., Wang, L., Lu, D., Lu, M., Gautam, S C., and Chopp, M. Intravenous bone marrow stromal cell therapy reduces apoptosis and promotes edogenous cell proliferation after stroke in female rat. *J. of Neuro. Res*. 2003; 73: 778-786.

**8.** Schmidt, A., Ladage, D., Schinkothe, T., Klausmann, U., Ulrichs, Ch., Klinz, FJ., Brixius, K., Arnhold, S., Desai, B., Mehlhorn, U., Schwinger, R H G., Staib, P., Addicks, K., and Bloch, W. Basic fibroblast growth factor controls migration in human mesenchymal stem cells. *Stem Cells.* 2006; 7: 1750-1758.

**9.** Cheng, NC., Wang, Sh., and Young, T H. The influence of spheroid formation of human adipose-derived stem cells on chitosan films on stemness and differentiation capabilities. *Biomaterials.* 2012; 33:1748-1758.

**10.** Beckermann, B.M., Kallifatidis,G., Groth, A., Frommhold,D., Apel,A., Mattern, J., Salnikov, A.V., Moldenhauer, G., Wagner, W., Diehlmann, A., Saffrich, R., Schubert, M., Ho, A.D., Giese,N., Büchler,M.W., Friess, H., Büchler,P., and Herr, I. VEGF expression by mesenchymal stem cells contributes to angiogensis in pancreatic carcinoma. *British J. of Cancer.* 2008;99:622-631.

**11.** Oswald, J., Boxberger,S.,Jorgensen,B., Feldmann, S., Ehninger, G., Bornhauser,M., and Werner, C. Mesenchymal stem cells can be differentiated into endothelial cells in vitro. Stem cells. 2004; 22: 377-384. Chappuis-Flament, S.; Wong, E.; Hicks, L.D.; Kay, C.M.; Gumbiner, B.M. *J. Cell Biol.* 2001, 154, 231-243.

**12.** Foty, R. A simple hanging drop cell culture protocol for generation of 3D spheroids. *J.Vis.Exp.* 2011. P.2720.

**13.** Lambert, M., Padilla, F.,and Mege, R-M. Immobilized dimmers of N-cadherin-Fc chimera mimic cadherin-mediated cell contact formation: contribution of both outside-in and inside-out signals. *J. Cell Sci.* 2000**;** 113: 2207-2219.

**14.** Chappuis-Flament, S., Wong, E., Hicks, L.D., Kay, C.M., and Gumbiner, B.M. Multiple cadherin extracellular repeats mediate homophilic binding and adhesion. *J. Cell Biol.* 2001; 154: 231-243.

**15.** Sivasankar, S., Brieher, W., Lavrik, N., Gumbiner, B., and Leckband, D. Direct molecular force measurements of multiple adhesive interactions between cadherin ectodomains. *Proc. Natl. Acad. Sci.* 1999; 96: 11820-11824.

**16.** DeVolder, R.J., Bae, H., Lee, J. and Kong, H. Direct blood vessel growth using an angiogenic microfiber/microparticle Composite Patch. *Adv. Mater*. 2011; 23:3131-3149.

**17.** Kolf, M C., Cho, E., and Tuan, S, R. Biology of adult mesenchymal stem cells: regulation of niche, self-renewal and differentiation. *Arthritis Research & Therapy*. 2007; 9: 204-213.

**18.** Arancibia-Cárcamo, L., Fairfax, B. P., Moss, S. J., and Kittler, J, T. Studying the localization, surface stability and endocytosis of neurotransmitter receptor by antibody labeling and biotinylation approaches. In: Kittler JT, Moss SJ, editors. The dynamic synapse: molecular methods in ionotropic receptor biology. *Boca Raton (FL): CRC Press*; 2006: Chapter 6.

**19.** Radice, G. L. N-Cadherin-Mediated adhesion and signaling from development to disease: lessons from mice. *Progress in Molecular Biology and Translational Science*. 2013; 116: 263-289.

**20.** Reis, M. and Liebner S. Wnt signaling in the vasculature. *Experimental cell research*. 2013; 319: 1317-1323.

**21.** Adams, R. H., Alitalo, K. Molecular regulation of angiogenesis and lymphangiogenesis. *Nature Reviews.* 2007; 8: 464-478.

**22.** Cébe-Suarez, S., Zehnder-Fjällman and Ballemer-Hofer, K. The role of VEGF receptors in angiogenesis; complex partnerships. *Cell. Mol. Life Sci.* 2006; 63: 601-615.

**23.** De Luca, A., Verardi, R., Neva, A., Benzoni,P, Crescini,E., Xia, Er., Almici, C., Calza, S., and Dell'Era, P. Comparative analysis of mesenchymal sromal cells biological properties. *ISRN Stem Cells.* 2013; 2013: 9 pages.

**24.** Vestweber, D., Winderlich, M., Cagna,G., and Nottebaum, A.F. Cell adhesion dynamics at endothelial junctions: VE-cadherin as a major player. *Trends in Cell Biology.* 2008; 19: 8-15.

**25.** Jeon, J. S., Berini, S., Whisler, J.A., Chen, M. B., Dubini, G., Charest, J. L., Moretti, M., and Kamm, R. D. Generation of 3D functional microvascular networks with human mesenchymal stem cells in microfluidic systems. *Integrative Biology*. 2014; 6: 555-563.

# Chapter 4: Soluble N-Cadherin can modulate the ratio of glia and neurons in Neuro-differentiation of BMSCs spheroids

## 4.1 Abstract

The capability of the bone marrow-derived mesenchymal stem cells (BMSCs) to secrete different factors that can aid the healing process at the site of injury make them an invaluable tool for biomedical devices. There have been several efforts to investigate how BMSCs can module the healing process in a stroke, acute injures and inflammatory diseases of the central nervous system (CNS), as well as brain tumors. Unfortunately, it is unknown how to modulate the mechanisms that trigger BMSC to induce a healing response. Here we used N-Cadherin and E-Cadherin, known cell adhesion molecules, that regulates the endothelial to mesenchymal transition (EMT) to modulate and induce the BMSCs to form spheroids by the hanging drop method. Further, BMSCs spheroids differentiated into neurons and glia when they were cultured with neural induction media. Interestingly, the differentiation of BMSCs spheroids cultured with N-Cad-Fc resulted in significantly lower numbers of glia than neurons when compared to BMSCs spheroids cultured with soluble E-Cadherin. Also, the BMSCs spheroids cultured with soluble N-Cadherin show a significantly lower network activity, even though there were significantly more neurons in the culture. These results suggest that N-Cadherin and E-Cadherin cell adhesion molecules can modulate the neural to glia differentiation ratio. Also, our analyses of the network activities of the different cultures correlate with the current knowledge that glia increase the activity in neural cultures.

## 4.2 Introduction

Bone marrow-derived mesenchymal stem cells (BMSCs) are known for their healing properties during brain injury [1]. Some studies have shown an improvement in the healing process at the site of injury where BMSCs were implanted [2]. Unfortunately, it is unknown if their healing capacities are due to the secreting factors by the BMSCs or the differentiation of the BMSCs taking place at the injury site [3]. It has been a difficult task to characterize what occurs at the site of injury, because BMSCs cells, after implantation as free cells, begin to migrate [4]. Several materials have been used to encapsulate the cells to keep them at the site of the injury [5]. Unfortunately, the implantation of foreign materials into the brain is challenging due to the high sensitivity of the system triggering the immune response [5,6].

Culturing cells in 3-D free of scaffold would be of great advantage since it allows studying complex interactions such as cell-cell and cell-matrix in the absence of exogenous subtracts, which might be beneficial for regenerative medicine [6,7]. It would also be able to maintain the cells at the site of injury without the use of a substrate [6]. Previous studies have shown that BMSCs can form spheroids using the hanging drop method and the spheroids can be cultured for long periods of time without exhibiting any evidence of necrosis [5].

Studies of co-cultured BMSCs with neural stem cells (NSC) promoted outgrowth and directional neurite extension from NSC and increased the NSCs differentiation into oligodendrocytes [8]. It was also found, that cell adhesion molecules such as N-Cadherin, Fibronectin and Laminin influence this response too [8]. Previously, we were able to induce BMSCs spheroids with N-Cadherin (N-Cad-Fc) and E-Cadherin (E-Cad-Fc), demonstrating that cell aggregation did occur in the presence of cell adhesion molecules (Chapter 3). We were also

able to induce blood vessel formation when BMSCs spheroids cultured with N-Cadherin were implanted in chicken embryos (Chapter 3). In this work, we investigated if N-Cadherin and E-Cadherin could modulate the neuron and glia differentiation ratio of BMSCs spheroids under the appropriate conditions. Because BMSCs maintain their multipotency and E-Cadherin and N-Cadherin modulate the Endothelial-to Mesenchymal-Transition (EMT) [9], we hypothesize that it would be possible to modulate the differentiation of BMSCs by E-Cad-Fc and N-Cad-Fc into neurons and glia. To test our hypothesis, we cultured BMSC spheroids with N-Cad-Fc or E-Cad-Fc, followed by treatment with neural differentiation inducing media. Then we analyzed the glia to neuron ratio in each of the different conditions in which BMSC spheroids were cultured and their calcium activity to see if they are functional differences.

## 4.3 Experimental

### *4.3.1 Cell Culture*

Bone marrow-derived mesenchymal stem cells (BMSCs) isolated from mouse's tissue with a passage number lower than 26 were used. Dulbecco's modified Eagle' Medium (DMEM; Invitrogen) supplemented with 10% fetal bovine serum (FBS; Invitrogen) and 100 units/ml penicillin-streptomycin (PS; Invitrogen) was used to culture the BMSCs. Cells were cultured in a tissue culture flask up to 70% confluence.

### *4.3.2 Spheroid Formation*

BMSCs were induced to form spheroids by culturing them with the hanging drop method (Fig.4.1) [10]. Spheroids were cultured for three days before beginning differentiation media. Thirty spheroids were used per condition and each spheroid was made with 30,000 BMSCs in

30µl of medium. Three conditions were evaluated: spheroids culture with N-Cadherin (N-Cad-Fc) or E-Cadherin (E-Cad-Fc) (100µg/ml of each) and with no protein (control).

### *4.3.3 N_Cadherin Protein*

HEK293 cells previously engineered to express soluble recombinant canine chicken N-cadherin-Fc constructs (N-cad)[11] were cultured in Dulbecco's modified Eagle' Medium (DMEM; Invitrogen) supplemented with 10% fetal bovine serum (FBS; Invitrogen) and 0.4mg/ml G418 (Sigma, St Louis, MO) as a selection marker. The ckN-cad-FC construct was purified from the conditioned medium using Protein A affinity column (Bio-Rad) followed by gel filtration chromatography, as described [12]. Bead aggregation measurements confirmed the functionality of the N-cadherin [13].

### *4.3.4 Soluble E-Cadherin (E-Cad-Fc)*

EBNA 293 cell sere previously engineered to express soluble recombinant canine epithelial cadherin fused to the human Fc domain [11]where cultured in Dulbecco's modified Eagle' Medium (DMEM; Invitrogen) supplemented with 10% fetal bovine serum (FBS; Invitrogen) and 0.1mg/ml Ampicillin (Sigma, St Louis, MO) as a selection marker. The E-cad-Fc construct was purified on a Protein A affinity column (Bio-Rad) followed by gel filtration chromatography, as described [12]. Protein functionality was confirmed by bead aggregation assay [13].

### *4.3.5 Spheroid Differentiation*

After three days, the spheroids culture medium was changed to neurogenic differentiation media (PromoCell). The media was exchanged once every other day for two weeks (30µl per spheroid). Spheroids were cultured during these two weeks in a hanging drop method. As a

control for our differentiation studies spheroids were also cultured with no differentiation media for two weeks in the same set up as the differentiation studies.

### *4.3.6 Immunofluorescence imaging of spheroids*

Spheroids were fixed with 4% (w/v) paraformaldehyde in PBS overnight at room temperature. Then cells were washed twice with PBS for 5 min each time, then permeabilized with 0.5% Triton-X 100 for 30 min, and again washed twice with PBS. Permeabilized cells were blocked with 5w/v% goat serum albumin solution (Sigma) and 0.1% sodium azide (Fisher) in PBS overnight and then washed twice with PBS. Then spheroids were incubated overnight with the following primary antibodies: rabbit polyclonal antibodies against neuronal marker Microtubule-Associated Protein-2 (anti-MAP2, 1:1000, Sigma Aldrich) and mouse monoclonal antibodies against the glial marker Glial Fibrillary Acidic Protein (anti-GFA, 1:5000, BD Bioscience). Followed by three washes with PBS and were then incubated overnight with secondary antibodies ( Alexa Fluor 488 goat anti-mouse and Alexa Fluor 568 goat anti-rabbit antibodies, Invitrogen) [14]. Spheroids were washed three times with PBS and incubated with 100 ng/ml DAPI solution for 30 minutes. DIC (Differential Interference Contrast) and fluorescence images were acquired with 40x and 63x oil objectives in the laser-scanning confocal microscope (LSM700, Zeiss).

### *4.3.7 Calcium Activity of the Spheroids*

Neural-network functionality of the spheroids was evaluated by fluorescent analysis of $Ca^{\pm}$ measured in the cells by Fluo-4 NW calcium assay kit (molecular probes). The calcium activity was evaluated and quantified in terms of the intensity acquired from the images. The manufacture protocol was followed. Images then were acquired with laser-scanning confocal microscope (LSM700, Zeiss). A minimum of 15 images were analyzed per condition and images were taken from different areas of four spheroids at random.

## 4.4 Results

We have previously demonstrating that BMSCs are able to form a spheroid in the presence of N-Cad-Fc or E-Cad-Fc (Chapter 3). Using the same hanging drop technique (Fig. 4.1) we have cultured BMSCs spheroids with no protein, with N-Cad-Fc and with E-Cad-Fc. The immunofluorescent images revealed the presence of neurons (MAP2) and glia (GFAP) in all of the conditions treated with neuro-differentiation media (Fig. 4.2 & Fig. 4.3). However, the spheroids that were formed in the absence of protein (Fig. 4.2A) showed average mean intensity (AMI) ratio of neurons 0.6 ± 0.03 and glia 0.5 ± 0.02. According to this data there is a 1.18 ratio, a 1 to 1 ratio of neurons per glia. On the contrary, there was a significant decrease in the ratio of AMI of glia (0.3±0.016) in the spheroids that were previously treated with E-Cad-Fc. The ratio of AMI of neurons in these spheroids was slightly decreased to 0.52±0.02. The decrease of glia cells in the spheroids yielded a ratio of 1.6 to 1, meaning approximately 2 neurons per one glia. Interestingly, spheroids that were cultured with N-cad-Fc showed a significant decrease in the ratio of AMI for neurons 0.45 ± 0.02 as well as a decrease of the ratio of AMI glia marker 0.16 ± 0.008, given a ratio of 2.8, which translates into 3 neurons per glia were present in the spheroid treated with N-Cad-Fc.

The neural network activity was analyzed by the relative calcium intensity in the spheroids (Fig. 4.4). Spheroids cultured without protein had significantly higher relative fluorescent units of calcium intensity (43 ± 2.2) than spheroids cultured with E-Cad-Fc (32.4 ± 1.6) or N-Cad-Fc ( 11.9 ±0.6) (Fig. 4.5). Surprisingly the spheroids cultured soluble with N-Cad-Fc had a significantly lower calcium activity that correlated with the significant decrease in glia, when compared to any other condition and compared to neurons found in the spheroid (Fig. 4.3).

Further, in order to determine that the presence of neurons and glia staining in the MSC spheroids that were cultured with neural differentiating media was a true signal, and not from accumulation of the dye in non-specific location in the cytosol of the cells, spheroids without differentiation media were also cultured for the same period of time (2 weeks) with DMEM media. Spheroids were cultured with no protein, with E-Cad-Fc and N-Cad-Fc in the same was as was describe for spheroids that were culture for neuro differentiation. Then the spheroids were stained for MAP2 and GFAP (Fig. 4.6). The AMI of neurons and glia present in the spheroids was quantified (Fig. 4.7). No significant intensity was detected for either neurons or glia in the spheroids. Confirming the undifferentiated state of the BMSCs and that MAP2 or GFAP did not stain the undifferentiated cells.

## 4.5 Discussion

In this work, we demonstrated that it is possible to manipulate the differentiation ratio of neurons and glia in spheroids of BMSCs, by culturing them with soluble cadherins in the media. BMSCs have been found to aid the CNS during the healing process [1,15]. Although, it is unknown what is the specific mechanism by which MSC are involved in the healing process of CNS [16, 15]. Some studies suggest that their secreted factors can support the healing process of the injured tissue [15]. Other studies proposed that they differentiate into the cells that are needed at the site of injury [15, 17]. It is well known that E-Cad and N-Cad are involved in the MET of BMSCs [9,18]. It is possible then that E-Cad and N-Cad can modulate the differentiation rate and ratio of the BMSCs at the site of injury by activating or inactivating the Wnt/β-catenin pathways [19,20].

Previously (Chapter 3), we analyzed the gene expression of spheroids cultured with N-Cad-Fc and E-Cad-Fc and we found a down regulation of the N-Cad and E-Cad occurred respectively of the treatment (Fig. 4.8A, in Chapter 3 Fig 3.10). This could indicate that there would be more β-Catenin available in the cytosol that can bind to Wnt and possibly activate the Wnt differentiation pathway toward glia or neurons [20,21]. It is unknown to us if the down-regulation of the Cadherins would prevail during the differentiation period. Further gene studies would need to be performed in order to confirm this hypothesis. Surprisingly, the down regulation of N-Cad (0.6 ±0.03 in Fig. 4.8A) expression and E-Cad (0.5±0.02 in Fig.4.8A) expression observed with spheroids cultured with N-Cad-Fc correlates with the significant decrease in glia numbers and calcium activity (Fig.4.8A,B and C). Although, there was a decrease of neurons in spheroids cultured with N-Cad-Fc, the decrease was not as significant as compared to the decrease of glia cells. There was also a decrease of gene expression on spheroids cultured with E-Cad-Fc (0.7±0.03 N-cad and 0.6±0.03 E-cad in Fig. 4.8A), which it did cause a decrease on the ratio of BMSCs differentiated into neurons and glia (Fig. 4.8A, B and C). This data suggest that even thought there was not a statistical significant difference in the gene down regulation between spheroids cultured with N-Cad-Fc and E-Cad-Fc, it seems that this subtle difference does have a significance in the biological response of the cells.

It is well known that glia are found in the brain and that they are involved in synapse formation, maturation and network function [22]. The organization of glia and neurons in the brain is critical to maintain the health and functionality of the tissue [23]. Cell adhesion molecules such as N-Cad are critical for the migration and polarity of the tissue [15]. Calcium experiments (Fig. 4.5), confirmed the importance of the presence of glia cells in the network to be functional [23, 24]. Comparison for the relative calcium intensity (Fig.4.8) showed that the

significant decrease of calcium activity on spheroids cultured with N-Cad-Fc (Fig.4.8C) correlates to the significant decrease of glia (Fig. 4.8B). This trend can also be seen on spheroids cultured with E-Cad-Fc (Fig. 4.8B & 4.8C). The decrease of calcium intensity correlates with the decrease of glia in all conditions cultured with cadherins. Spheroids cultured with no protein yield significantly higher calcium activity and glia (Fig. 4.8B and 4.8C). Although, there was a decrease in the neurons present in the spheroids cultured with E-Cad-Fc in relation to the neurons in spheroids with no protein (Fig.4.8), it was not as significant as the decrease observed in glia expression.

Control experiments confirmed that the spheroids did differentiate into neurons and glia (Fig.4.6) and no false positive were observed due to the dye possibly staining undifferentiated cells due to its accumulation in the cytosol when spheroids were analyzed (Fig.4.7) The AMI confirmed that cells were in the undifferentiated state thus confirming that MAP2 and GFAP stained neuro differentiated data yielded a true positive result.

## 4.6 Conclusion

We were able to modulate the differentiation ratio of neurons and glia from BMSCs by cultured the BMSCs shperoids in the presence of N-Cad-Fc and E-Cad-Fc. Also, our calcium activity data correlates with the literature confirming that the increased in activity by the network correlates with the increase in number of glia present in the culture. Further, subtle changes in gene expression of the cadherins can affect the biological response of the cells. More genetic studies would need to be performed during the differentiation stages of the cells in order to confirm this hypothesis. Also, to identify if the down regulation of E-Cad or N-Cad in regulating

the cells to commit to either neurons or glia, or if both gens are involve and there is a precise amount of one of the genes need it to be present in order to favor one cell type more than the other.

*Acknowledgement*

This work was supported by National Science Foundation (CAREER: DMR-0847253 to H.K., STC-EBICS Grant CBET-0939511 to H.K., NSF CMMI 10-29871 to L.D., NSF Graduate Fellowship to J.V.), and The University of Illinois' Research Board.

## 4.7 Figures and Tables

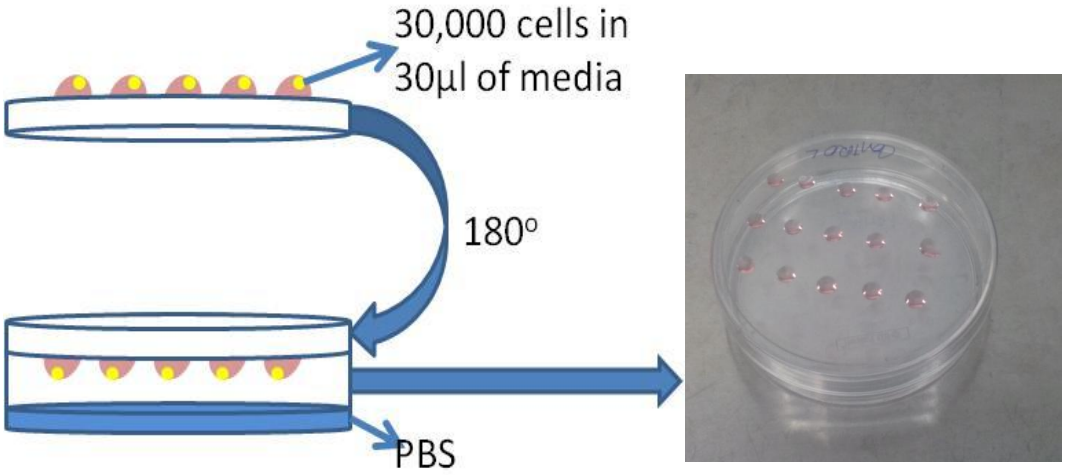


**Figure 4.1. Schematics of BMSCs cultured in a hanging drop method.** BMSCs were cultured in DMEM media with/out N-Cadherin or E-Cadherin. Spheroids were formed with 30,000 cells per drop in 30 µl of media. Fifteen spheroids were cultured per condition. The spheroids form in three days and after this media was changed for neural differentiation media. Spheroids were cultured in hanging drop method for two weeks with the neural differentiation media. Media was change every two days.

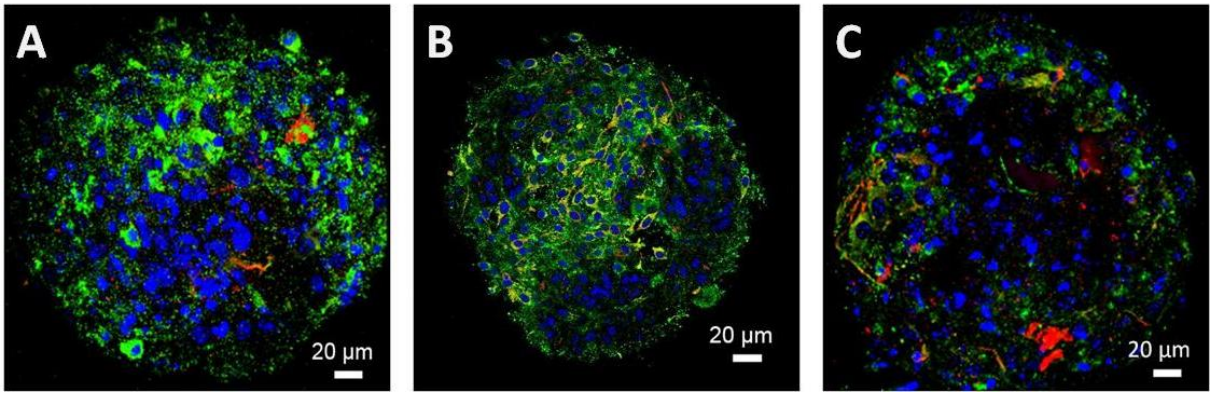


**Figure 4.2. Fluorescence microscopy images of neurons and glia present in the differentiated spheroids.** Spheroids cultured with no protein (A), N-Cad-Fc (B) and E-Cad-Fc (C) were cultured with neurogenic differentiation media. MAP2, GFAP and DAPI.

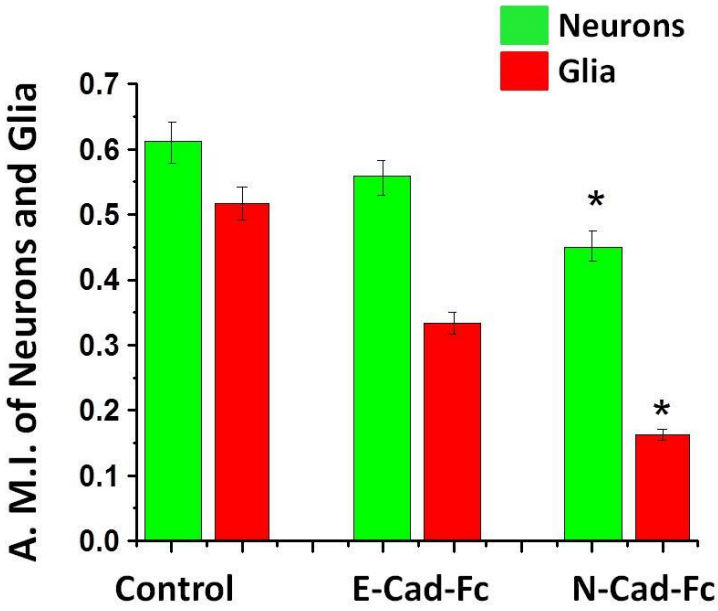


**Figure 4.3** were stained and quantified (D). A statistically significant decrease on glia and neurons was found in the spheroids that were previously treated with N-Cad. p-value <0.05

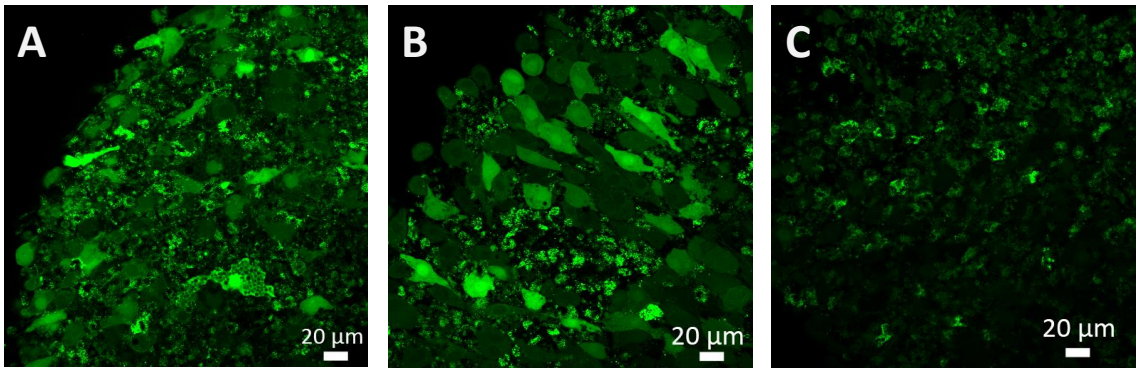


**Figure 4.4. Cells calcium activity.** The network like structure activity was checked by measuring the calcium activity in the spheroids cultured with no protein (A), E-Cad (B) and N-Cad (C).

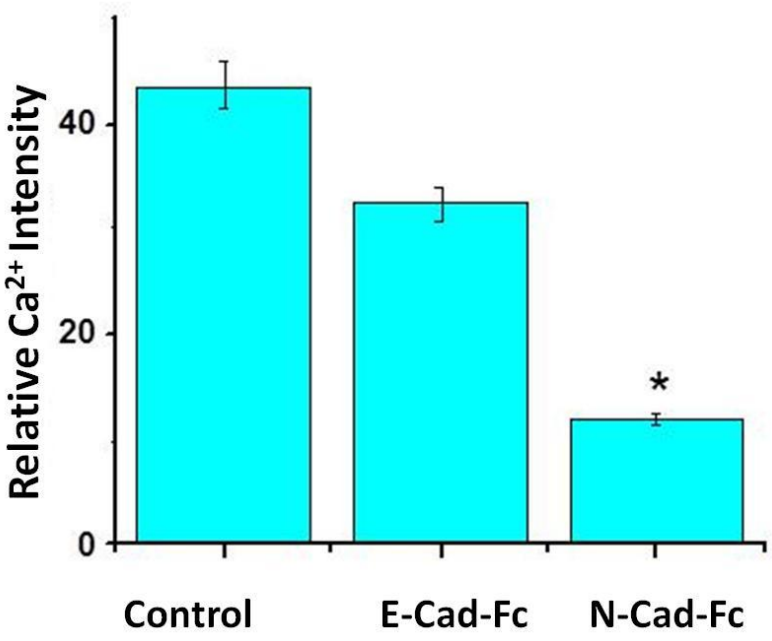


**Figure 4.5.** The relative calcium intensity was analyzed. Significantly lower calcium activity was obtained from spheroids cultured with N-Cad.

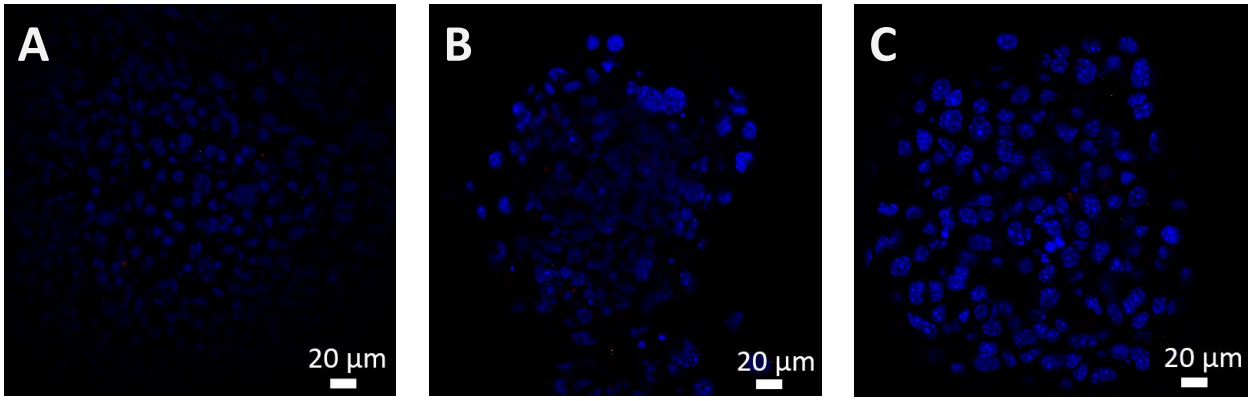


**Figure 4.6 Fluorescent images of undifferentiated spheroids stained for neurons and glia.** Spheroids cultured with no protein (A) E-cad (B) and N-Cad (C) for two weeks without differentiated media were stained for MAP2, GFAP and DAPI **.**

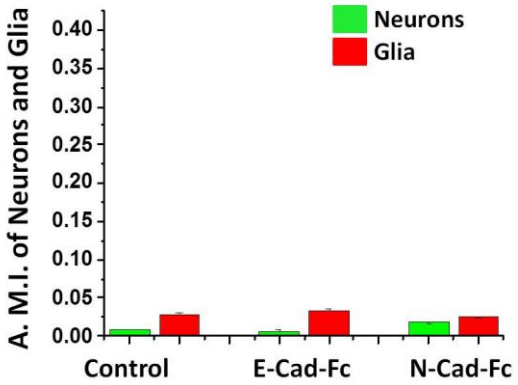


**Figure 4.7.** Analysis of the average mean intensity (AMI) was plotted (D). No neurons or glia were found in these spheroids.

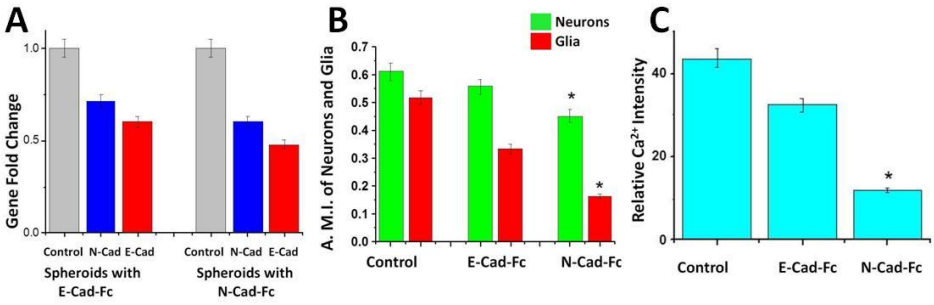


**Figure 4.8.** mRNA gene expression of N-Cad and E-Cad on BMSCs spheroids to the neurons, glia and calcium activity found in the differentiated cells. mRNA gene expression of N-Cad and E-cad was determined on spheroids cultured on E-Cad-Fc and N-Cad-Fc prior to begin differentiation studies (A) this data is also in Chapter 3 (Fig. 3.10). Analysis of the neurons and glia present of spheroids in relation to the nucleus (B). Calcium activity measures of the spheroids, a minimum of 15 images were analyzed from four spheroids at random(C) p-value<0.05.

## 4.8 References


**1.** Scheibe, F., Klein, O., Klose, J., and Priller, J. Mesenchymal stromal cells rescue cortical neurons from apoptotic cell death in an in vitro model of cerebral ischemia. *Cell. Mol. Neurobiol.* 2012; 32:567-576.

**2.** Kim, M., Kim, K. H., Park, S. R., and Choi, B. H. Mesenchymal stem cells for treatment of neurological disorders: a paracrine effect. *Tissue Eng. and Reg. Med*. 2013; 10: 234-245.

**3.** Baksh, D., Song, L., and Tuan, R.S. Adulth mesenchymal stem cells: characterization differentiation, and application in cell and gene therapy. *J. Cell Mol. Med.* 2004; 8:301-316.

**4.** Alagesan, S., and Griffin, M. D. Autologous and allogeneic mesenchymal stem cells in organ transplantation: what do we know about their safety and efficacy? *Stem Cell Trans.* 2014; 19: 65-72.

**5.** Barania, P.R., and McDevitt, T. C. Scaffold-free culture of mesenchymal stem cells spheroid in suspension preserves multilineage potential. *Cell Tissue Res.* 2012; 347: 701-711.

**6.** Crapo, P. M., Medberry, Ch.J., Reing, J. E., Totey, S. Van der Merwe, Y., Jones K. E., and Badylak, S. F. Biologic Scaffolds composed of central nervous system extracellular matrix. *Biomaterials.* 2012; 33: 3539-3547.

**7.** Banerjee, M., and Bhonde, R. R. Application of hanging drop technique for stem cell differentiation and cytotoxicity studies. *Cytotechnology.* 2006; 51:1-5.

**8.** Li, QM., Fu, YM., Shan, ZY., Shen, JL., Zhang, XM., Lei, L., and Jin, LH. BMSCs guide neurite directional extension and promote oligodendrogenesis in NSCs. *Biochem. and Biophy. Res. Comm.* 2009; 384: 372-377.

**9.** Gheldof A., and Berx, G. Cadherins and Epithelial to Mesenchymal Transition. *Progress in Mol. Biol. and Trans. Science.* 2013:116: 317-336.

**10.** Foty, R. A simple hanging drop cell culture protocol for generation of 3D spheroids. *J.Vis.Exp.* 2011. P.2720

**11.** Lambert, M., Padilla, F.,and Mege, R-M. Immobilized dimmers of N-cadherin-Fc chimera mimic cadherin-mediated cell contact formation: contribution of both outside-in and inside-out signals. *J. Cell Sci.* 2000**;** 113: 2207-2219.

**12.** Chappuis-Flament, S., Wong, E., Hicks, L.D., Kay, C.M., and Gumbiner, B.M. Multiple cadherin extracellular repeats mediate homophilic binding and adhesion. *J. Cell Biol.* 2001; 154: 231-243.

**13.** Sivasankar, S., Brieher, W., Lavrik, N., Gumbiner, B., and Leckband, D. Direct molecular force measurements of multiple adhesive interactions between cadherin ectodomains. *Proc. Natl. Acad. Sci.* 1999; 96: 11820-11824.

**14.** Intracellular calcium assays in dissociated primary cortical neurons: Doering, L. C., Editor. Springer protocols handbooks. 4th ed. McMaster University, Hamilton, ON, Canada. *Humana Press;* 2010: 125-136.

**15.** Ma, S. Xie, N., Li, W., Yuan, B., Shi, Y and Wang, Y. Immunogiology of mesenchymal stem cells. *Cell Death and Diff.* 2014; 21: 216-225.

**16.** Voulgari-Kokota, A., Fairless, R., Kramita, M., Kyrargyri, V., Tseveleki, V., Evangelidou, B., Delorme, B., Charbord, P., Diem, R., and Probert, L. Mesenchymal

stem cells protects CNS neurons against glutamate excitotoxicity by inhibiting glutamate receptor expression and function. *Exp. Neuro.* 2012; 236:161-170.

**17.** Kolf, C.M., Cho, E., and Tuan, R. S. Biology o adult mesenchymal stem cells: regulation of niche, self-renewal and differentiation. *Arthritis Res.&Therapy*. 2007; 9:204, 10 pages.

**18.** Lu,K.V., Chang,J.P., Parachoniak, Ch.A., Pandika, M.M., Aghi, M.K., Meyronet,D., Isachenko, N., Fouse, Sh.D., Phillips,J.J., Cheresh, D.A., Park, M. and Bergers, G. VEGF inhibits tumor cell invasion and mesenchymal transition through a MET/VEGFR2 complex. *Cancer Cell.* 2012; 22:21-35.

**19.** Yeh, HY., Liu BH., and Hsu, SH. The calcium-dependent regulation of spheroid formation and cardiomyogenic differentiation of MSC on chitosan membranes. *Biomaterials.* 2012; 33: 8943-8954.

**20.** Adherens Junctions: From molecular mechanism to tissue development and disease. *Subcellular Biochemistry*. 2012; 60: 9- 62 and 171-249.

**21.** Radice, G. L. N-Cadherin-Mediated adhesion and signaling from development to disease: lessons from mice. *Progress in Molecular Biology and Translational Science*. 2013; 116: 263-289.

**22.** Halbleib, J.M., and Nelson J. Cadherins in development: cell adhesion, sorting, and tissue morphogenesis. *Genes and Devel.* 2006; 20:3199-3214.

**23.** Nedergaard, M., Ransom, B., and Goldman, S.A. New roles for astrocytes: Redefining the functional architecture of the brain. *Trends in Neuro.* 2003; 26:523-530.

**24.** Mori, T., Buffo, A., and Gotz, M. The novel roles of glial cells revisited: the contribution of radial glia and Astrocytes to neurogenesis. *Current Topics in Devel. Bio*. 2005; 69:67-99.

# Chapter 5: The biological conjugation of N-Cadherin to 3D microchannel alginate gels is permissive to cells and allows the active neural network formation.

## 5.1 Abstract

In the brain, neurons and glia are arranged in what could be seen as random but in reality, there is a highly specialized system that maintains a tight organization of geometry and signals. The study of this has been challenging because it has been difficult to gain accurate knowledge from a system that is three dimensional *in vivo* and until now most cultures have been in monolayers or 2-D. With this in mind, increase studies in 3-D have been developed. Here we cultured rat E19 cortical neurons in a 3-D microchannel alginate hydrogel biologically coupled with Fc-tag-N-Cadherin (N-Cad-Fc). The presence of N-Cad-Fc along with the parallel arrangement of the porous alginate gel provided a suitable environment for neurons and glia adhesion with a high neural network activity. In contrast, neural network activity in 3-D microporous alginate gels biologically coupled with N-Cad-Fc was significantly lower. These results suggest that there is a synergistic effect between the geometry of the material and N-Cad-Fc that can influence the neural cell adhesion and neural network activity.

## 5.2 Introduction

The complex structure of the brain contains different cell types that allow the response of the motor and sensory input and output through the body [1,2]. Unfortunately, a clinical treatment is not currently available to restore the function of the central nerve system (CNS) after brain injury [3,4]. Development of a three-dimensional (3-D) model that can mimic the brain tissue can enable the cells to behave similar to the *in vivo* models in an *in vitro* set up where studies of CNS can be performed and the variables can be controlled [5]. Providing further understanding on what are the permissive cues needed in the environment for the CNS to regenerate [5]. *In vitro* models facilitate the control of the components that are in the extracellular matrix (ECM) and to make measurements and observations that are not possible *in vivo* [5]. There are different inhibitory responses that form during the CNS repair in the brain and it would be logical to learn how to overcome these in a 3-D artificial environment [6].

It is well known that neurons behave differently in a 2-D than in a 3-D environments [6]. Hydrogels are crosslink polymer networks with high water content and are suitable for mimicking a 3-D environment [6]. Unfortunately, 3-D hydrogel cultures are typically randomly oriented making it difficult to replicate the tissue architecture *in vitro* [6]. Several studies have established that the extracellular molecular cues are the critical stimulus that initially direct axons to their targets, and that is the synaptic activity that refines the neural circuits [7]. Parallel arrangement and protein gradient have shown to promote axon guidance and synapse formation [7].

Alginate is a natural polymer (polysaccharide) derived from the cell walls of brown algae [8]. This polymer has been extensively used in the encapsulation of mammalian cells because it is biocompatible and has low toxicity [9]. Alginate can be used to study the protein interaction of

the ECM with the cell, since it inherently lacks mammalian cell adhesivity [9]. Previous studies have demonstrated the used of alginate to encapsulate a variety of neural cell types and glia cells, demonstrating the cells are viable and that their morphology changes in a 3-D cell culture when compared to a 2D [8].

In this work we hypothesized that the use of N-Cad-Fc to modify microchannels in a 3-D alginate hydrogels would be advantageous for culturing cortical neurons providing a permissive environment for functional cortical neurons networks to form. The use of microchannels would allow the fluid exchange, as well as providing an adequate mechanical and chemical support for neurons to survive, synapse, and form a network [10]. In comparison to mircorporous alginate gel, which has a randomly oriented structured we expect that would be a less advantageous environment for a functional neural network to form.

## 5.3 Experimental

### *5.3.1 Fc-tagged N-Cadherin (N-Cad-Fc) synthesis*

Fc-tagged chicken N-cad constructs (N-Cad-Fc) was obtained from previously engineered HEK293 cells to secrete the recombinant N-Cad-Fc [11]. Cells were cultured in Dulbecco's modified Eagle Medium (DMEM, Invitrogen) supplemented with 10% fetal bovine serum (FBS, Invitrogen) and 0.4 mg/ml G418 (Sigma) as a selection marker. The cell supernatant was collected, filtered and N-Cad-Fc was isolated by using protein A affinity column (Bio-Rad) followed by gel filtration chromatography, as described [12]. Protein functional activity was confirmed by bead aggregation measurements [13].

*5.3.2 Cortical Neurons Cell Culture*

All procedures involving animals were reviewed and approved by the Institutional Animal Care and Use Committee at the University of Illinois Urbana-Champaign in accordance with the guidelines of the U.S. National Institutes of Health (Hee Jung Chung's Protocols 10199, 12240). Cortices were obtained and dissected from rats embryos at 18-19 days (E18-E-19) and the cortical neurons were isolated as previously described [14]. Cortices were incubated with 3 mg/ml protease 23 (Sigma) in 1X slice dissection solution (82 mM $Na_2SO_4$, 30 mM $K_2SO_4$, 10 mM HEPES, 10 mM Glucose, 5 mM $MgCl_2$ and 0.001 % Phenol Red pH 7.4) for 10 minutes at 37$^{o}$C followed by washing them with plating medium (10 % Fetal Bovine Serum (FBS), 20 % (w/v) glucose, 1% sodium pyruvate (100 mM), and 2 mM L-Glutamine in MEM mixed with Earle's BSS without L-glutamine), and dissociation into single cells took place in 3 mL of plating medium. Single cells were seeded on a monolayers (2-D) and three-dimensional (3-D) (microporous and microchannel) alginate gels were modified with N-Cad-Fc or Fc-Antibody-Fc- N-Cad at 1 x $10^5$ cells/cm.$^2$ The medium was replaced after 4 hrs with the maintenance medium (neural basal serum free media (invitrogen) containing B27 (invitrogen) extract, 2mM L-Glutamine and100 units/ml PS).

*5.3.3 Alginate Gel Preparation*

Alginate gels were prepared by 2 wt% alginate (Mw ~ 50,000 g/mol, FMC Biopolymer) dissolved in MES buffer (0.1 M 2-(N-morpholino) ethanesulfonic acid (MES, pH6.5), followed by filtration. Then 1-hydroxybenzotriazole (Hobt, Fluka), 1-ethyl-3-(3-dimethylaminopropyl) carbodiimide (EDC, Thermo Scientific), and adipic acid dihydrazide (AAD, Sigma-Aldrich) were added, and the pH was adjusted to 6.0. EDC:Hobt:AAD molar ratio was of: 1.0:0.5:0.2.

Gels were made in a sandwich configuration between two glass slides. Hydrogel disks were punched out with diameters of 5 mm and swollen in DI water at room temperature overnight before the freezing process, followed by lyophilization (Fig. 5.1). All hydrogels had a 5mm in diameter and 0.68 mm of thickness. The microporous gels and microchannel gels were prepared as described previously elsewhere [10].

### *5.3.4 Biological/Chemical conjugation of N-Cad-Fc to Alginate hydrogel using Fc-antibody and EDC/NHS*

After lyophilization, microporus and microchannel gels were modified by 1-ethyl-3-(3-dimethylaminopropyl) carbodiimide (EDC, Thermo Scientific) and 1-hydroxybenzotriazole (Hobt, Fluka). Biological conjugation (Fig. 5.2) was accomplished by dissolving EDC and Hobt in DI water at a concentration of 0.4mg and 1.1 mg per 1ml of Di $H_2O$ respectively. Gels were cover with this solution and left overnight at 4$^{o}$C, followed by three washes with PBS. Anti-Fc-antibody (Sigma) was dissolved in PBS at 250 µg/ml and was add it to the gels and left overnight at 4$^{o}$C. Then three washes with PBS were used to remove the unbound anti-Fc-antibody. Finally, the gel was incubated overnight at 4 $^{o}$C with N-Cad-Fc in HEPES buffer (20 mM HEPES, 50 mM NaCl, 5 mM CaCl) at concentration of 250 µg/ml. Then the gel was washed three times with D-PBS to remove unbound N-Cad-Fc [15].

Chemical conjugation of N-Cad-Fc to alginate hydrogel was accomplished by directly adding the N-Cad-Fc in HEPES buffer at 250 µg/ml concentration, after previously treating the gel with EDC/NHS. The protein solution was left at 4$^{o}$C overnight, followed by three washes with D-PBS [15].

The compressive analysis of the alginate microchannel and microporous gels was accomplish by scanning electron microscopy (SEM) and has been previously reported by our lab elsewhere [10].

### *5.3.5 Cortical neuron function*

The neural-network function was evaluated by fluorescent analysis of $Ca^{+2}$ measured in cortical neuron cultures in 2-D and 3-D alginate gels. The Fluo-4 NW calcium assay kit (molecular probes) was used to evaluate and quantify the activity in the cortical neuronal cultures. The protocol was followed as described by the company. Images then were acquired with laser-scanning confocal microscope (LSM700, Zeiss). A minimum of 10 images were analyzed per condition and images were taken from different areas of the gels at random.

### *5.3.6 Immunofluorescence imaging of neural networks*

At three weeks after seeding the cells, neurons were fixed with 4% paraformaldehyde for 1hr, and rinsed with D-PBS three times. Following permeabilization with 0.3 % Triton-X in D-PBS for 30 min at room temperature, neurons were blocked with 5% goat serum diluted in D-PBS overnight, and sequentially incubated with primary and secondary antibodies. The primary antibodies used were rabbit polyclonal antibodies against neuronal marker Microtubule-Associated Protein-2 (anti-MAP2, 1:1000, Sigma Aldrich) and mouse monoclonal antibodies against the glial marker Glial Fibrillary Acidic Protein (anti-GFA, 1:5000, BD Bioscience). Secondary antibodies used were Alexa Fluor 488 goat anti-mouse and Alexa Fluor 568 goat anti-rabbit antibodies [16]. Neurons were rinsed 3 times with PBS and incubated with 100 ng/ml DAPI solution for 20 minutes. The DIC and fluorescence images were acquired with laser-scanning confocal microscope (LSM700, Zeiss).

### *5.3.7 Statistical Analysis*

All average data are presented as means ± SE. To determine significance, comparisons between groups were performed by one-way ANOVA followed by Tukey's Multiple Comparison Test ($p < 0.05$).

### *5.3.8 Scanning Electron Microscopy images*

At three weeks neurons were fixed by 4% paraformaldehyde for 1hr, and were washed three times with D-PBS. Followed by freezing the samples overnight at 20$^{o}$C and lyophilized for one day. Then the samples were analyzed by cryo-fractured cross section with a field emission scanning electron (FESEM, S-4800 Hitachi) microscope at an accelerating voltage of 5kV after coating samples with an Au by ion sputtering.

## 5.4. Results

Based on our previous work (Chapter2) [15], alginate hydrogels were modified by the biochemical (Fig. 5.1) and chemical method (no shown). Alginate pours were aligned forming microchannels as we previously described [10] and were compared to microporous gels (Fig. 5.1A & 5.1B respectively). This modified alginate constructs (microchannels and microporus) were favorable for stability and viability of cortical neural cultures. Cultures were viable for up to four weeks and all studies were performed between the second and third week of been in cultured. The microchannel provided an organized pattern and multiple layers for the cells to interact and develop a network, as well as providing an easy fluid exchange environment (Fig. 5.1B and 5.3). In contrast, microporous gels did not provide organized structured with patterns

for the cells to form a network on the contrary it increased the cell clumping formation (Fig. 5.1A and 5.5).

Cortical neurons cultured in microchannel and micropores gels with no protein showed no statistical difference in the approximate number of cells that adhere to gels (Fig. 5.3A-I & Fig.5.5B-I), with an average ratio of intensity of 0.276 ± 0.08 and 0.28±0.06 from neurons in microchannels and micropores respectively. However, there was a significant difference in the number of ratio of intensity from glia cells that adhere to the microchannels (0.04 ± 0.002) and microporous (0.006± 0.001). Relative calcium intensity was also significantly higher in microchannel gels (13. ±0.6) then microporous gels (6.3±0.3) (Fig. 5.7A-I, Fig.5.7B-I and Fig.5.8). Suggesting that, microchannel gels would probably enable higher neurons and glia cell adhesion, which explained the increase in calcium activity. The only difference between these gels is the geometrical arrangement. The SEM images of each condition show the arrangement of the material and the cells that adhere (Fig. 5.3a-I and Fig. 5.5b-I).

In contrast chemically bound N-Cad significantly increases the amount of cells that adhere to the hydrogels compared to gels with no protein (Fig.5.4 &Fig. 5.6). However, no significant difference was found in the average mean intensity of neurons between microchannel (0.29 ± 0.01) and microporous (0.29 ±0.01) gels with or without N-cad-Fc (Fig 5.3A-II, 5.4 & 5.5B-II, 5.6) On the other hand, the number of glia adhering to microporous gels did increase as was detected by the analysis of the average mean intensity in microchannel (0.12 ± 0.07) and microporous (0.13 ± 0.03)gels, in comparison with gels without protein (Fig. 5.4 &5.6). Analysis of calcium activity yielded a significant statistical difference between chemically modified N-Cad-Fc to microchannel (31.4 ± 1.5) and microporous (19.5 ± 0.9) gel (Fig. 5.8). However, the

network like structure that formed in these two conditions was predominantly formed by clumping of the cells (Fig.5.3A-II, 5.3a-II & Fig. 5.5B-II, 5.5b-II).

Biologically modified N-Cad-Fc microchannel and microporous alginate gels allowed a significant increase on neural cell adhesion to the gels as well as functionality (Fig. 5.3A-III, 5.5B-III, and 5.8), when compared to chemically modified alginate gels or gels with no protein. Statistically significantly higher relative calcium intensity was obtained for neurons (0.6 ± 0.03) and glia (0.18 ±0.09) in microchannels (Fig.5.4) than in microporous gels (0.4±0.02 neurons and 0.14 ± 0.007glia) (Fig. 5.6). The biological coupling of N-Cad-Fc significantly influenced the cell adhesion to the gles. The relative calcium intensity also significantly increased in biologically modified microchannels (47.5 ± 2.4) and microporous (28.6 ±1.6) gels (Fig. 5.8). When compared to any other condition microchannels biologically coupled with N-cad-Fc showed higher cell adhesion and network functionality (Fig. 5.13). Also, cell clumping decreased (Fig. 5.3A-III), as can be seen in the SEM (Fig. 5.3a-III), cells grow along the gel fibers.

Per comparison, cortical neurons were also cultured on monolayers on N-Cad-Fc alginate gels chemically and biologically modified as well as alginate gels without N-Cad-Fc and their calcium activity was also analyzed (Fig. 5.11 & 5.12). Cells adhere in all three conditions, only in the biologically modified N-Cad-Fc alginate gel was observed a network like structure that was form due to the clumpling of the cells (Fig. 5.11C-III). Higher calcium activity was also observer in biologically couple N-Cad-Fc when compared to cells cultured on gels without N-Cad-Fc or chemically modified N-cad-Fc (Fig. 5.12E). However, when this was compared to the cell adhesion and the calcium activity obtained on biologically couple N-Cad-Fc microchannel and microporous alginate gels it was significantly less (Fig. 5.9, 5.10D, 5.10E and Fig.5.13).

## 5.5 Discussion

Cortical neural network formation and function was examined within 3-D biologically and chemically coupled N-Cad-Fc alginate gels. First, the fabrication method enabled the control of the alignment of the porous in the gels, forming in this way channels that interconnect and form an aligned geometry of the gel fibers [10]. These microchannels not only create layers in the gel but also aligned open pores that enable the rapid exchange of solutions [16]. The alignment of fibers in the gel provided the support for cortical neurons to extend their axons and form active synapses with other neurons and glia as was confirmed by the calcium measurements (Fig. 5.4). The alginate microchannel along with biologically tethered N-Cad-Fc provided a permissive matrix to culture cortical neurons in 3-D. In contrast, random arrangement of microporous biologically modified N-Cad-Fc was permissive for cell adhesion, unfortunately higher cell clumping was observe (Fig. 5.5B-III). Also, the calcium activity reported in these cultures it was significantly lower than microchannel gels biologically couple with N-Cad-Fc (Fig. 5.10). It is possible that the random arrangement of the pores in the gel prevented cells from extending their axons or migrating, due to the lack of continuality of the layers and fibers. Also, the decrease in glia numbers as well as the cell clumping can possibly contribute to the significantly decrease in calcium activity (Fig. 5.10). Another variable to consider is the presentation of the N-Cad-Fc binding domains, which could have been compromised duet to the lack of continuity of the material preventing cells to adhere and form synapses [15]

It has been widely accepted that even though neurons can be cultured in random surfaces they lack the structure that normally is present in their niche [2]. This implies that the cells will function abnormally as it would in their natural environment [2]. Therefore, there have been great efforts to develop techniques and materials that would favor natural network connectivity

in vitro [18]. In this work we demonstrated that patterned gels aid the neurons to adhere and form synapses. Furthermore, restricting neurons to patterns enhances their network and cellular calcium activity, in comparison when cultures in surfaces with random geometries (Fig. 5.10). These findings suggest the matrix structure can modulate the neural network formation and function.

Calcium activity measurements reveal low activity on hydrogels that did not present N-Cad-Fc protein for cell adhesion. Calcium activity increase as glia was present on these gels (Fig. 5.4, 5.6, 5.12D and 5.12E). This suggests findings correlate with the knowledge that glia can increase the calcium activity [19]. It is known that glia increases its intracellular calcium activity in response to neurotransmitters secreted by neurons such as glutamate, GABA, adrenaline, ATP, serotonin Ach and several other peptides [19]. Of the glia cells found in the mammalian brain, astrocytes are the most abundant in the brain [2]. Neurons co-cultured with astrocytes have shown an increase of sevenfold more synapses and activity in the presence of astrocytes [20,21]. Since our cell cultures were obtained from E19 rats' cortex, we expect to have astrocytes in our cultures. So, the increase of activity can correlate to the increase of glia in the cultures (Fig. 5.13), the absence or decrease of glia cells correlates with low calcium activity (Fig. 5.13B and 5.13D).

Increase knowledge about astrocytes has suggested that they may regulate the formation, maturation and maintenance of synapses [21]. Currently, the concept of "tripartite synapse," view astrocytes as an integral modulatory elements of the synapses [22]. In the central nerve system, the distribution of astrocytes is determined by contact spacing, such as, they can be evenly separated and their cell bodies processes are not in contact with each other [20]. Our biologically N-Cad-Fc modified 3-D microchannel alginate showed that not only allowed

neurons and glia to adhere to the gel but also form a functional network which was confirmed by the calcium measurements (Fig. 5.3, 5.4 and 5.13). The 3-D microchannel structure along with N-Cad-Fc biologically couple to the gel enable the culture of cortical neural networks that were significantly more active than biologically N-cad-Fc couple microporous gels (Fig 5.13C). This difference can be due to the difference in the structure of the material which was enhancing by the biological N-Cad-Fc coupled to the microchannel gel.

## 5.6 Conclusion

In this work, we were able to demonstrate that the organized arrangement of the hydrogel structure such as microchannels along with biological coupled N-Cadherin can significantly result in an advantageous environment for cell adhesion and increase of the functional activity of the neural network in a 3-D culture. This is an invaluable tool to further study the implications that N-Cad can have in the synapses and neural activity and how this compares to what occurs in vivo. Recreating the neural network complexity present in vivo, would be an invaluable tool to study how neural function and network formation is affected by different proteins, diseases and other molecules *in vitro*.

*Acknowledgment*

This work was supported by National Science Foundation (CAREER: DMR-0847253 to H.K., STC-EBICS Grant CBET-0939511 to H.K, NSF CMMI 10-29871 to L.D, NSF Graduate Fellowship to J.V.), and The University of Illinois' Research Board.

## 5.7 Figures and Tables

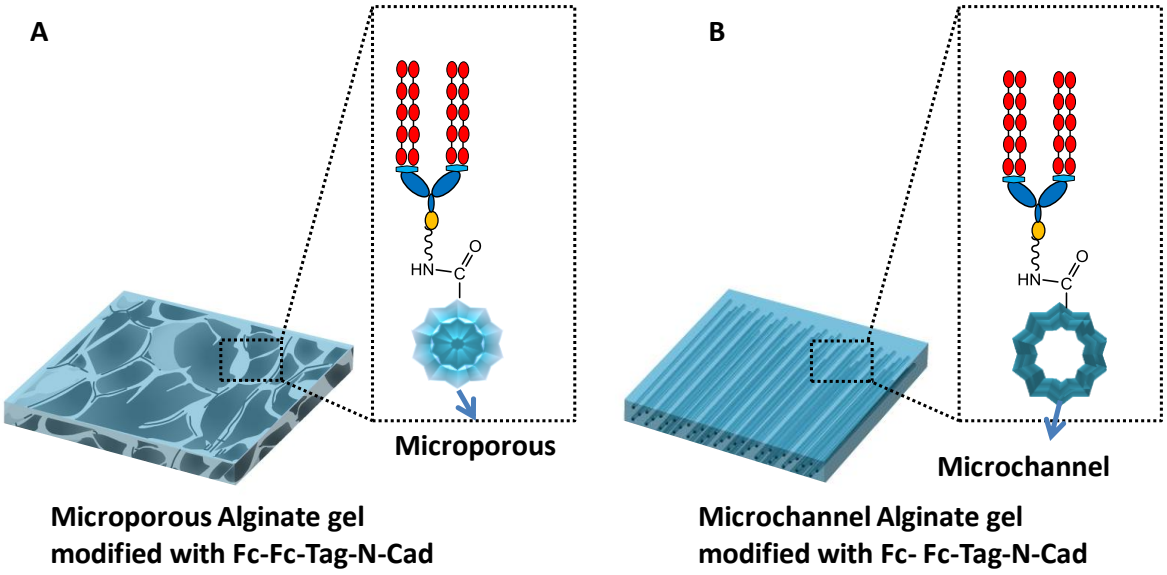


**Figure 5. 1**. **Schematics of biologically modified alginate gels with N-Cad.** Microporus alginate gel (A) modified with anti-Fc and Fc-Tag-N-Cad (biological modification), allowing complete exposure of the binding domains of N-Cad. The porous structure has been magnified. Microchannel alginate gel (B) biologically modified with N-Cad-Fc and magnification of the microchannel structure.

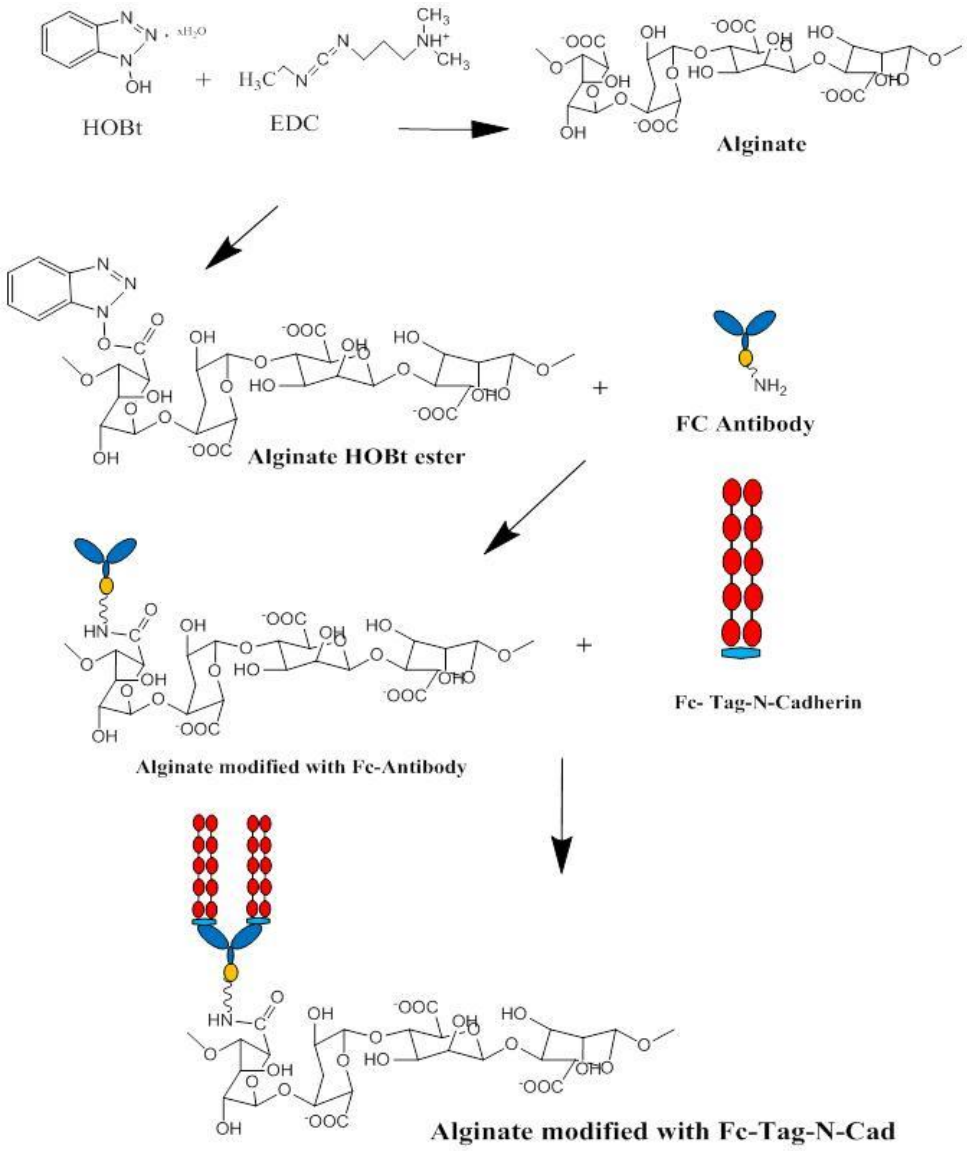


**Figure 5.2** Schematics of how alginate gel it is polymerized to form a hyrogel and further, biologically conjugated with Fc-Tag-N-Cad (N-Cad-Fc)

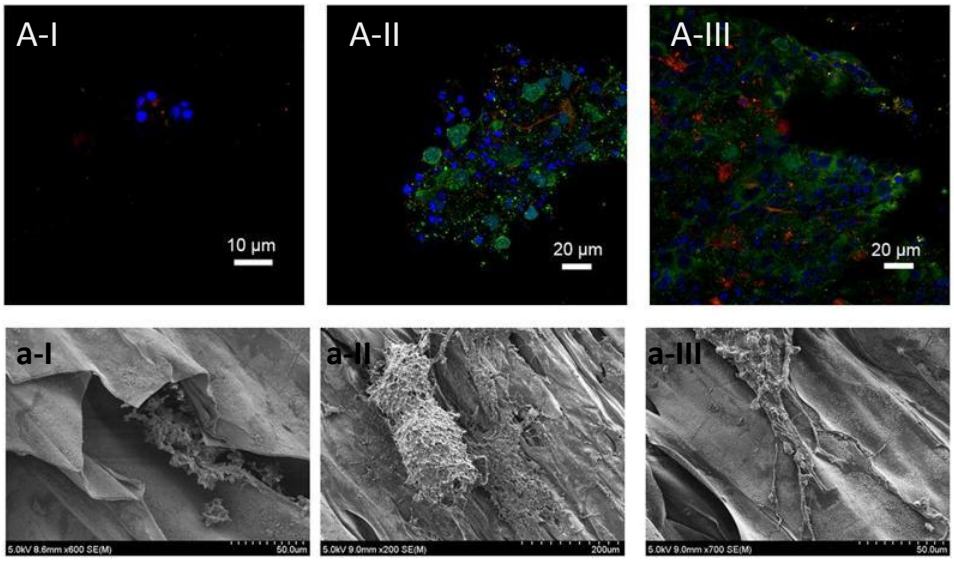


**Figure 5.3.** Fluorescent Images of Cortical Neurons on alginate microchannel gel without surface modification (AI-III) and SEM images of each condition. A-I control, A-II surface with N-Cad-Fc and A-III biological modification with Fc-antibody and N-Ca-Fc. Neurons were identified with MAP2, glia cells with GFAP and cellular nuclei was identified with DAPI.

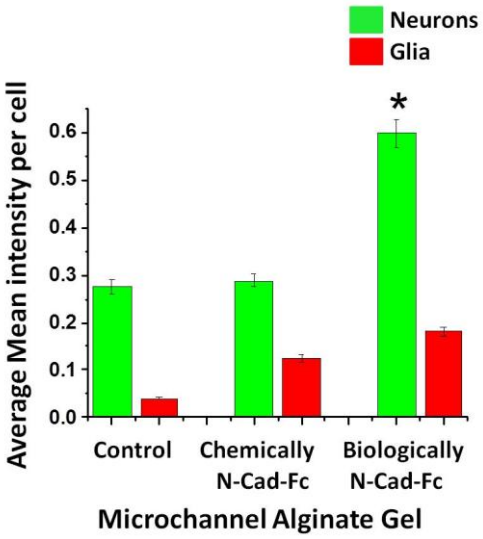


**Figure 5.4.** Depicts the statistical analysis of the neurons and glia present on each condition. Cortical neurons cultured on microchannel gels with biological linkage of N-Cad-Fc show a significant increase on neurons that adhere to the surface when compared to any of the other conditions.

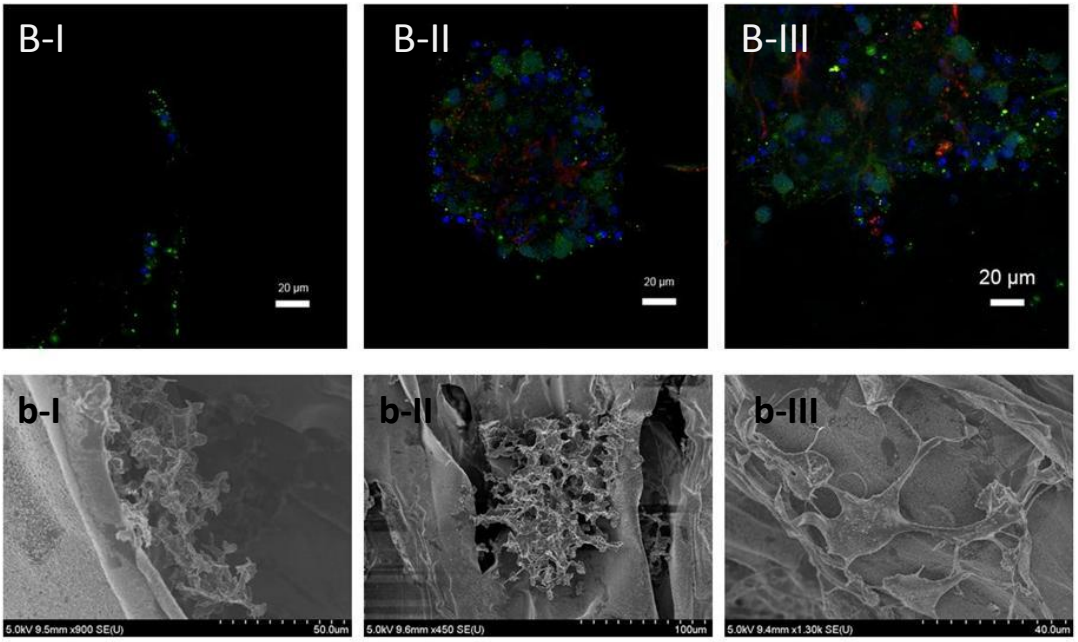


**Figure 5.5**. Fluorescent Images of Cortical Neurons on alginate microporous gel without surface modification (BI-III) and SEM images of each condition. B-I control, B-II surface with N-Cad-Fc and B-III biological modification with Fc-antibody and N-Cad-Fc. Neurons were identified with MAP2, glia cells wih GFAP and cellular nuclei was identified with DAPI.

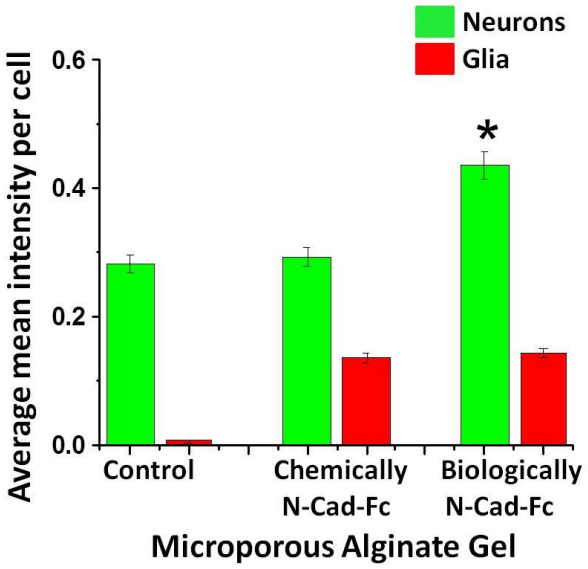


**Figure 5.6.** Depicts the statistical analysis of the neurons and glia present on each condition. Cortical neurons cultured on microchannel gels with biological linkage of N-Cad show a significant increase on neurons that adhere to the surface when compared to any of the other conditions.

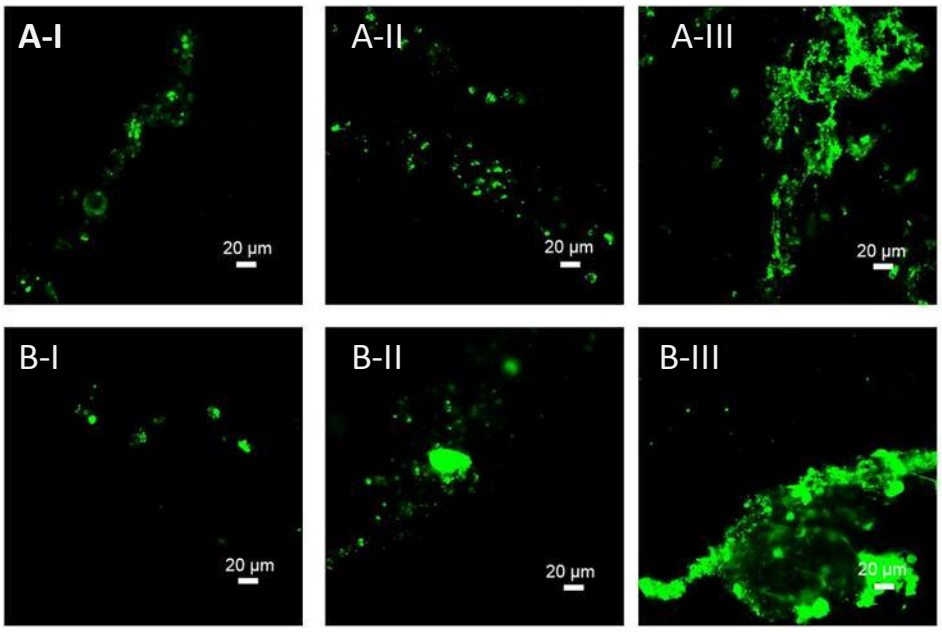


**Figure 5.7.** Calcium measurements of E19 cortical neurons cultured either on microchannel (AI – III) or microporous (BI-III) alginate gels modified with N-Cad-Fc. A-I neurons were cultured with no protein on the gel, A-II shows the neurons cultured on the gel modified directly with N-Cad-Fc, while on A-III the protein was biologically linked to the gel by the use of Fc-Antibody. B-I neurons were cultured with no protein on the gel, B-II shows the neurons cultured on the gel modified directly with N-Cad-Fc, while on B-III the protein was biologically linked to the gel by the use of Fc-Antibody.

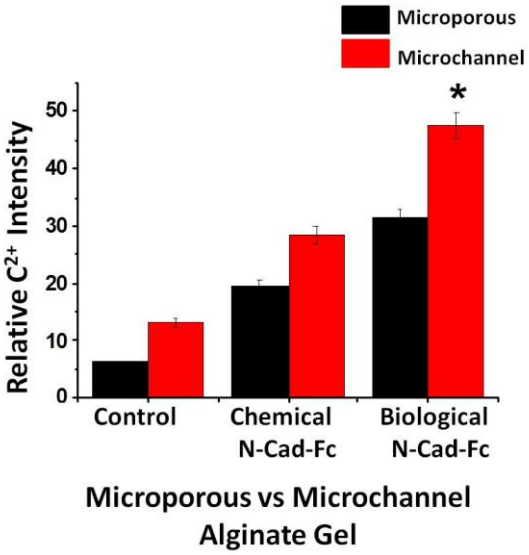


**Figure 5.8.** Presents the statistical analysis of the calcium activity on the neural cultures and shows the comparison between conditions. Cortical neurons show a statistically significant increase on activity when they were cultured on microchannel gels biologically modified with N-Cad-Fc when compared with any of the other conditions.

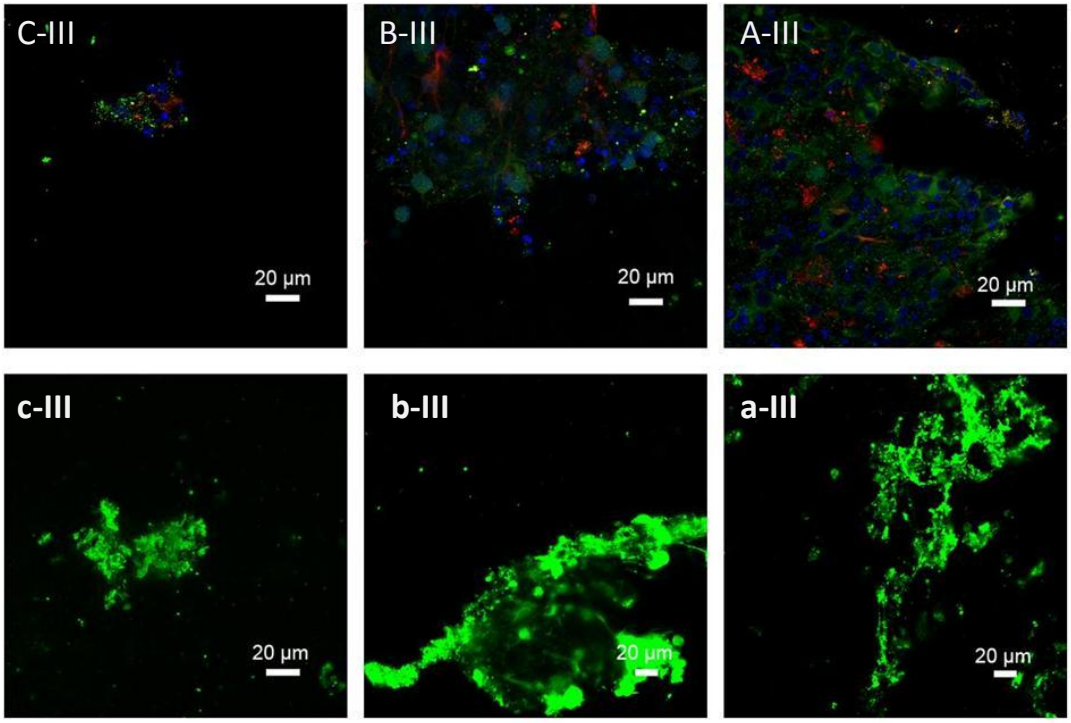


**Figure 5.9. Comparison biologically couple N-Cad in 2D microporous and microchannel alinate gels.** Fluorescent images of 2D (C-III) , microporous (B-III) and microchannel (C-III) E-19 cortical neurons stained for MAP2 , GFAP and DAPI.

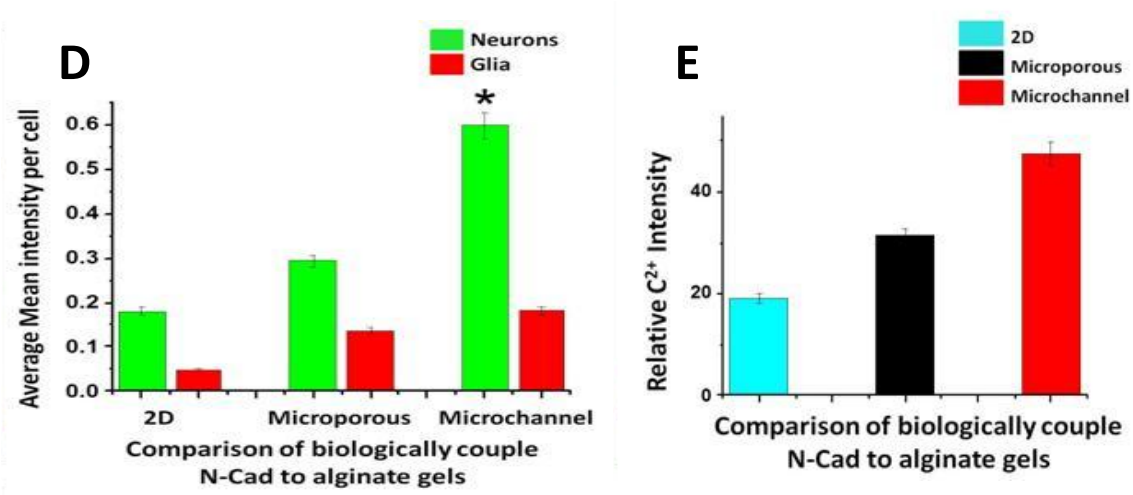


**Figure 5.10.** The average mean intensity of neurons and glia was analyzed against the nuclei per image (D). Calcium intensity images of 2D (c-III), microporous (b-III) and microchannel (a-III). The intensity was acquired from 15 images per condition and the average was plotted (E). p-value < 0.05.

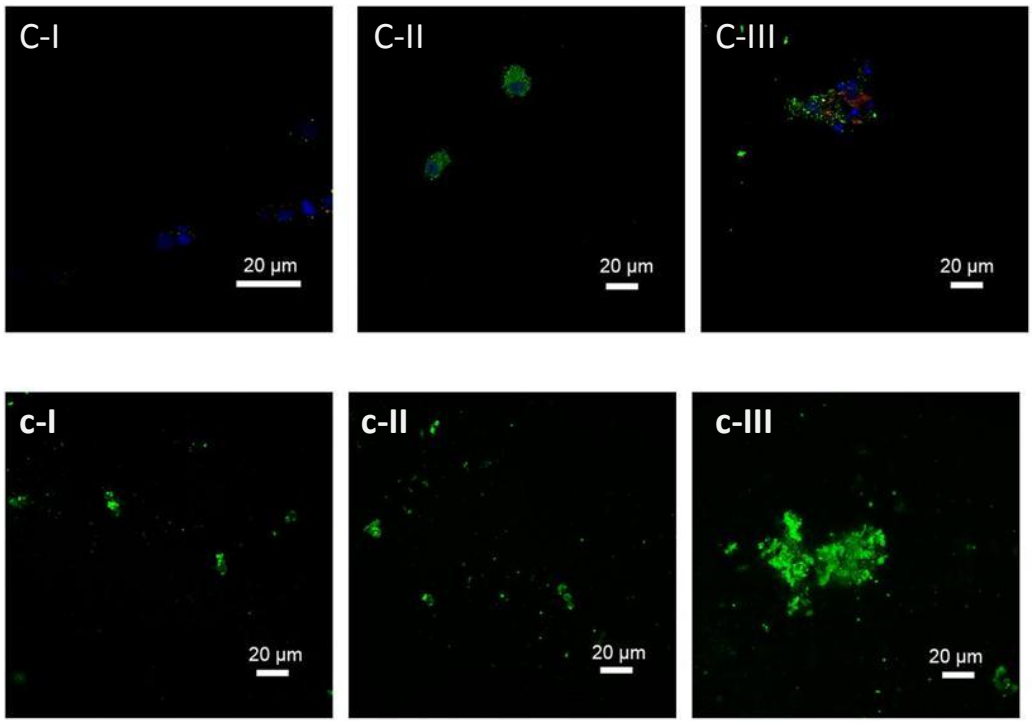


**Figure 5.11. Monolayer cultures of cortical E19 neurons on alginate gels.** Fluorescent images of cortical neurons cultured on gels with no protein (C-I), chemical (C-II) and biological (C-III) conjugation of N-Cad-Fc depicts MAP2 , GFAP and DAPI.

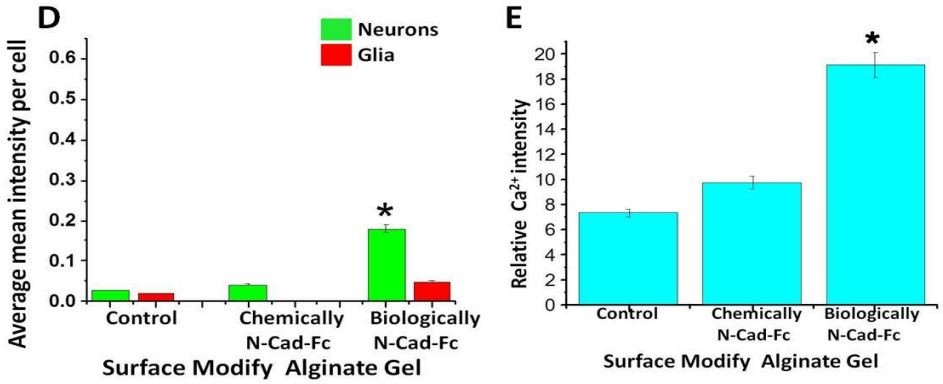


**Figure 5.12.** Images were analyzed and neuron and glia were quantified as an average mean intensity per cell (D). Calcium images of no protein (C-I), chemical (C-II) and biological (C-III) were used to analyzed the calcium activity (E) in the cultures. p-value <0.05

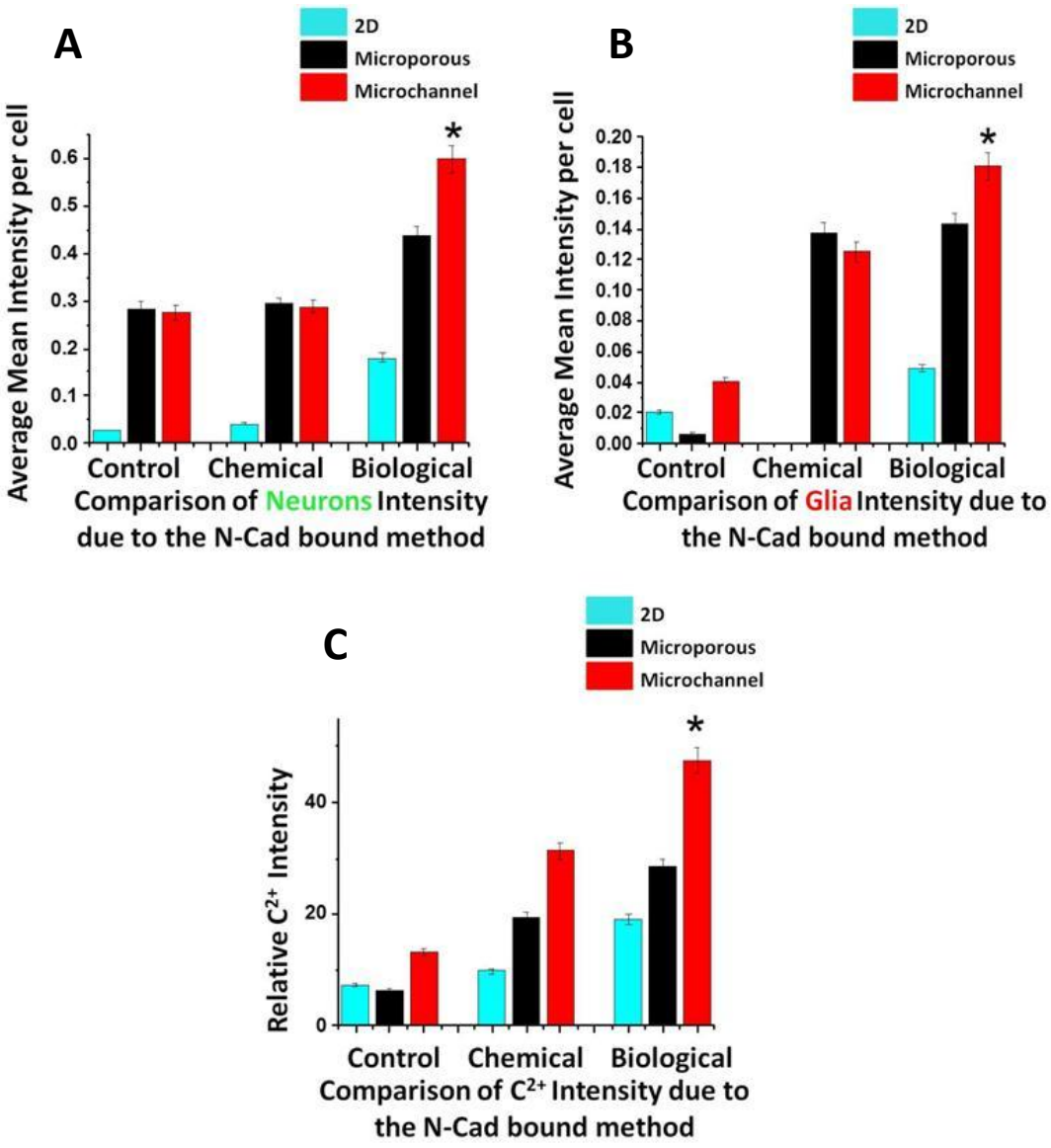


**Figure 5.13. Statistical comparison of neurons, glia and calcium intensity in all the conditions.** Neurons (A), glia (B) and calcium intensity (C) were analyzed and compared for 2-D, microporous, and microchannel gels without N-Cad-Fc and chemically and biologically modified with N-Cad-Fc. Statistically significant increase of neurons, glia and calcium intensity of cortical neurons cultured on biochemical modified N-Cad-Fc microchannel alginate gels was found when compared to any other condition. Chemically modified N-Cad-Fc microchannel gels had higher calcium activity when compared to chemically coupled N-Cad-Fc to microporous gels. Biologically modified N-Cad-Fc micropours gel had significantly lower calcium activity in comparison with biologically bound N-Cad-Fc to microchannel hydrogel. (p-value <0.05).

## 5.8 References


1. Willerth, S.M. & Sakiyama-Elbert, S.E. Approaches to neural tissues engineering using scaffolds for drug delivery. *Adv. Drug Deli. Rev.* 2007; 59: 325-338.
2. Linne, ML. and Jalonen, T. O. Chapter Nine- Astrocyte-Neuron Interactions: from experimental research-based models to translational medicine, In: Kim T. Blackwell, Editor(s), *Progress in Molecular Biology and Translational science, Academic press.* 2014; 123: 191-217.
3. Schmidt, C.E. & Leach, J. B. Neural tissue engineering: strategies for repair and regeneration. *Ann. Rev. of Biomed. Eng.* 2003; 5: 293-347.
4. Gumera,C., et al. Materials for central nervous system regeneration: bioactive cues. *J.Mater.Chem.* 2011; 21: 7033-7051.
5. East, E. Golding, J.P., and Philips, J.B. Engineering an integrated cellular interface in three-dimensional hydrogel cultures permits monitoring of reciprocal astrocyte and neuronal responses. *Tissue Engineering Part C: Methods*. 2012;18:526-536.
6. Irons, H.R., Cullen Dk., Shapiro, N. P., Lambert, N.A., Lee, R.H., and LaPlaca, M.C. Three-dimensional neural constructs: novel platform for nurophysiological investigation. *J. Neural Eng.* 2008; 5: 333-341.
7. Roy, J., Kennedy, T.E., and Costantino, S. Engineered cell culture substrates for axon guidance studies: moving beyond proof of concept. *Lab Chip.* 2013; 13: 498-508
8. Frampton, J. P. Hynd, M R., Shuler, M. L. and Shain, W. Fabrication and optimization of alginate hydrogel constructs for use in 3D neural cell culture. *Biomed. Mater.* 2011; 6: 18pp.

9. Lee, K.Y. and Mooney, D. J. Alginate: properties and biomedical applications. *Progress in polymer science.* 2012; 37:106-126.

10. Lee, M. K., Rich, M. H., Shkumaov, A. Jeon, J. H., Boppart, M. D., Bashir, R., Lee, J., and Kong, H. Glacier moraine formation-mimicking colloidal particle assembly in crochanneled, bioactive hydrogel for guided vascular network construction. *Adv. Healthcare Mater.* 2014; 00: 1-6.

11. Lambert, M., Padilla, F., and Mege, R-M. Immobilized dimmers of N-Cadherin-Fc chimera mimic cadherin-mediated cell contact formation: contribution of both outside-in and inside-out sitnals. J. Cell Sci. 2000;113: 2207-2219.

12. Chappuis-Flament, S., Wong, E., Hicks, L.D., Kay, C.M., and Gumbiner, B.M Multiple cadherin extracellular repeats mediate hemophilic binding and adhesion. . *J. Cell Biol.* 2001;154: 231-243.

13. Sivasankar, S., Brieher, W., Lavrik, N., Gumbiner, B., and Leckband, D. Direct molecular force measurements of multiple adhesive interactions between cadherin ectodomains. *Proc. Natl. Acad. Sci.* 1999; 96: 11820-11824.

14. Lee, H.K.; Kameyama, K.; Huganir, R.L.; Bear, M.F. NMDA induces long-term synaptic depression and dephosphorylation of the GluR1 subunit of AMPA receptors in hippocampus. *Neuron.* 1998; 21: 1151-1162.

15. Vega L. J.C.M., Lee, M.K., Jeong, J.H., Smith,C.E., Lee, K.Y., Chung, H.J., Leckband, D.E., and Kong, H. Recapitulating cell-cell adhesion using N-cadherin biological tethered to substrates. *Biomacromolecules.* 2014; 15:2172-2179.

16. Samitsu, S., Zhang, R., Peng, X., Krishnan, M.R., Fujii, Y., and Ichinose, I. Flash freezing route to mesoporous polymer networks. *Nature Communications.* 2013; 4:2653.

17. Intracellular calcium assays in dissociated primary cortical neurons: Doering, L. C., Editor. Springer protocols handbooks. 4th ed. McMaster University, Hamilton, ON, Canada. *Humana Press*. 2010: 125-136.

18. Wheeler, B. C. and Brewer, G. J. Designing neural networks in cultured. *Proceedings of the IEEE*. 2010; 98:398-406.

19. Newman, E. A. New roles for astrocytes: Regulation of synaptic transmission. *Trends in Neuro.* 2003;26: 536-542

20. Nedegaard, M., Ransom, B., and Goldman, S.A. New roles for astrocytes: redefining the functional architecture of the brain. *Trends in Neuro*. 2003; 26: 523-530.

21. Allen, N.J. and Barres, B. A. Glia and synapse formation: An overview. Encyclopedia of Neuroscience, ed. By Larry R. *Squire, Academic Press, Oxford*. 2009: 731-736.

22. Slezak, M. and Pfrieger, F. W. New roles for astrocytes: Regulation of CNS synaptogenesis. *Trends in Neuro.* 2003; 26: 531-535.